ABSTRACT

DETAILED LITHOSTRATIGRAPHIC CHARACTERIZATION OF CHICO MARTINEZ CREEK, CALIFORNIA

By

Annie G. Mosher

December 2013

A 6012-foot Monterey Formation succession at Chico Martinez Creek, San Joaquin basin, is characterized at high spatial resolution by spectral gamma-ray data in 2-foot increments, 5-foot lithologic descriptions, and qualitative XRD and FTIR analysis. Based on these data, the 4 Monterey members–the Gould, Devilwater, McDonald and Antelope shales–are subdivided into 7 distinctive lithofacies. New paleomagnetic data, combined with industry-provided biostratigraphy establishes a chronostratigraphic framework and allows determination of linear sediment accumulation rates. Condensed sedimentation at the onset of McDonald deposition (~14 Ma) is also observed in correlative members in the Pismo, Santa Maria and Santa Barbara basins. This regional event is associated with eustatic regression from the Mid-Miocene highstand related to formation of the East Antarctic Ice Sheet and ongoing thermotectonic basin subsidence. A surge in linear sediment accumulation rates in the siliceous upper McDonald and Antelope (~10.4 Ma) is attributed to a regional increase in diatom productivity.

DETAILED LITHOSTRATIGRAPHIC CHARACTERIZATION OF CHICO MARTINEZ CREEK, CALIFORNIA

A THESIS

Presented to the Department of Science Education

California State University, Long Beach

In Partial Fulfillment

of the Requirements for the Degree

Master of Science in Geology

Committee Members:

Richard Behl, Ph.D. (Chair)
Stanley C. Finney, Ph.D.
Gregg Pyke, M.Sc.

College Designee:

Robert D. Francis, Ph.D.

By Annie Mosher

B.S., 2008, University of California, Santa Cruz

December 2013

WE, THE UNDERSIGNED MEMBERS OF THE COMMITTEE,

HAVE APPROVED THIS THESIS

DETAILED LITHOSTRATIGRAPHIC CHARACTERIZATION OF
CHICO MARTINEZ CREEK, CALIFORNIA

By

Annie G. Mosher

COMMITTEE MEMBERS

Richard J. Behl, Ph.D. (Chair)	Geological Sciences
Stanley C. Finney, Ph.D.	Geological Sciences
Gregg Pyke, M.Sc.	Occidental Oil and Gas Corporation

ACCEPTED AND APPROVED ON BEHALF OF THE UNIVERSITY

Robert D. Francis, Ph.D.
Department Chair, Department of Geological Sciences

California State University, Long Beach

December 2013

Copyright 2013

Annie G. Mosher

ALL RIGHTS RESERVED

ACKNOWLEDGMENTS

First and foremost I would like to thank Dr. Richard Behl for giving me the opportunity to study under his advisement at CSULB. These last two years have proved to be some of the most challenging and rewarding, yet. You have taught me to see the Monterey Formation as a complex puzzle, one that cannot be solved with a single explanation, but is open to many interpretations and possibilities. It seems your enthusiasm is not limited to the earth sciences, but all things in life. Thank you for making me a better researcher, effective communicator, and for pushing me to do more than I thought possible.

I would like to extend my gratitude to all other people and parties who have been involved with this project. To my committee members, thank you for putting in the time and effort to review my manuscript and share your knowledge and feedback with me. Thank you to Dr. Stan Finney for making my writing more concise, organized and grammatically accurate, and to Gregg Pyke, whose editorial remarks brought laughter during times of pre-submission stress. To my undergraduate field assistants, David Dillion and Bryan Petry, thank you for helping me endure the monotonous exercise of collecting spectral gamma-ray readings. Your assistance and company were invaluable, and at times, saved my sanity.

To the MARS consortium affiliates, thank you for providing the knowledge and resources that made this research effort possible. A special thanks to Plains Exploration

& Production, Aera Energy, Occidental Petroleum and Venoco, for providing me with their data and expertise.

This project was also made possible by Kevin Bohacs from Exxon Mobil, who generously loaned a portable handheld scintillometer, the data from which is at the core of this thesis. Also by Epoch Well Services which not only allowed me to utilize their software to generate a surface mudlog for this project, but also gave me the opportunity and experience as a mudlogger prior to graduate school. Those two exciting and exhausting years working on oil rigs inspired my interest in petroleum geology and was the catalyst that motivated me to pursue an advanced degree. A special thanks to my mudlogging mentor and friend Mike Campbell who convinced me that I had what it took to be a successful graduate student, without your encouragement, I may have never taken this leap.

I would like to extend my gratitude to Karl Twisselman who generously, and without question allowed me to conduct this study on his private ranch. You have a keen interest in science and an amazing recollection of the geologists who have worked the Chico Martinez Creek section over the decades. Without your consent, this study would not have been possible.

To my family, thank you for being a strong foundation of support throughout this process. Mom, you are my inspiration. You have shown me that with hard work and dedication almost anything is possible. I would like to thank my brother and sister for providing encouragement and support with their kind words and actions. And for always reminding me of who I am, as only siblings can do. To my stepfather, our backpacking journeys to alpine terrain have rekindled my passion for geology at times when I thought

the fire was fading. Lastly, I would like to thank my father for inspiring my love for science at a young age by entertaining discussions of physics and planetary science with an 8 year old, you are never too young learn.

Last, but certainly not least, I would like to express my gratitude to my cohorts and dear friends Heather Strickland and Eric Arney whose work ethic and high standard for excellence have raised my own personal bar for achievement. The sky is the limit!

In geology, no stoned should be left unturned when searching for understanding. This is a philosophy I have found to be not only applicable to science, but to all aspects of life.

TABLE OF CONTENTS

LIST OF TABLES

TABLE Page

LIST OF FIGURES

FIGURE Page

FIGURE Page

CHAPTER 1

INTRODUCTION

The siliceous Miocene Monterey Formation is of great economic importance in the San Joaquin basin and the state of California, both as a hydrocarbon source and reservoir. This intraformational petroleum system exists due to the variable lithologic nature of the Monterey Formation, which contains both source rocks with high total organic carbon (TOC) and highly fractured biosiliceous chert and porcelanite reservoirs capable of storing commercial quantities of hydrocarbons. According to a recent survey conducted by the U.S. Geological Survey to assess hydrocarbon potential in the San Joaquin Basin, there exists an estimated 393 million barrels (MMBbls) of technically recoverable undiscovered oil, 332 MMBbls of which is trapped in Miocene sediments (Gautier et al., 2003). These estimates become potentially greater when considering continued improvement in recovery methods in known Monterey reservoirs.

In an industry where the perception exists that most conventional accumulations have already been discovered and exploited, new excitement surrounding untapped unconventional shale plays has thrust the Monterey Formation back into the spotlight as an exploration target in California. Although long known to be the key source of oil in California, enhanced understanding of this heterogeneous succession may prove pivotal to discovering new hydrocarbon accumulations and enhancing recovery from existing accumulations.

Chico Martinez Creek (CMC), located in the foothills of the Temblor Range (fig. 1), has served as a stratigraphic reference section for the Miocene Monterey Formation in the San Joaquin basin for nearly 100 years (Gaylord and Hanna, 1924) and is considered to be one of the thickest and most continuous surface exposures (greater than 6000 stratigraphic feet) of the Monterey Formation in California (Bramlette, 1946). The section has also been the site for lithologic studies, groundbreaking silica diagenesis research, and numerous field guides (Woodring, Stewart and Richards, 1940; Bramlette, 1946; McMichael, 1959; Karp, Elliott and Young, 1968; Foss and Blaisdell, 1968; Dibblee, 1973; Murata and Nakata, 1974; Murata and Larson, 1975; Murata and Randall,

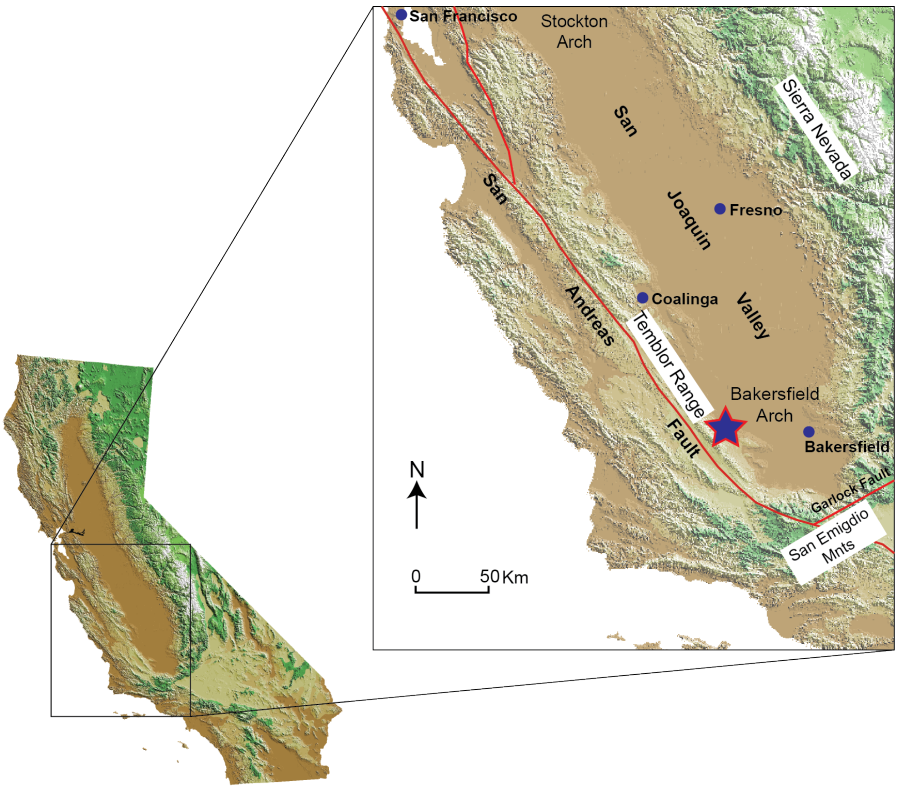

FIGURE 1. Index map illustrating the location of Chico Martinez Creek (blue star) with respect to the San Andreas fault and Temblor Range.

1975; Murata et al., 1977; Friedman and Murata, 1979; Williams, 1982; Williams et al., 1982; Graham and Williams, 1985; Williams, 1990). In spite of this long interest, the lithostratigraphy of the section has never been studied in detail. In fact, only a brief one-page general description exists in the academic literature (Woodring, Stewart and Richards, 1940), and it is only a small component of a larger, more regional research effort. In essence, the Chico Martinez section offers a wealth of untapped data that could potentially yeild valuable insight into subsurface stratigraphy. This succession, considered to be continuous, may also provide an uninterrupted record of major Miocene climatic changes and cycles. Establishing the detailed stratigraphy and timing of depositional events can provide an important basis for understanding global events.

Objective

This study aims to rectify the lack of detail in the academic archives, by providing a detailed lithostratigraphic characterization of the Monterey Formation via acquisition of surface spectral gamma-ray data and detailed lithologic descriptions at CMC. Gamma-ray spectrographic data will be used as a proxy for sediment geochemistry and can be useful for interpretations of sequence stratigraphy that allow for identification of major paleoceanographic events, such as changes in sea level and bottom-water oxygenation. Because gamma-ray logs are routinely collected while drilling oil and gas wells, surface spectral and total gamma-ray data can be collected and compared to established subsurface stratigraphy and provide more valuable insight into lateral thickness variations of the Monterey Formation members than can be accomplished by lithologic descriptions alone.

This research effort will use biostratigraphic data previously acquired by industry

for chronostratigraphic correlation of the section and, in effect, bring previously unpublished proprietary data into the realm of publically accessible literature. To further refine age control, the remanent paleomagnetism in dolostone beds across a key interval will be determined to identify magnetic reversals in the Upper Miocene succession. These chronostratigraphic data allow for determination of sediment accumulation rates– fluctuations in which may provide insight into paleoceanographic events and basin architecture during deposition.

Although the Belridge Diatomite (referred to as the Reef Ridge in other areas of the basin) is accepted as the top of the Monterey Formation in the San Joaquin basin, it was not included in the study due to its poor exposure. Consequently this thesis is limited to the Gould, Devilwater, McDonald and Antelope Shale members of the Monterey Formation. Ultimately, this new detailed lithostratigraphic characterization will be of value to geoscientists working on the Monterey Formation in the southwestern San Joaquin basin and may ultimately aid in the overall understanding of how accumulation of these siliceous sediments varied between different Neogene basins in California.

Geologic Setting

CMC is located in the foothills of the Temblor Range where Oligocene to Miocene strata overlie crystalline Cretaceous rocks (Hudson and White, 1941; Johnson and Graham, 2005). The Temblor Range marks the western boundary of the San Joaquin basin and is bound to the west by the northwest-southeast trending San Andreas Fault (fig. 1). Although, CMC is located in a structural high influenced by Temblor Range tectonic uplift, it is still considered to be part of the southwestern San Joaquin basin.

Figures 2 and 3 are detailed location maps showing the field location with respect to proximal oil fields, major roads and nearby towns. More specifically, CMC is located on the Twisselman Ranch in the northern part of the McKittrick quadrangle in Township 29S, Range 20E. The Monterey Formation exposure begins to the west in section 9, continues eastward across sections 10 and 11 and terminates to the northeast in section 2.

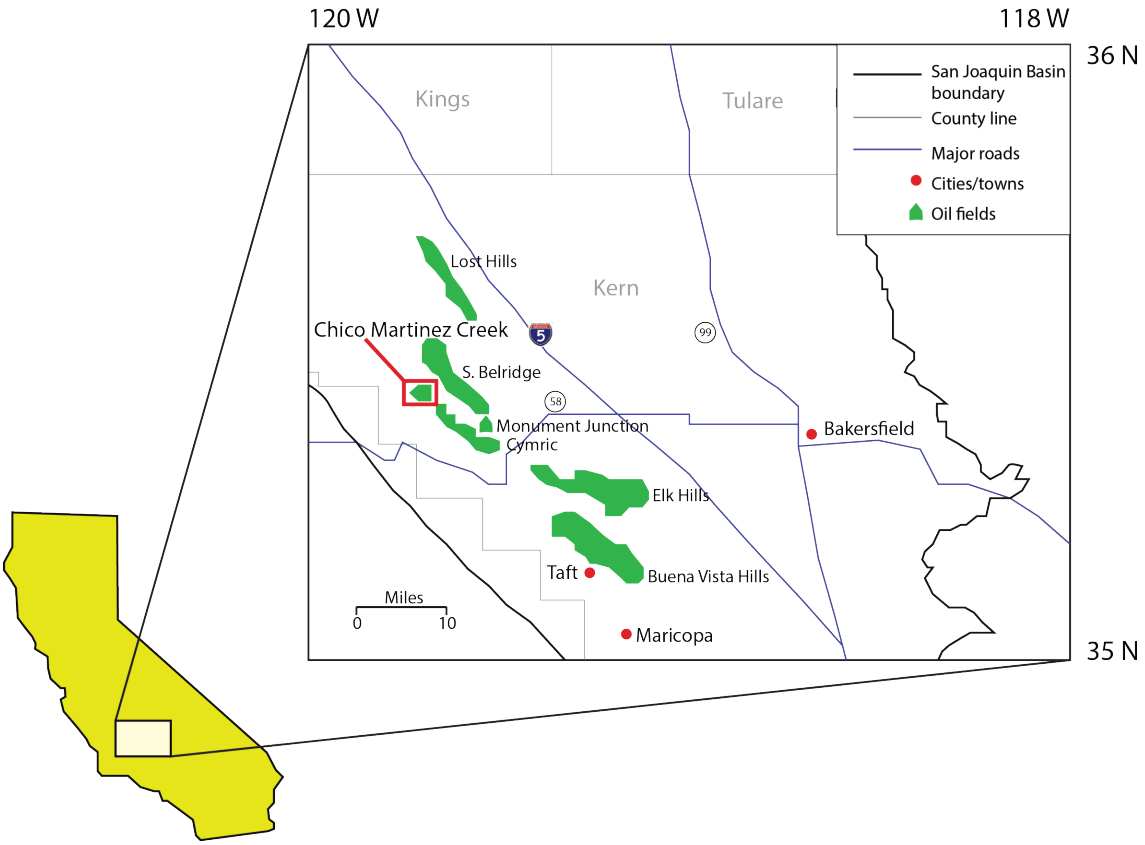

FIGURE 2. Map illustrating the location of Chico Martinez Creek (red star) with respect to major oil fields.

The San Joaquin basin, located west of the Sierra Nevada, is an asymmetric synclinal depocenter with a gently dipping eastern limb and a more structurally deformed steeply dipping western limb (Bartow, 1991). The basin is located in the southern part of

the Great Valley, originally a forearc basin from the Late Mesozoic through Early Cenozoic when subduction-related tectonics dominated the California continental margin (Dickinson and Seely, 1979). The sedimentary fill is more than 25,000 feet (>7.6 km) thick and provide a record of over 100 million years of local tectonics, eustatiyc and global climatic events (Graham and Williams, 1985; Scheirer and Magoon, 2007). Jurassic ophiolites underlie this thick succession in the western part of the basin, and plutonic and metamorphic rocks, exposed in the Sierra Nevada, serve as basement in the east (Bartow, 1991). The limits of the basin are defined by the San Andreas fault and Coast Range system to the west, the Sierra Nevada foothills to the east, the Stockton Arch to the north and the San Emigdio Mountains to the south (fig. 1).

Geologic History and Basin Development

A series of tectonic events from approximately 29 Ma to 7.5 Ma lead to the development of the deep Neogene basins within which Monterey sediments accumulated and underwent syn- and post-depositional deformation (Harding, 1976; Blake et al., 1978). Cessation of subduction along the California continental margin and the inception of the current-day San Andreas fault system began in the Middle Oligocene (29 Ma) during which time the East Pacific Rise converged with the North American Plate (Atwater and Molnar, 1973; Dickinson and Snyder, 1979). This collision resulted in a transition from a compressional to shear stress regime along the continental margin, with the majority of movement occurring along the San Andreas fault (Atwater, 1970). This transition in plate motion was complex and time-transgressive–propagating northwestward and southeastward from the initial point of contact at varying rates.

Slip along the present-day inboard San Andreas fault system did not begin until

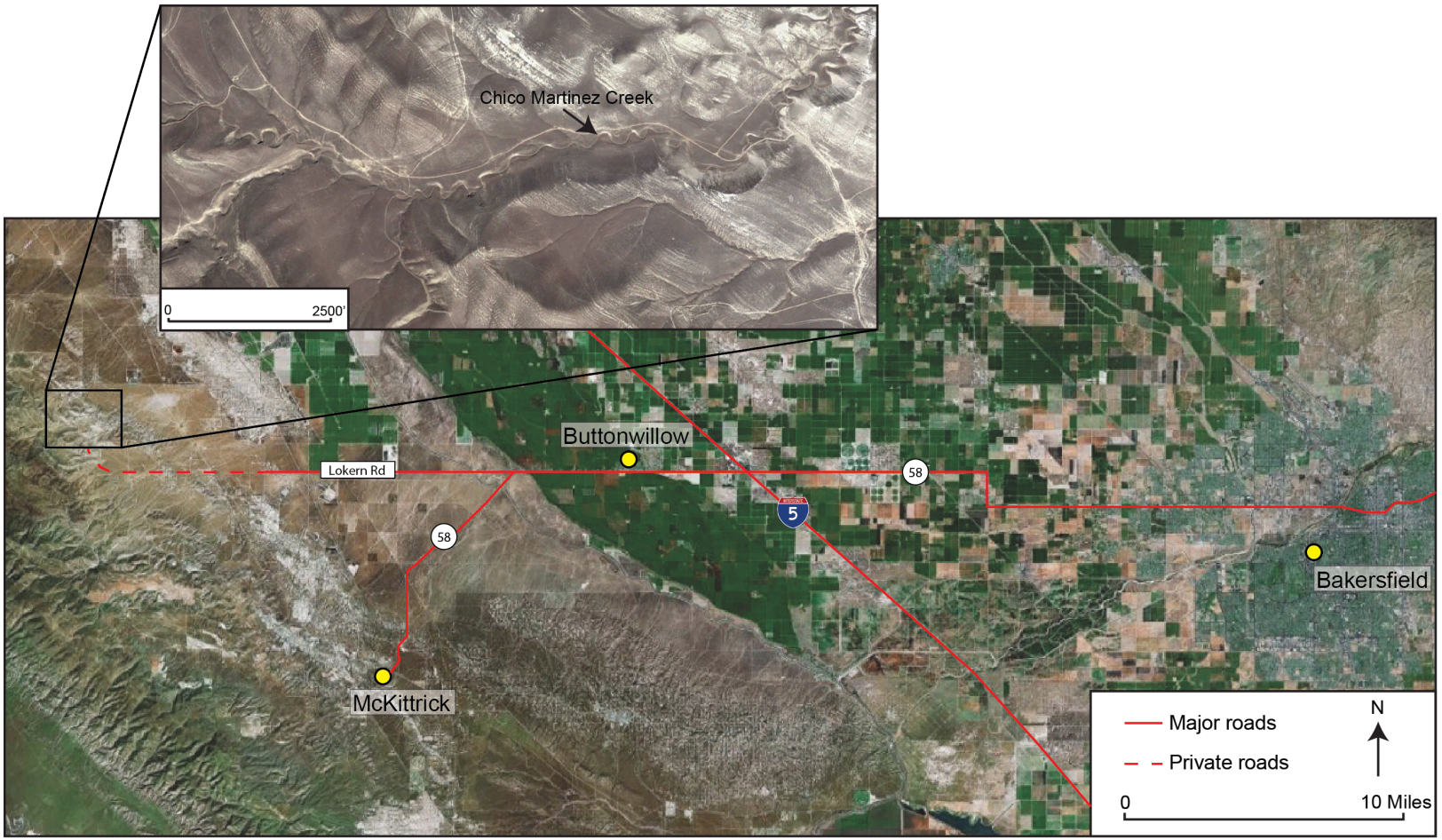

FIGURE 3. Detailed location map illustrating the position of Chico Martinez Creek with respect to major roads and nearby towns.

the Middle Miocene (16-17 Ma). This inland migration of transform motion coupled with a shift to more westerly-oriented shear along the fault system resulted in a transtensional stress regime that lead to Neogene basin development (Blake et al., 1978). In the CMC section, this tectonically induced basin subsidence is marked by a shift from the shallow-marine sandstone deposits of the Buttonbed Sandstone member of the Temblor Formation to the deep-marine hemipelagic sediments of the Monterey Formation (Graham and Williams, 1985). During this time of rapid basin subsidence, Monterey deposits filled the San Joaquin basin as northward migration of the Salinian block west, of the San Andreas fault further isolated the basin from the Pacific Ocean (Graham and Williams, 1985).

According to Harding (1976), uplift of the Temblor Range–the southernmost extent of the California Coastal Ranges–occurred contemporaneously with deposition of the Monterey Formation. This is evidenced by the abundance of growth folds and updip thinning in middle Miocene strata (Harding, 1976). Compared to Miocene deformation, Eocene and Oligocene structural deformation is minor and likely associated with the inception of strike slip motion in the Middle Oligocene (Harding, 1976). This deformation accelerated in the Late Miocene-Early Pliocene (Mohnian and Delmontian stages), when slip rate along the San Andreas fault increased (Harding, 1976).

Besides being tilted, the Monterey Formation at CMC have undergone relatively little structural deformation. The sediments form a gentle basinward-dipping (40° ENE) homoclinal structure with no known faults or unconformities within the Monterey section (fig. 4). As such, this section is ideal for a stratigraphic study, that requires continuity of section to determine accurate changes in sediment accumulation rates.

Monterey Formation Deposition

In addition to tectonic-induced basin subsidence, Monterey Formation deposition was controlled by paleoceanographic and climatic events that occurred coeval with deposition of strata at the base (17.5 Ma) and top (6 Ma) of the formation (Barron, 1986). These events resulted in enhanced biologic productivity of microorganisms along the California margin, and, consequent high rates of biomass decomposition resulted in the development of oxygen-starved basins, promoting the preservation of organic material (Pisciotto and Garrison, 1981).

The proportions of different types of planktonic organisms and organic matter that were preserved varied throughout the Miocene succession, depending on climate and oceanographic conditions. This resulted in compositional variability on a multitude of scales, from laminations to members (Pisciotto and Garrison, 1981). In general, the Monterey can be subdivided into three major stratigraphic depositional facies as defined by Pisciotto and Garrison (1981): a basal calcareous facies, a middle phosphatic facies, and an upper siliceous facies. All three facies are present in the Monterey Formation members at CMC and include the Gould, Devilwater, McDonald and Antelope Shale members (fig. 5). This facies subdivision occurs in several other Neogene depocenters of California including the Santa Barbara, Santa Maria and Salinas basins (Pisciotto and Garrison, 1981)

Although there are local variations, the three-part facies subdivision of Pisciotto and Garrison (1981) is widespread and can be explained by paleoclimatic and paleoceanographic events that occurred during the Miocene. Prior to growth of the East Antarctic Ice Sheet, a warm global climate and high sea level dominated from the

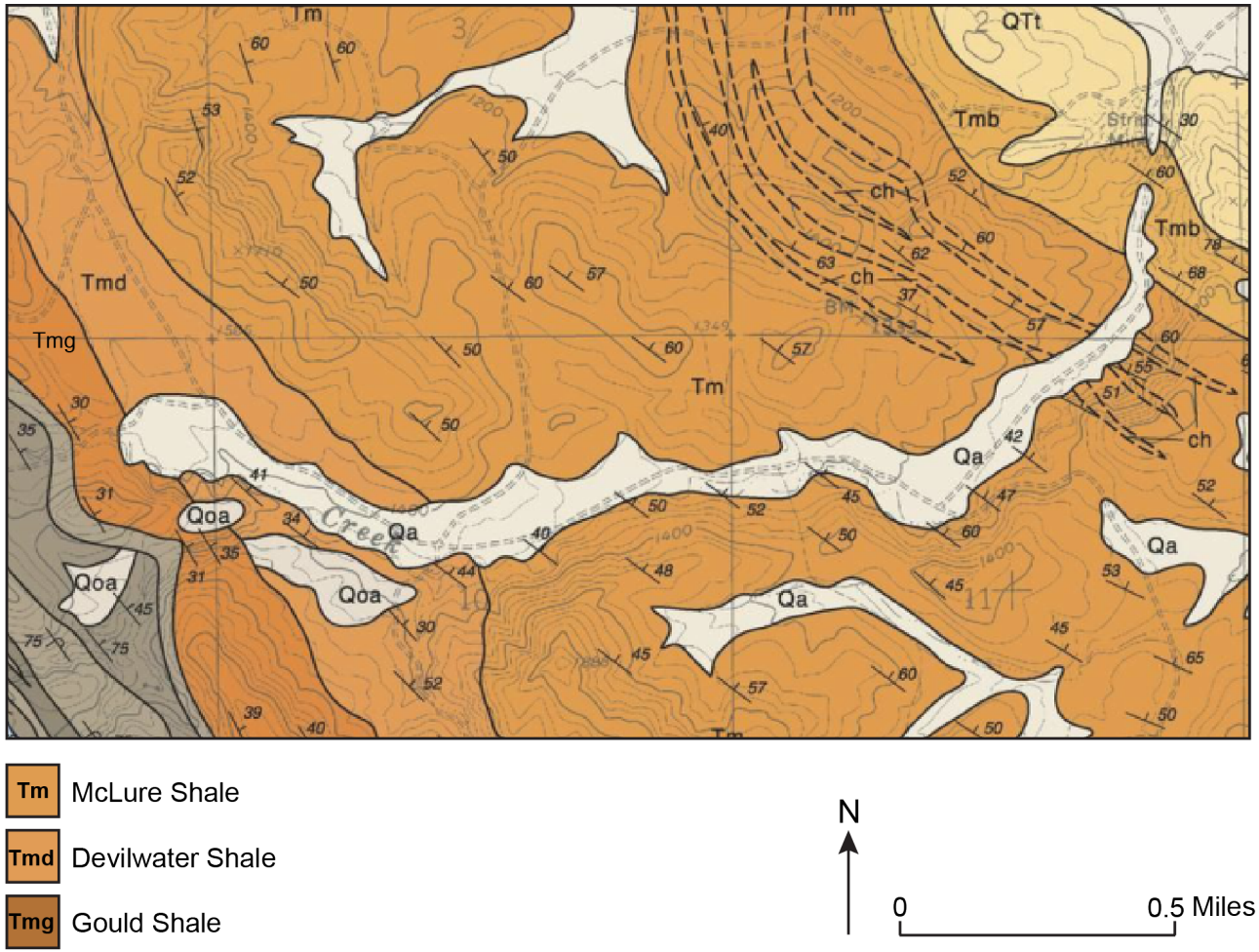

FIGURE 4. Geologic Map of the Chico Martinez Creek section highlighting the shallow eastward-dipping homoclinal structure. Modified from Dibblee (2006).

Saucesian to Luisian (20 to 14 Ma) allowing calcareous plankton to thrive (Barron, 1986). Even though other pelagic sedimentary components are included in this member, production and deposition of abundant coccoliths and foraminifera resulted in the formation of the basal, distinctly calcareous lithofacies (Pisciotto and Garrison, 1981). At CMC the lithology of the Gould, Devilwater and lower McDonald members are characteristic of this lower calcareous basinal facies (fig. 6).

Deposition of the middle phosphatic facies marks the transition between the lower calcareous and upper siliceous facies, approximately 12 to 13 Ma (Pisciotto and Garrison, 1981). The combined effects of slow sedimentation rates, prevailing anoxic conditions and the convergence of the seafloor with the oxygen minimum zone allowed for significant accumulation and preservation of organic and diagenetic phosphatic material (Pisciotto and Garrison, 1981). The phosphatic facies is an important component to the

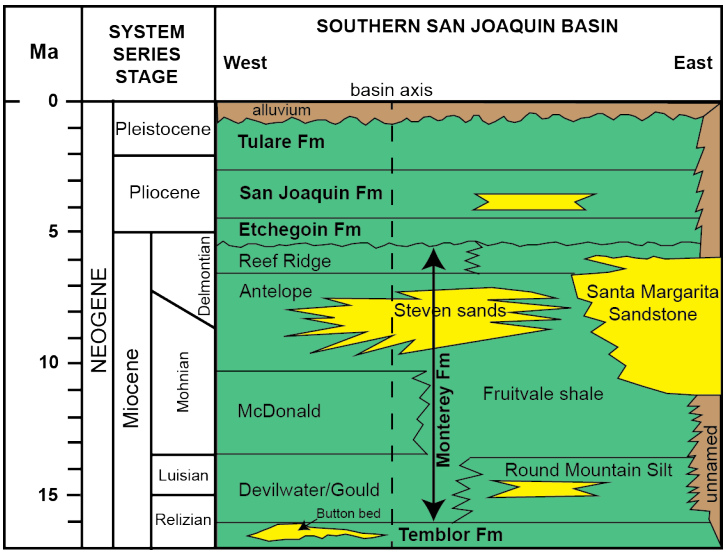

FIGURE 5. Stratigraphic column of the southern San Joaquin basin trending west to east. Modified from Scheirer and Magoon (2007). Note the sandstone units are colored yellow and shale units are green.

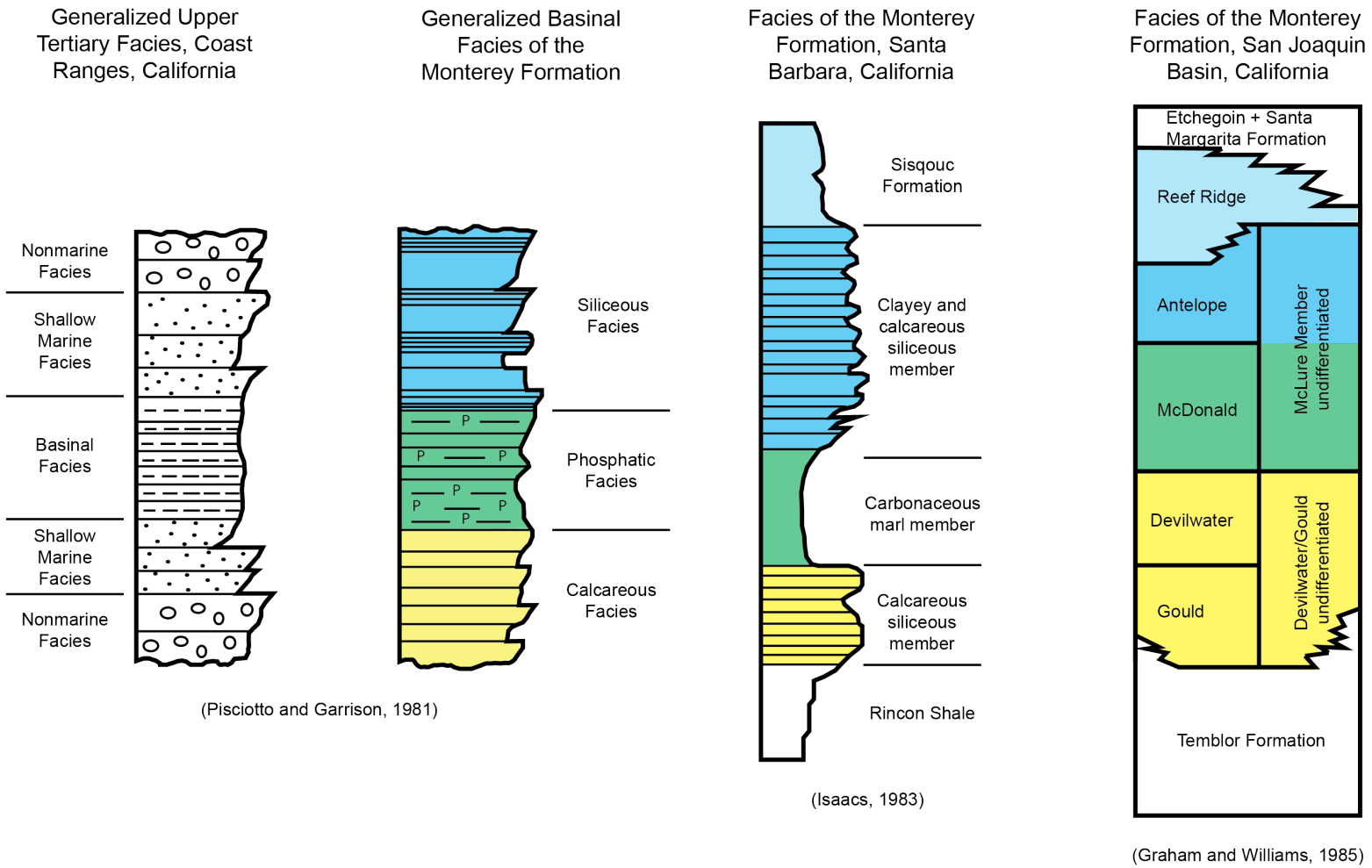

FIGURE 6. Generalized lithostratigraphic facies subdivision of the Monterey Formation as defined by Pisciotto and Garrison (1981). This includes the lower calcareous facies (yellow), middle phosphatic facies (green) and upper siliceous facies (blue) - faded blue is indicative of detrital-rich siliceous facies.

Monterey Formation petroleum system within the San Joaquin basin, offering the richest source potential, with TOC values reaching up to 9.16 weight percent (Graham and Williams, 1985). At CMC, the middle phosphatic member of the Monterey Formation corresponds to the McDonald Shale member (fig. 6).

Oxygen isotope data indicate that global sea-level fell 53-59 meters between 16.5 and 13.9 Ma at which point 90 percent of the East Antarctic Icesheet had formed marking the beginning of a major global cooling event (John et al., 2011). The resulting positive oxygen isotope excursion occurred contemporaneous with an increase in diatom productivity and resulted in the formation of the upper siliceous facies (Pisciotto and Garrison, 1981; Ingle, 1981; Barron, 1986). Thick and widespread Miocene diatomaceous deposits are not limited to California's Neogene basins, but are present both onshore and offshore along the Pacific Rim, supporting the global nature of this event (Ingle, 1981). This global cooling phase resulted in an increase in upwelling along the continental margin, which led to an increase in the supply of nutrient-rich water, and ultimately enhanced diatom (and other planktonic) productivity. As diatomaceous material accumulated, the eventual decomposition of organic matter starved basins of oxygen, resulting in the development of anoxia. These anoxic conditions subsequently allowed for mass preservation of carbonaceous and biosiliceous material. It has been postulated that burial of this abundant organic carbon developed a positive feedback that enhanced global cooling (Vincent and Berger, 1985; Mawbey and Lear, 2013). In CMC, the upper informal Antelope Shale member, which is highly siliceous, is characteristic of the upper siliceous facies as defined by Pisciotto and Garrison (1981). This siliceous member is overlain by the poorly exposed Belridge Diatomite.

Westside San Joaquin Basin Stratigraphy

The Monterey Formation is predominantly restricted to the central and southwest margin of the San Joaquin basin. It has an average thickness of approximately 5,000 feet (1,500 meters) and a maximum known thickness of 10,000 feet (3,000 meters) at CMC when including the Belridge Diatomite member (Johnson and Graham, 2004; Scheirer and Magoon, 2007; Scheirer, 2013). The Monterey Formation thins to the north and east (fig. 7) as documented by numerous stratigraphic studies that have used both outcrop and subsurface well data (Foss and Blaisdell, 1968; Graham and Williams, 1985; Callaway, 1990; Johnson and Graham, 2004; Scheirer and Magoon, 2007; Scheirer, 2013).

Recently, published research has been increasingly focused on understanding the relationship between sedimentary units of the San Joaquin basin within a sequence stratigraphic framework (Johnson and Graham, 2004). This is a useful way to make chronostratigraphic correlations in basinal strata where coeval, but lithologically distinct facies occur in different paleogeographic settings within a depocenter. During deposition of the Monterey Formation, terrigenous sediment was delivered to the San Joaquin basin by rivers draining from the ancestral Sierra Nevada–principally the ancient Kern River to the east with some input from the Tejon River to the south (Callaway, 1990). In the Late Miocene, northward translation of the Salinian block west of the San Andreas fault both isolated the basin from the Pacific Ocean and provided an additional source of coarse granitic sands from the west (Graham and Williams, 1985). Graham and Williams (1985) postulate that the Salinian block is the provenance of the Stevens sands, a prolific turbidite sandstone reservoir in the upper Antelope Shale member of the Monterey Formation on the west side of the San Joaquin basin (fig. 5).

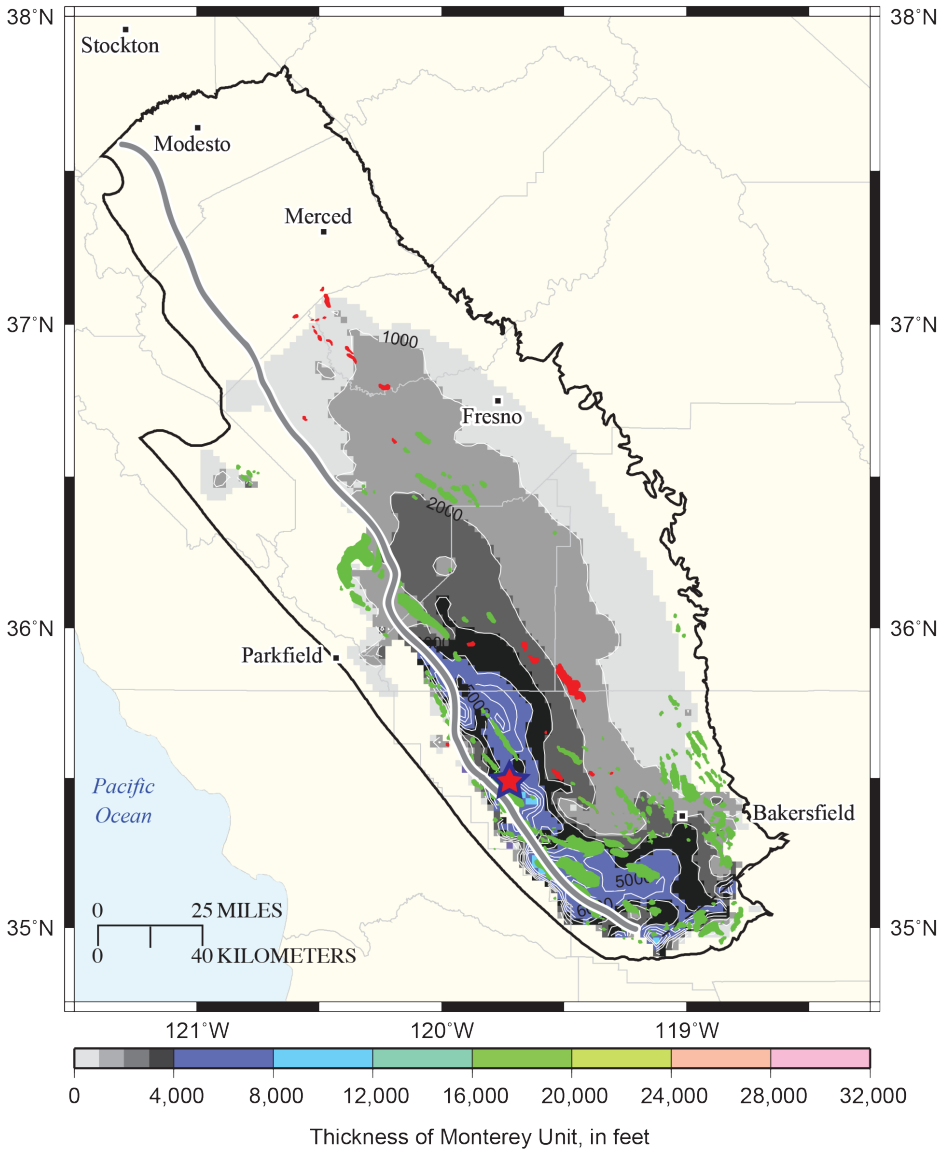

FIGURE 7. Thickness of the Monterey Unit in the San Joaquin basin. Modified from Scheirer, 2013. Red star indicates the location of the Chico Martinez Creek section.

In spite of the abundance of sediment entering the San Joaquin basin during the Miocene, Monterey Formation depocenters, for the most part, were isolated or had reduced terrigenous input. The bathymetry of the basin during the Miocene consisted of structurally isolated silled basins that developed over the ancient forearc basin landscape due to San Andreas-related wrench tectonics (Graham and Williams, 1985). The depocenters were starved of clastic input and hemipelagic sedimentation processes dominated (Graham and Williams, 1985). Relative to other Neogene basins located farther oceanward, the Monterey Formation in the San Joaquin basin has a higher detrital:silica ratio due to the closer proximity of the Sierra Nevada (Graham and Williams, 1985).

A combination of San Andreas-related tectonics and sea-level fluctuations resulted in the preservation of several transgressive and regressive cycles within the Miocene sediments (Callaway, 1990; Johnson and Graham, 2004). In order to better understand these cycles Johnson and Graham (2004) classified the San Joaquin basin fill into 4 distinct lithofacies to assess sequence stratigraphic significance: (1) distal deepwater shale and siltstone, (2) sandstone and siltstone of a transgressive systems tract (3) shelf and slope sandstones (4) and slope and basin-floor turbidite fan systems. The Monterey is characteristic of the distal deepwater shale facies (fig. 8) and shoals to the shelf-and-slope sandstone facies of the Santa Margarita Formation to the northwest (Johnson and Graham, 2004).

The conformable contact between the Buttonbed Sandstone and the overlying Gould Shale member (fig. 8) marks a major transition to a trangressive systems tract (Callaway, 1990; Johnson and Graham, 2004). This was followed by a relative lowstand

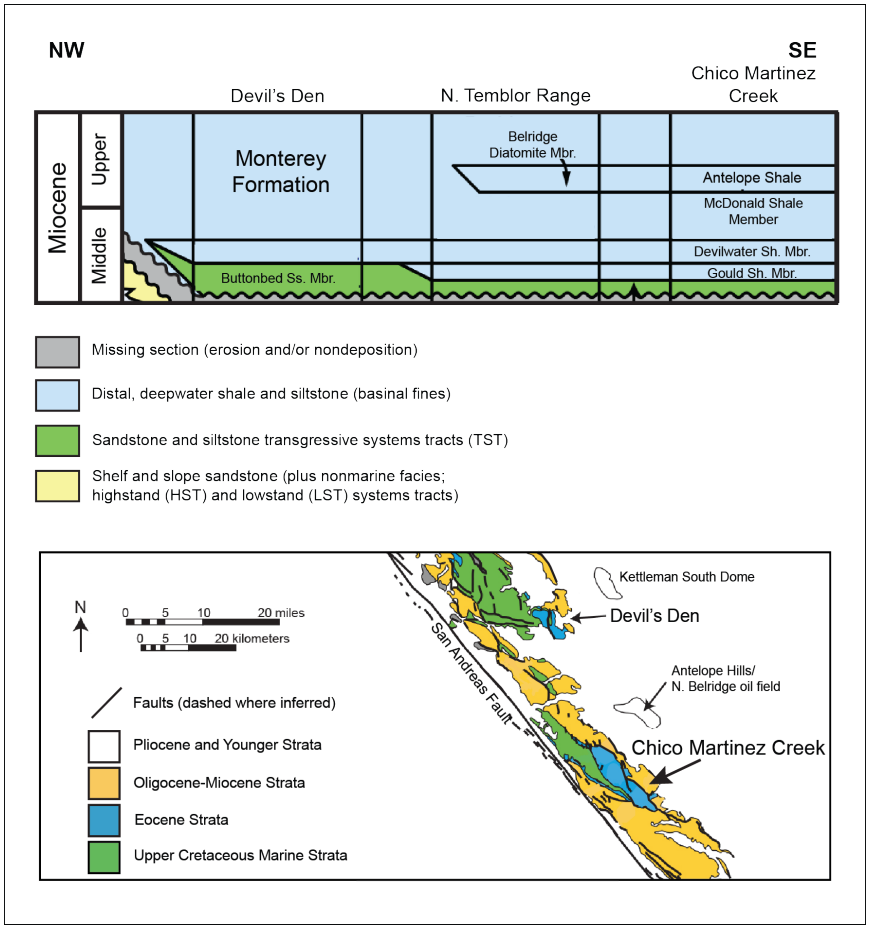

FIGURE 8. Chronostratigraphic correlation chart for the west-side San Joaquin Basin trending northwest-southeast from Devil's Den to Chico Martinez Creek. Below is outcrop geology of the southwestern San Joaquin basin illustrating the location of Devil's Den relative to Chico Martinez Creek. Figure modified from Johnson and Graham (2004).

system represented by the deposition of the silty Devilwater Shale, characteristized by onlapping deposits with a higher clastic composition (Johnson and Graham, 2004). The overlying McDonald and Antelope Shale members of the Monterey Formation were deposited during transgressive and highstand conditions. During this time, coeval with a global sea level highstand, the Monterey Formation reached its maximum eastward extent, coeval with a global sea level highstand (Graham and William, 1985; Vail and

Hardenbol, 1979). Clastic strata overlying the Monterey Formation, and including the upper diatomaceous Reef Ridge member of the Monterey Formation, represents a major regressive shift, and the ultimate filling of the San Joaquin basin (Graham and Williams, 1985).

Monterey Formation Member Ages

Published numerical ages interpreted for the members of the Monterey Formation are based on a variety of sections with a numerical timescale that has evolved over time (Foss and Blaisdell, 1968; Graham and Williams, 1985; Scheirer and Margoon, 2007). Ages in the San Joaquin basin are based on calcareous nanofossil zones of Bukry (1973, 1975), Okada and Bukry (1980), and Martini (1970, 1971); planktic foraminiferal zones of Berggren and Miller (1989), and Berggren (1972); California benthic foraminiferal zones of Kleinpell (1938); and diatom zones of Barron (1981a, 1981b). The Miocene geologic timescale (fig. 9) was constructed using a combination of Barron and Isaacs (2001) updated version of the chronostratigraphic framework for the California Miocene and McDougall's California biostratigraphic framework (2007), to which numerical ages were assigned based on paleomagnetic reversals that were previously dated.

The earliest published work to determine ages in the Monterey Formation in the CMC section was that of Foss and Blaisdell (1968) and later Graham and Williams (1985). In a more recent regional stratigraphic study, Scheirer and Magoon (2007) compiled information from previous studies to give the most up-to-date interpretation of unit ages in the San Joaquin basin. It is important to note that these ages assigned to the member, particularly their upper and lower boundaries, are variable throughout the basin due to the time-transgressive nature of Monterey Formation deposition (Graham and

Williams, 1985). Furthermore, an added complexity is that the stratigraphic terminology has varied over time as well. Formal rock stratigraphic terms used in this thesis were obtained from the geologic names lexicon of the USGS national geologic names database.

Scheirer and Magoon (2007) combined the Gould and Devilwater Shale members into one undifferentiated unit due to difficulty differentiating them in subsurface logs. However, Foss and Blaisdell (1968) derived dates for each separate member using benthic foraminifera from outcrop. In the Gould Shale, foraminifers characteristic of Kleinpell's (1938) *Siphogenerina branneri* zone are Relizian in age and correlate to the lower to middle part of the N8 planktonic foraminiferal zone which is between 16.5 and 15.5 Ma (Scheirer and Magoon, 2007) giving the Gould an average age of 16 Ma. The Gould Shale is conformably underlain by the Buttonbed Sandstone member of the Temblor Formation and conformably overlain by the Devilwater Shale member (fig. 5) (Foss and Blaisdell, 1968).

The age of the Devilwater is well constrained by biostratigraphic zones at both the top and the base of the member (Scheirer and Magoon, 2007). According to Foss and Blaisdell (1968), the lower Devilwater Shale member contains foraminifera of Kleinpell's (1938) *Siphogenerina reedi* zone (lower Luisian), whereas the upper part of the section contains foraminifera characteristic of the *Siphogenerina nuciformis* zone (upper Luisian). The Devilwater Shale was therefore deposited between 15.5 to 13.5 Ma (Scheirer and Magoon, 2007), and is conformably overlain by the McDonald Shale and grades into the Round Mountain Silt to the east (fig. 5) (Foss and Blaisdell, 1968).

The McDonald Shale member of the Monterey is early Mohnian to late early

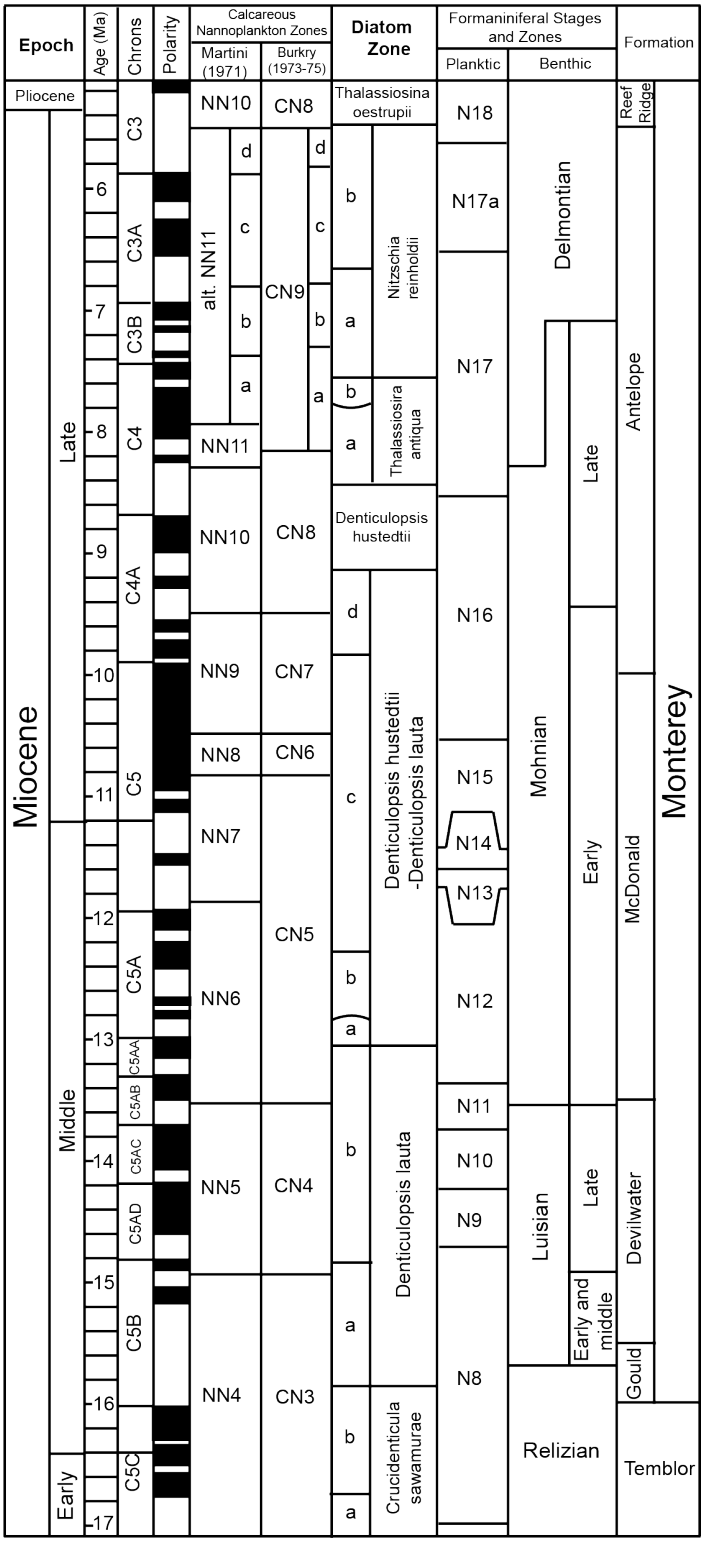

FIGURE 9. Miocene geologic timescale with combined data from Barron and Isaacs (2001) and McDougall (2007).

Mohnian in age as determined by Foss and Blaisdell (1968). The lower McDonald Shale has foraminifera characteristic of Kleinpell's (1938) *Bolivina modeloensis* zone, which correlates to the lower part of the Mohnian Stage. This zone is correlative with the planktonic formaniniferal zones N11 to N12 (13 to 12.5 Ma) according to Bartow's (1992) timescale (Scheirer and Magoon, 2007). The upper McDonald Shale has benthic foraminifera characteristic of the *Bolivina modeloensis* zone of lower Mohnian Stage. This zone correlates to calcareous nannoplankton zones NN9 and CN7, to which Bartow (1992) gave a numerical age of 9.5 Ma. Callaway (1990) correlated the top of the McDonald to a slight sea level transgression, which he interpreted to be 10 Ma. As such, the McDonald Shale was deposited from 13.5 to 10 Ma. The McDonald grades into the Fruitvale Shale to the east (fig. 5) and the undifferentiated McLure Shale to the north (Foss and Blaisdell, 1968).

Based on benthic foraminifera, the informal Antelope Shale member has fauna characteristic of the Kleinpell's (1938) Mohnian Stage (Graham and Williams, 1985). A commonly identified subsurface log signal known as the "N-marker" is widely interpreted to indicate the top of the Antelope and dated to be 6.5 Ma based on correlation with benthic foraminiferal fauna (Scheirer and Magoon, 2007). According to Foss and Blaisdell (1968), the Antelope is upper Mohnian on the basis of stratigraphic position and benthic foraminifera. Callaway (1990) placed the member between sequence stratigraphic boundaries dated at 10 Ma and 6 Ma. As such, the Antelope is determined to be 10 to 6.5 Ma and grades into the undifferentiated McLure Shale to the north (Scheirer and Magoon, 2007).

It is important to note that although these ages for the members of the Monterey

Formation are widely accepted, the members, likely vary in age across the San Joaquin basin due to their time-transgressive nature. This is particularly true for the top of the Antelope where differential Temblor Range uplift and basin subsidence have either truncated the Antelope or resulted in deposition of a thicker succession (Graham and Williams, 1985). As such, these dates are not definite and will merely serve as a general guide for interpreting ages for the CMC Monterey Formation succession. In this study, ages are assigned to the section strictly on the basis of biostratigraphy but further refined by magnetostratigraphy.

Previous Studies

Over the past century, CMC has been the site of both academic and industry-funded proprietary research. These studies vary in scope and detail from brief field guides to more extensive multidisciplinary research efforts. The section was first referenced in published literature in the early 19th century (Gaylord and Hanna, 1924; Hanna, 1928; Taff, 1933; Goudkoff, 1934, Simpson and Krueger, 1942), but was not intensively studied until the 1970's when breakthrough research on carbonates, silica diagenesis and oxygen geochemistry was published (Murata and Larson, 1975; Murata and Randall, 1975; Murata et al., 1977; Friedman and Murata, 1979). Even 90 years ago (Gaylord and Hanna, 1924), the CMC outcrops were recognized as an extraordinarily thick and complete stratigraphic succession. However, many of the publications discussed in this chapter were not exclusively conducted at CMC, but rather incorporated the section in larger, more regional, studies as a means to understand the lithostratigaphy of the Monterey Formation. The proprietary studies discussed in this chapter were

principally biostratigraphic in nature and provided the basis for chronostratigraphic correlation of the CMC section described in this thesis.

Published Literature

Lithostratigraphy. The first significant lithostratigraphic characterization of the Monterey Formation at CMC was that of Bramlette (1946) in his comprehensive overview of siliceous Monterey rocks in California. In this study, the section was measured, briefly described, and compared with other Monterey Formation outcrops in an effort to determine stratigraphic relationships throughout California. Bramlette confirmed that the 6,404-foot exposure at CMC was one of the thickest and most well exposed sections of Miocene strata in California. Bramlette subdivided the Monterey Formation at this locality into three distinctive members: the McLure Shale (later subdivided into the lower formal McDonald and upper informal Antelope Shale members), Devilwater Shale and Gould Shale members.

Woodring, Stewart and Richards (1940) included Bramlette's measured section per communication in their USGS Professional Paper on the geology of the Kettleman Hills oil field. They further subdivided the section into 11 members (10 unnamed members and the basal Gould member) and published the first descriptions of the Monterey Formation at CMC. They described the Gould Shale member as a cherty calcareous shale, and the Devilwater Shale was characterized as a silty calcareous mudstone. The overlying McDonald and Antelope Shales were described as brown calcareous shale and lighter diatomaceous shale. Bramlette's section was also cited in Dibblee's (1973) professional paper in which the stratigraphy of the Southern Coast Ranges was mapped. In this publication, the McLure Shale was mapped as one

undifferentiated unit due to difficulty in differentiating the McDonald Shale member from the Antelope Shale member in the field (Dibblee, 1973).

In 1968, Foss and Blaisdell published a report on the stratigraphy of the west side of the southern San Joaquin Valley. This paper aimed to serve as a reference guide for geologists working in the basin, and for each formation it provided the type locality, lithologic characteristics, fauna and age and stratigraphic relationships. At the time, many of the Monterey Formation members were considered informal and there were discrepancies in how different geologists and companies lithologically distinguished and defined their subdivisions of the Monterey Formation. Though controversial, this paper was to define member boundaries in an effort to establish industry-wide consistency in nomenclature. This was a foundational study that is regularly referenced today when discussing stratigraphic nomenclature and ages in the western San Joaquin basin (Scheirer and Magoon, 2007). Many of the stratigraphic relationships and contacts illustrated in Figure 5 are based on this study.

Williams (1982) published a study that identified nine distinctive lithologies within the Monterey Formation on the basis of outcrop exposures: diatomite and diatomaceous shales, porcelanite, siliceous shales and siliceous mudstones; mat-laminated sediments, clay shales and claystones, chert, dolomite, calcareous siliceous sediments, and siltstones and fine-grained sandstones. Her classification scheme was based on field observations, thin sections and Scanning Electron Microscopy (SEM) analysis, and was in part based on previous work by Isaacs (1981). Williams also evaluated how these lithogies vary laterally across the San Joaquin basin.

Graham and Williams (1985) combined lithostratigraphy and biostratigraphy from

outcrops, cores and well logs to understand the depositional and diagenetic history of the Monterey Formation in the San Joaquin basin. They showed with the stratigraphic cross sections that the Monterey Formation is predominantly a north-south trending body surrounded by siliciclastics strata. In general, the Monterey thickens to the south and west, but abruptly terminates along the western margin of the San Joaquin basin due to tectonic uplift along the San Andreas fault. Intraformational correlation by well log characteristics and paleontologic makers demonstrated the top of the Monterey Formation was time-transgressive.

Graham and Williams (1985) further documented the increasingly terrestrial character of organic matter content in the northern and eastern areas of the basin, compared to the marine kerogens that are more prevalent along the western margin of the basin. This provided insight into the basins overall architecture and sediment distribution patterns, and demonstrated that the basinal depositional environment in the western San Joaquin basin shallowed to shelfal environments in the north and east.

Field Guides. The first field guide for CMC was published by the San Joaquin Geologic Society guidebook in 1959 (McMichael). In 1968, a Pacific Section AAPG guidebook featuring the geology and oil fields in the southwestern San Joaquin basin included multiple stops at the CMC exposures (Karp, Elliott and Young). In 1990, Williams published the most comprehensive field guide in which distinctive lithologies, diagenetic boundaries and geomorphic features were described throughout the section.

Unpublished Proprietary Reports

Additional important work at CMC has not been published because of its proprietary nature, but has become available for this thesis. Although the company

reports were not externally peer reviewed, they contain data that is highly relevant and valuable for this research effort.

Shell Oil (1937). In 1937, Shell Oil completed a detailed paleontologic study in which approximately two miles of trenches were excavated along the ridges lining the creek to achieve full exposure (fig. 10). The lithology was described and benthic foraminifera were sampled in 10-foot increments. The Monterey Formation was measured to be 6,970 stratigraphic feet thick and was compared to that obtained in previous studies (figs. 10 and 11).

Unocal (1986). In 1986, Unocal conducted a multidisciplinary stratigraphic study that incorporated paleontologic data, geochemistry (x-ray diffraction) and total gamma ray data to lithostratigraphically characterize the section and provide age control for subsurface correlation (Heitman, 1986). Sediment accumulation rates were determined using key biostratigraphic horizons, and subsurface correlations were made using the surface gamma ray data. Samples and data used in this study were collected along creek exposures (fig. 12). Using these transects, the section was measured to be 5,615 feet thick (fig. 11). The Unocal study also includes organic carbon/carbonate and Rock-Eval analyses.

In this study, 376 stratigraphic levels were sampled for calcareous nanofossils, siliceous microfossils and benthic foraminifera. Fresh samples were collected with a gasoline-powered augur equipped with a five-foot long drill bit where exposure permitted and brief lithologic descriptions were noted between sample localities. Biostratigraphic correlations were based on Kleinpell (1938), Okada and Bukry (1980), and Barron (1981). In addition, gamma-ray measurements were collected every five stratigraphic

feet by Cedar Strat–a third party consultant out of Ely, Nevada. These reading are stated to be accurate to (plus or minus) 10 counts per second and didn't include a spectral gamma breakdown of uranium, potassium and thorium energy levels.

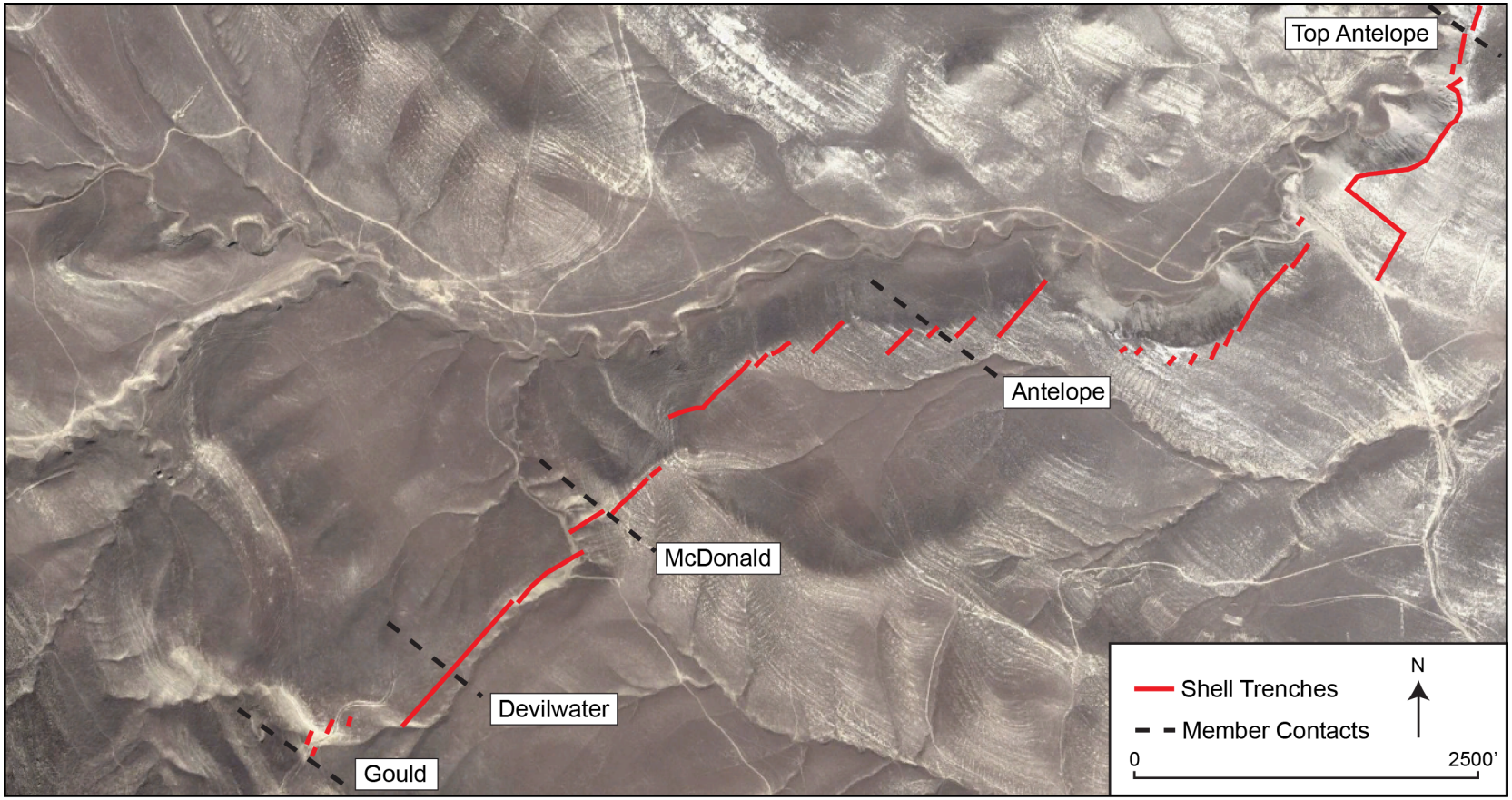

FIGURE 10. Location of trenches excavated by Shell in 1937.

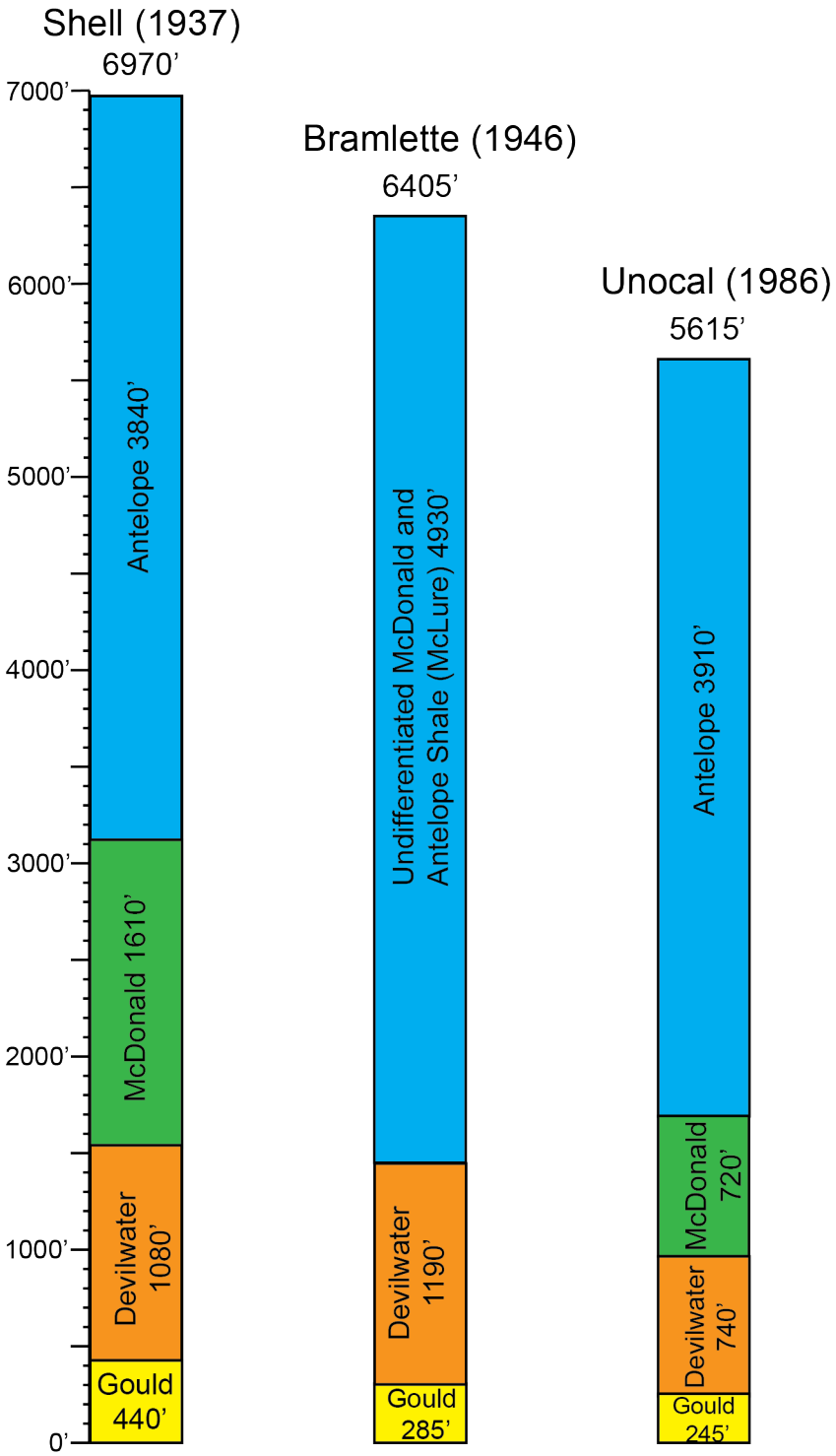

FIGURE 11. Measured sections from previous studies conducted at Chico Martinez Creek.

FIGURE 12. Location of sample transects from Unocal's 1986 study.

CHAPTER 2

METHODOLOGY

Data Collection

Locations of Data Acquisition

Historically, studies conducted in the CMC section have been restricted to exposed outcrop along the creek where the majority of the Monterey Formation is covered by colluvium and vegetation. In 1937, however, Shell conducted a micropaleontological study, which employed trench excavation along ridges flanking the creek as a means to maximize exposure (fig. 10). Since that time, the 2-foot wide by 3-foot deep trenches were either backfilled or naturally infilled with sediment. For the purposes of acquiring more complete data, a series of these trenches were re-excavated by Golden Construction & Excavation using a 420D loader backhoe with a 24-inch bucket. Most of the trenches could not be reopened due to their location on government owned BLM property, where surface land disruption is prohibited without an extensive review and environmental assessment procedure. Where the original Shell Oil trenches were on BLM land, either new laterally offset trenches were excavated, or data were collected from exposures along the creek (fig. 13). Re-excavated Shell trenches include T1, T2, T3, T4, T6 and T7, whereas T5, T8 and T9 are new trenched sections. New trenches were oriented perpendicular to strike, except where rugged and steep terrain did not permit.

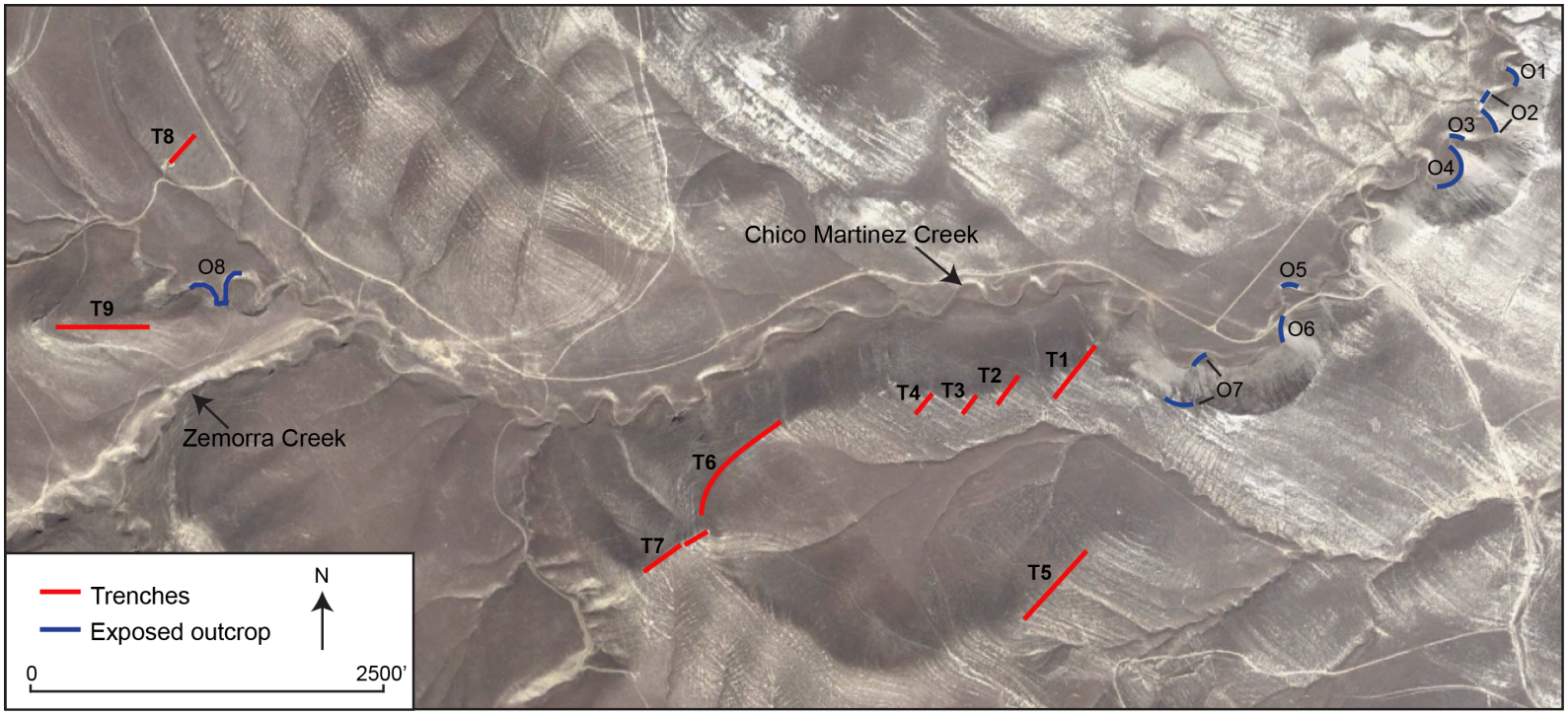

FIGURE 13. Sample locations along trenches (red) and exposed outcrop (blue).

In total, 2,440 stratigraphic feet (731 meters) of trenches were either re-excavated or newly unearthed, and 1,220 stratigraphic feet (366 meters) of section were measured in outcrop (fig. 13). The lengths of the covered intervals between trenched and exposed strata were calculated using the trigometric function: stratigraphic thickness = sin (dip angle)×(outcrop width). The dip was assumed to be an average value between the two bounding exposed sections, and outcrop width was measured on satellite images in a direction perpendicular to strike. In total, 2,352 feet (717 meters) of the Monterey Formation were inaccessible, approximately 40 percent of the section. Measurements are presented in feet in order to compare the CMC section with subsurface well data.

Handheld Spectral Gamma-Ray Data

Spectral Gamma-Ray data were collected using a portable handheld BGO Super Spec RS 230 scintillometer in order to facilitate correlation with subsurface successions and to determine uranium, thorium and potassium content at Chico Martinez Creek. Measurements were collected in two-foot stratigraphic intervals because the resolution best approximates that of subsurface logs (typically 0.5-1-foot). The stratigraphic thickness between sampling stations was measured with a Jacob's staff.

Measurements were taken in a standardized and consistent manner in order to minimize error and produce accurate and meaningful data. Each measurement was collected with the instrument oriented parallel to the dip azimuth with an assay time of 3 minutes per station. Average count rate is directly proportional to the amount of radioactive isotopes in the formation (Ward, 1982) and the volume of rock sampled. The 3-minute sampling interval allowed the machine to detect more counts, resulting in a more accurate measurement. Three consecutive 3-minute measurements were collected

at a discrete sampling station each day to calculate instrumentation error. During the duration of this study the calculated error associated with uranium, thorium and potassium was determined to be 7.4, 11.4 and 10.2 percent, respectively. The measurement error was calculated using the following formula: [(average of the 2 additional measurements – actual measurement) ÷ (actual measurement)] × 100. Total gamma-ray (API) was derived from the uranium, thorium and potassium data using the following formula: total gamma = [8×uranium(ppm) + 4×thorium(ppm) + 16×potassium(%)] (Ellis, 1987).

The spectral breakdown of gamma-ray data into uranium, thorium and potassium is a powerful tool that can provide insight into rock composition (Schwalbach and Bohacs, 1996). Potassium (largely present in clays, micas, and feldspars) serves as a proxy for detrital content because it is directly related to aluminum based on the equation: $Al_2O_3(\%) = 5.38 \times K_2O(\%) + 0.16$ in the Monterey Formation of the Pismo basin (Schwalbach and Bohacs, 1992). Thorium is also related to aluminum content with the exception of tephra horizons where spikes in thorium are attributed to high radioactivity rather than abundant aluminosilicate detritus. Uranium is indicative of organic content, which is present in high concentrations due to anoxic conditions and low rates of sedimentation.

In an effort to fill covered intervals of missing gamma ray data, the gamma-ray profile from Chico Martinez Creek was correlated with well USL 57-11, located approximately 1,500 feet (457 meters) to the south (fig. 14). Because the well logs only start in the lower Antelope Shale, gaps in the upper ~2200’ (671 meters) in the CMC section could not be filled. AnalySeries 2.0 was used for correlation and data from USL

57-11 were spliced between tie points bounding covered intervals (fig. 15). Prior to splicing the interpreted data into the CMC section, the values were first normalized by subtracting the mean total API from each discrete data point and dividing by the standard deviation. The mean total API from CMC was then added to the normalized subsurface data and multiplied by the standard deviation of the CMC data. This normalization process adjusts for variations in values between the two datasets caused by differences in instrumentation and data acquisition techniques and conditions. It also corrects for any natural variation in gamma-ray values that may occur between the subsurface and the weathered surface outcrop. The newly spliced values increased the gamma-ray profile from encompassing only approximately 60 % coverage of the section, to approximately 80 % coverage (Fig. 16), leaving gaps only in the uppermost sections of the Antelope Shale.

Lithologic Descriptions

Lithology was documented at every 2-foot spectral gamma-ray station. Samples were collected every 10 feet and packaged into 30-foot composite samples for microscope analysis. These lithologic data, along with the spectral gamma-ray data were then logged in five-foot intervals using mudlogging software (Plate 1). The log was generated using a combination of the field-documented lithology and laboratory reflected-light microscope analysis. Microscope analysis allowed for more accurate determination of physical and chemical rock properties such as: color, hardness, luster, texture, carbonate content and composition of visible grains. Lithology, detailed sample descriptions, member contacts, and total and spectral gamma ray data are documented in detail in Plate 1 (i.e., the mudlog).

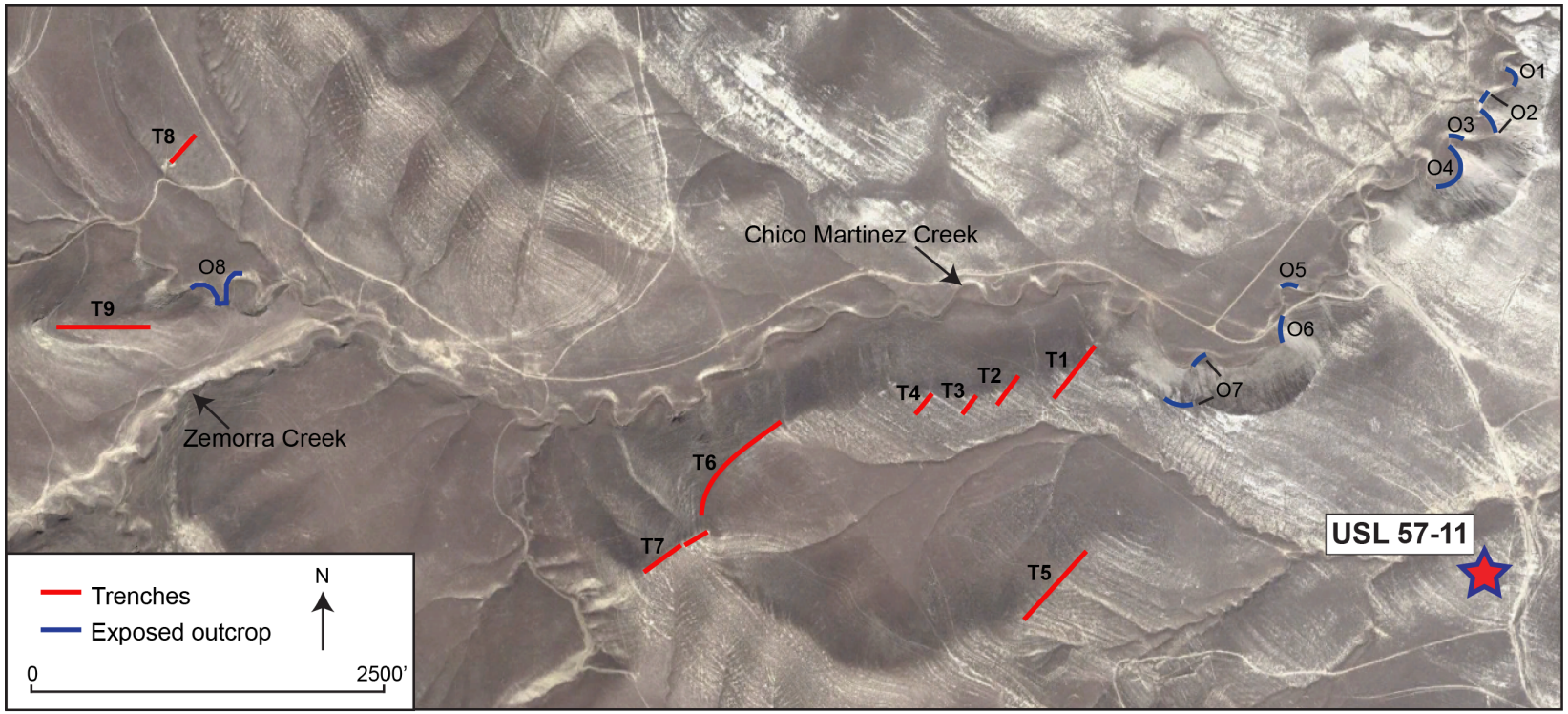

FIGURE 14. USL 57-11 (red star) location map.

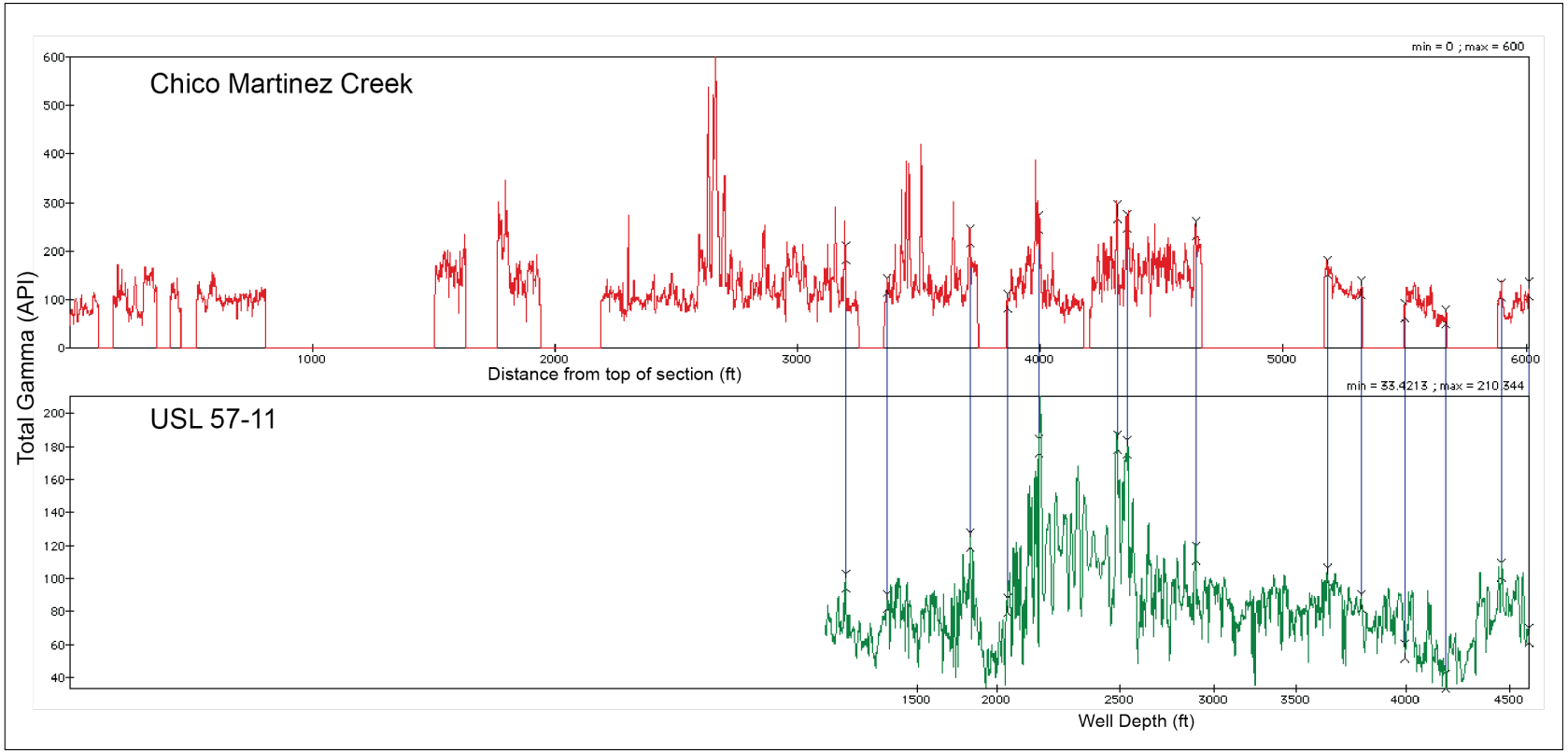

FIGURE 15. USL 57-11 correlation to the Chico Martinez Creek section.

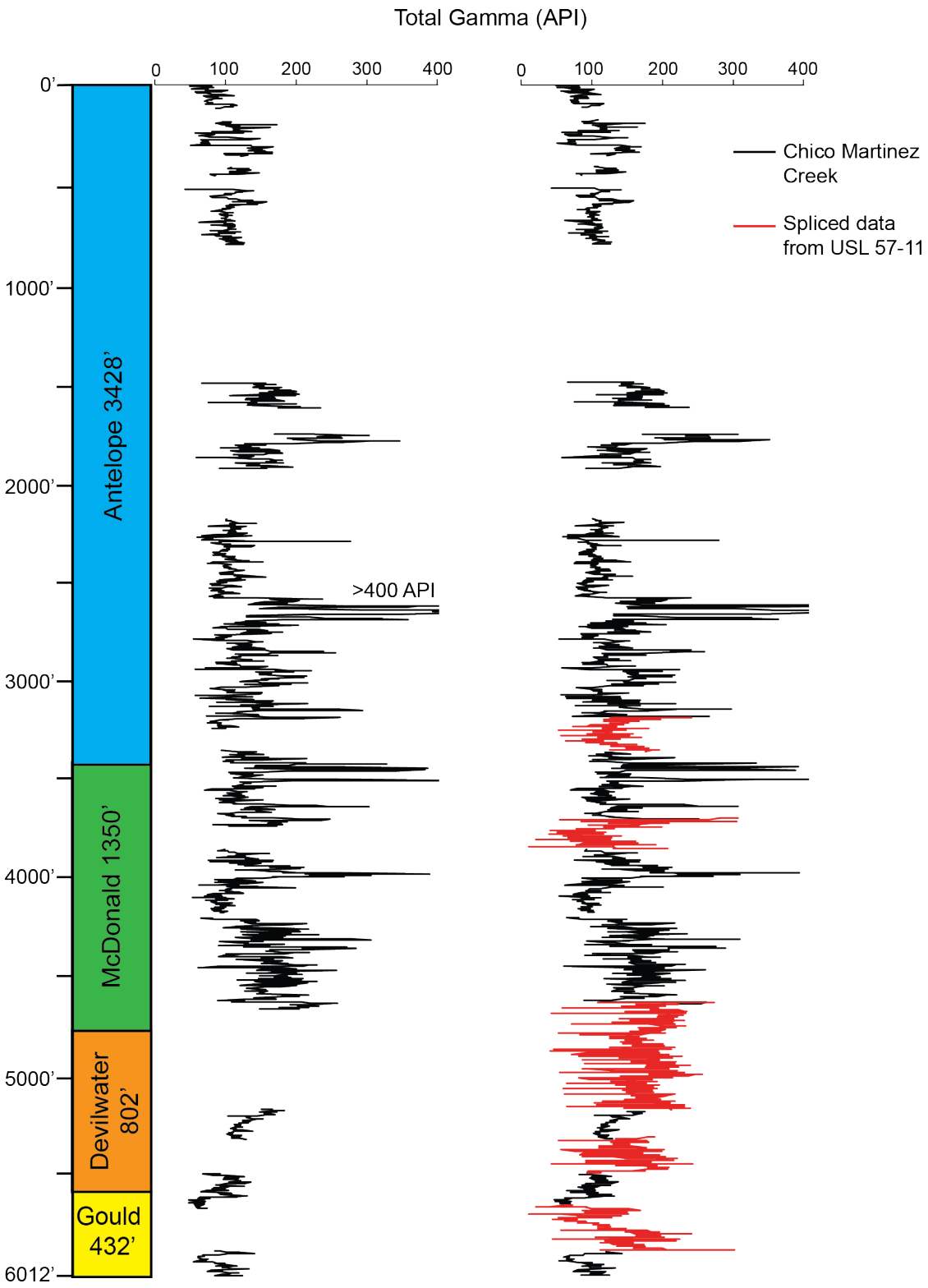

FIGURE 16. Total gamma-ray curve before (left) and after (right) splicing data from USL 57-11.

Integration of Biostratigraphy Data

Key biostratigraphic horizons were integrated into the measured trench and outcrop sections from the proprietary Unocal (Heitman, 1986) and Shell Oil (Bell, 1937) studies. The Unocal study provided biostratigraphic data for calcareous nanofossils, diatoms and benthic foraminifera; the Shell study provided biostratigraphic data for benthic foraminifera. The disparity in data between these two studies can be attributed to their different vintages because it wasn't until the 1970s and 1980s that published research made coccolith and diatom biostratigraphy a reliable tool for correlation. Numerical dates for the biostratigraphic horizons are taken from Barron and Isaacs (2001).

Paleomagnetic Core Collection and Processing

Paleomagnetic cores were collected from 33 unaltered dolostone beds in the McDonald Shale member of the Monterey Formation in order to obtain additional age control in this poorly dated section. The cores were acquired from prominent dolostones exposed along the creek and northern ridge by Jonathan Guillaume using a gasoline powered diamond-tipped drill (fig. 17). He later analyzed the cores at Occidental College Paleomagnetism Lab facilities using a 2G Cryogenic Magnetometer. The cores were oriented during collection in the field using a nonmagnetic orienting sleeve and the *in situ* bedding attitude was measured and used to calculate tilt-corrected directions. The sampled dolostones were later tied into the trenched intervals by stratigraphic correlation. A stratigraphic column was generated for both the creek-ridge and trenched sections from the base of the McDonald Shale, and dolostones were correlated based on similar stratigraphic distance from this contact.

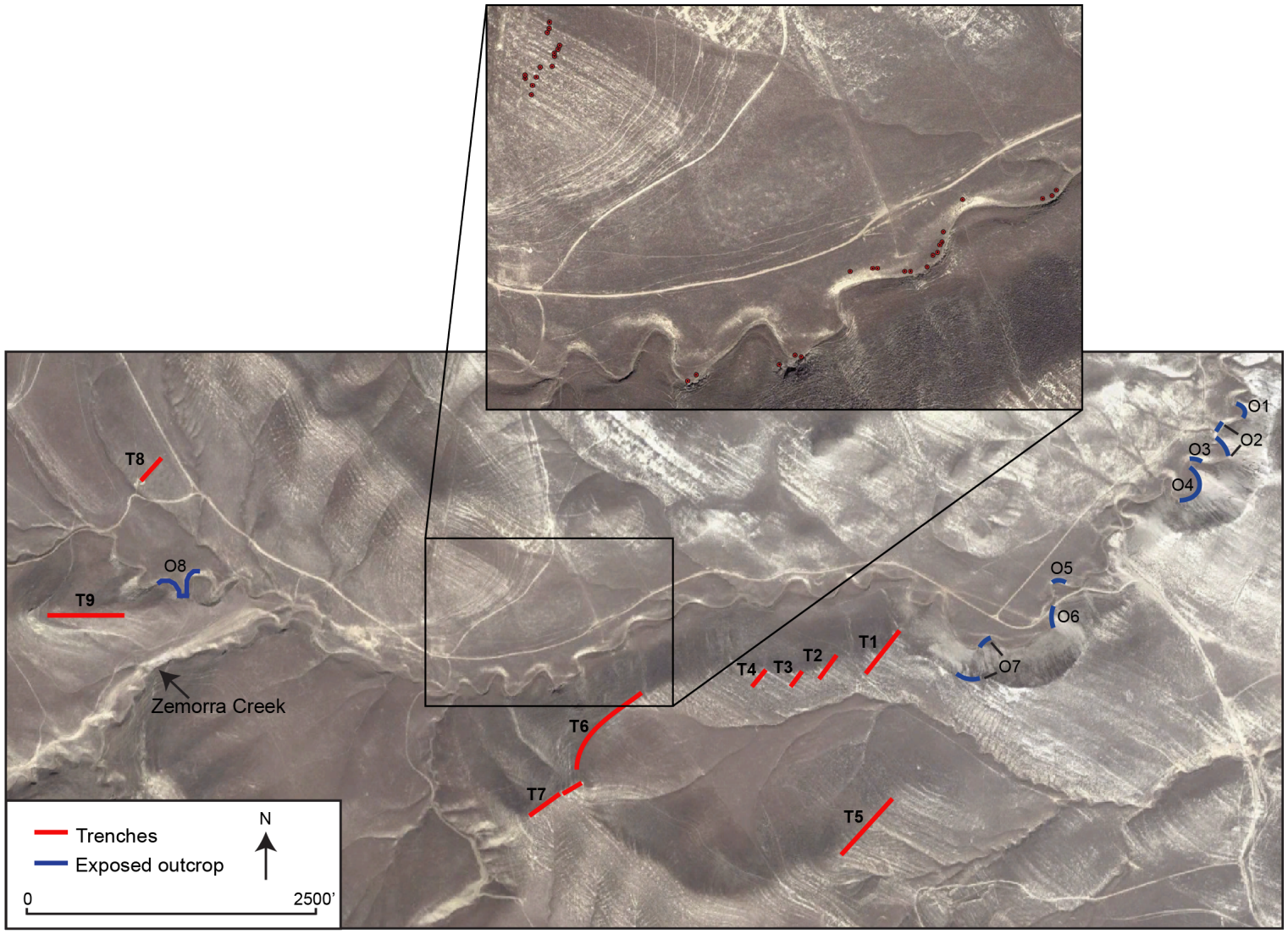

FIGURE 17. Dolostone core sample locations along the creek and northern hill.

X-ray Diffraction and Fourier Transform Infrared Spectroscopy

A Rigaku MiniFlex X-ray diffractometer and PANalytical X'Pert Highscore Plus software were used to identify the mineralogic composition of 10 discrete samples. Based on peak position and intensity, the presence of minerals was qualitatively assessed as either a major or minor component. Bruker Alpha Diamond Attenuated Total Reflection device was used for FTIR analysis, and Bruker's Opus software was used for data interpretation. FTIR was used to quantitatively detect the presence of minerals not easily detected or quantified using XRD, specifically clays.

Total Organic Carbon (TOC)

An average Total Organic Carbon (TOC) value was calculated for the Gould, Devilwater, McDonald and Antelope Shale members using the following formula: TOC (weight %) = 0.75× U (ppm) - 3.63. This formula was generated by Schwalbach and Bohacs (1996) based on based on graphic correlation of empirical TOC (weight %) and uranium (ppm) data from Naples Beach, California.

Subsurface Correlation

The total gamma-ray profile from CMC was correlated to two wells: 51X-33 ST, located 4.5 miles to the northeast, and Bacon #1, located 3.5 miles due north, in order to assess variation in stratigraphic thickness (Fig. 18). These locations were chosen as tie points because they likely lie within the same paleodepocenter as the CMC section, and the stratigraphic thicknesses in the wells have not been structurally compromised. 51X-33ST was converted to true stratigraphic thickness (TST) by incorporating directional survey and dipmeter data in the following formula: $TST = MT \times (\cos\psi - \sin\psi \times \cos\alpha \tan\phi) \times \cos\phi$, where MT is measured thickness, ψ is borehole inclination from vertical, α

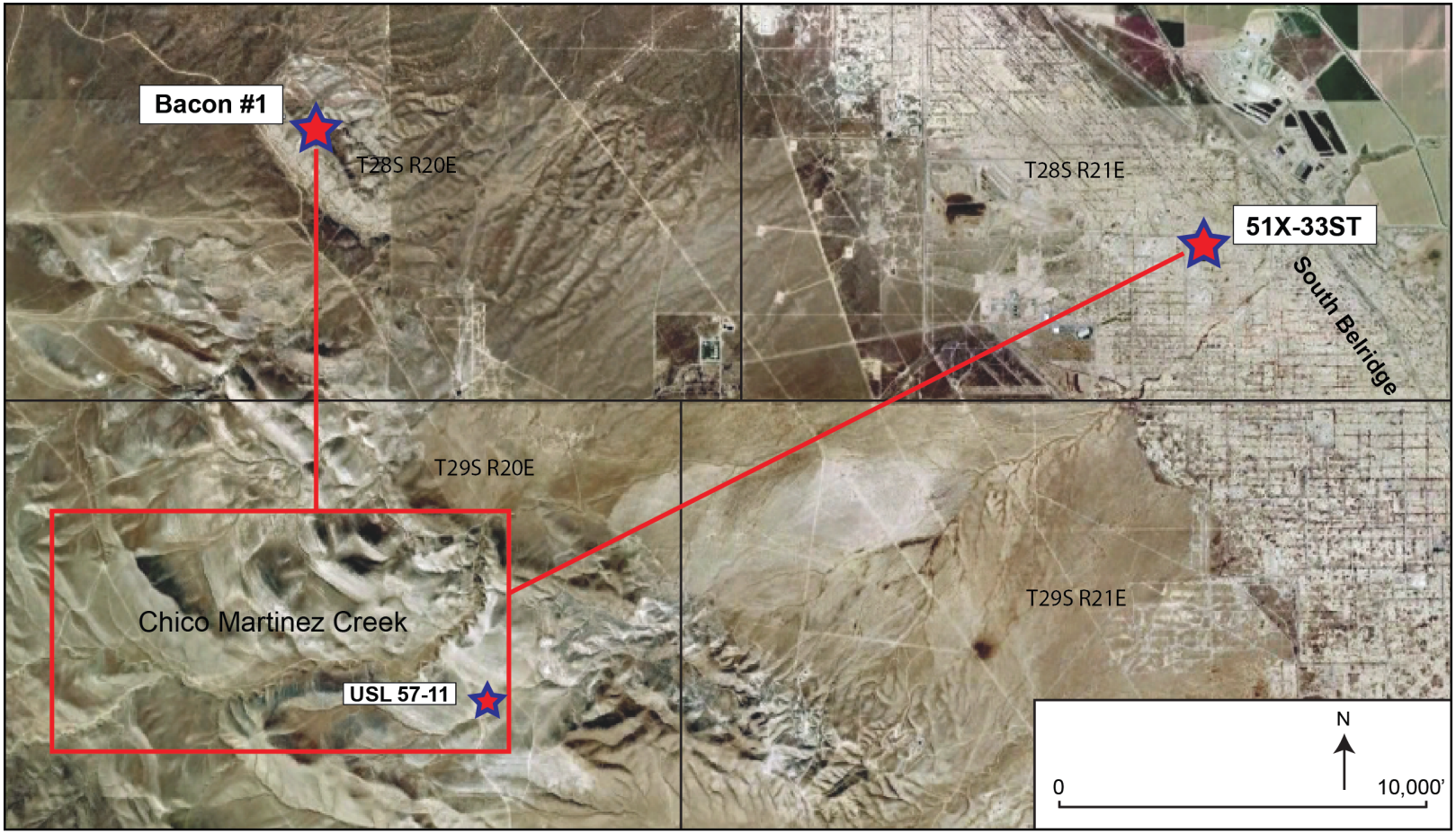

FIGURE 18. Location of 51X-33ST and Bacon #1 with respect to Chico Martinez Creek.

is the dip azimuth minus the borehole azimuth, and ϕ is the dip (Tearpock and Bischke, 1991). No dipmeter or directional survey data were available for Bacon #1, however, this well is considered to be a relatively vertical hole with a regional dip of 40 degrees (pers. commu. Aera Energy).

CHAPTER 3

RESULTS

Based on a detailed lithostratigraphic investigation of the CMC section using a combination of field and microscope analysis, XRD (x-ray diffraction) and FTIR (Fourier transform infrared spectroscopy), and spectral gamma-ray data, the Monterey Formation has been subdivided into 7 distinctive lithofacies. In ascending order, these are calcareous porcelanite, calcareous silty claystone, phosphatic shale, calcareous siliceous shale, siliceous shale, arkosic sandstone, and porcelanite and chert. These distinctive lithofacies are briefly described in this section; detailed descriptions are in Plate 1 (i.e., the mudlog). Linear sediment accumulation rates were determined based on 5 biostratigraphic horizons and 6 paleomagnetic ages. Finally, subsurface correlations were made using the total gramma-ray profile from CMC to 51X-33 ST, located 4.5 miles to the northeast and Bacon #1, located 3.5 miles to the north.

Lithostratigraphic Characterization

Gould Shale

The Gould Shale member of the Monterey Formation is estimated to be 432 feet thick with approximately 208 feet covered (52 % exposure). Its contact with the underlying Buttonbed Sandstone member of the Temblor Formation is sharp and marks an abrupt change from clastic to hemipelagic facies (figs. 19 and 20, Plate 1). The Gould Shale consists predominantly of calcareous shale and mudstone, but is distinguished from

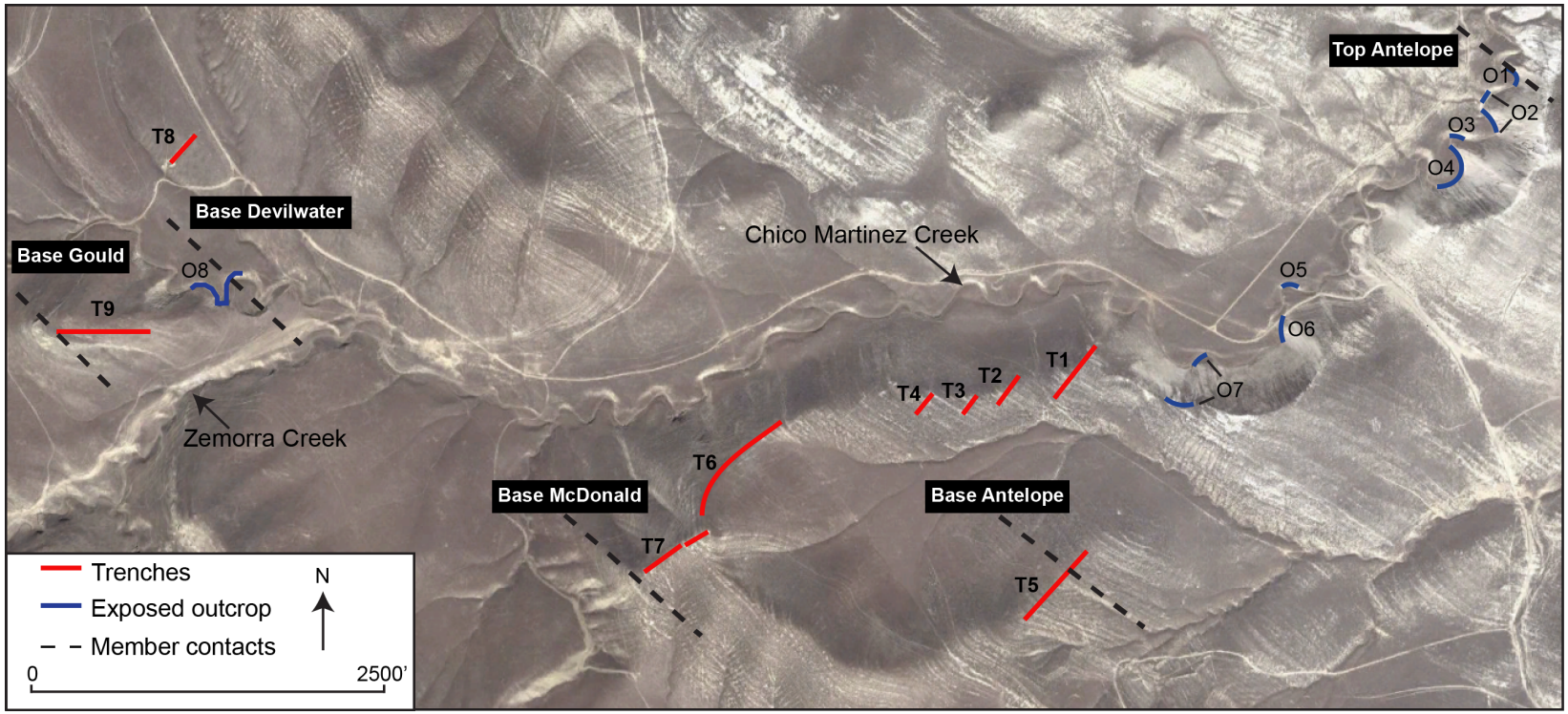

FIGURE 19. Member contact locations.

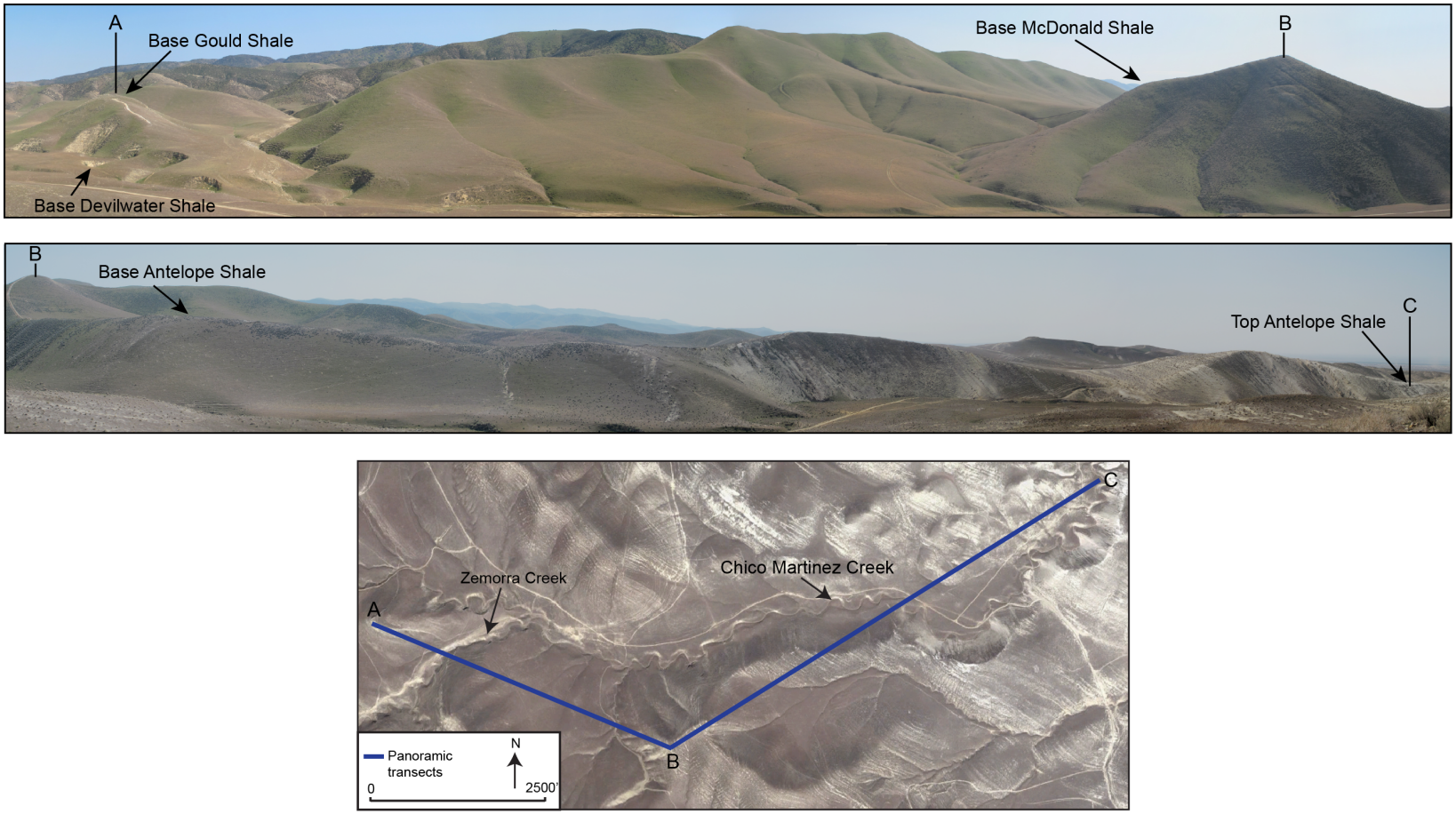

FIGURE 20. Panoramic view of the Chico Martinez Creek section from west (A) to east (B). Top: panoramic images of the Monterey Formation at Chico Martinez Creek trending from the base of the section (A-B) to the top of the section (B-C). Bottom: satelite image illustrating transects along which panoramic photos were captured.

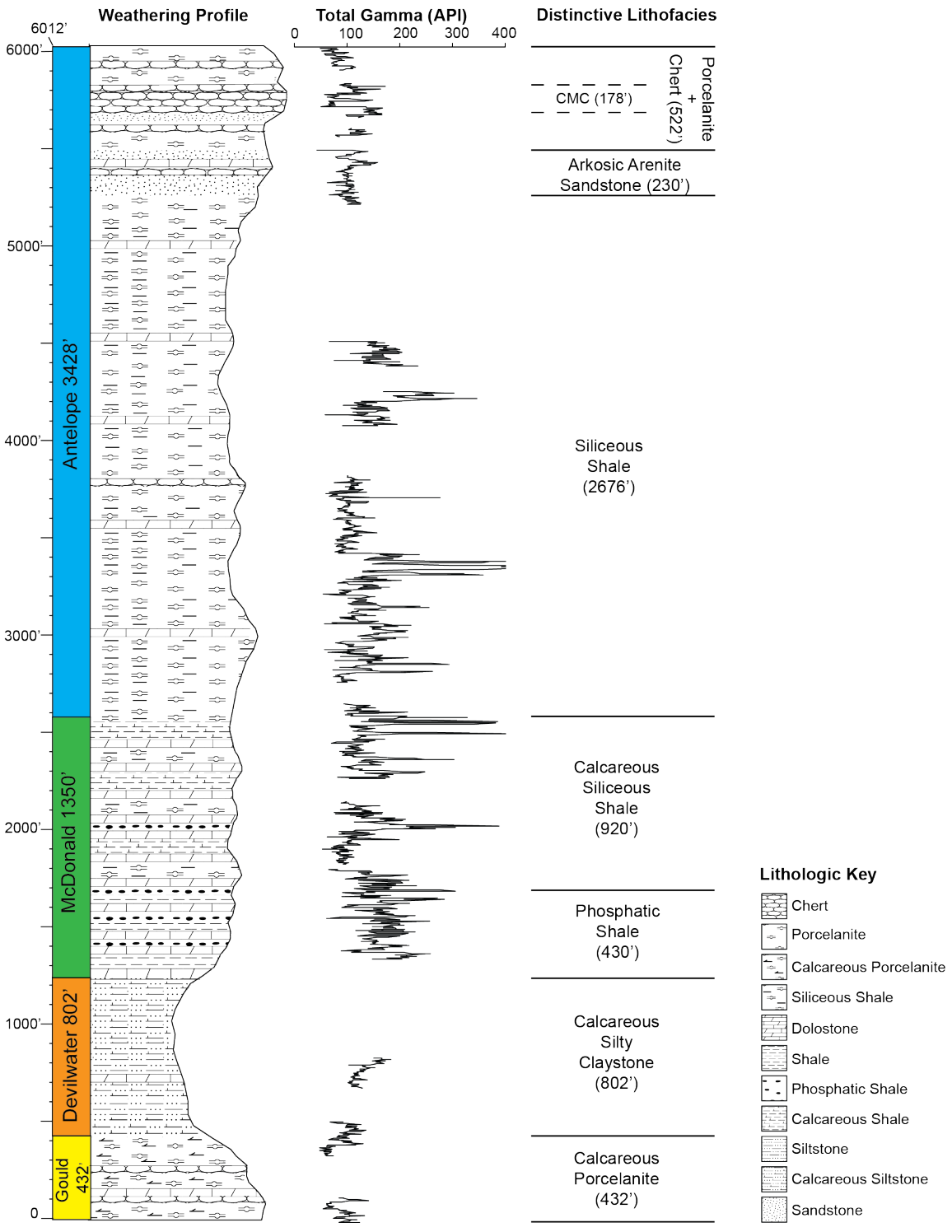

FIGURE 21. Generalized lithologic weathering profile with total gamma ray profile and distinctive lithofacies at Chico Martinez Creek. Number-designated arrows are the stratigraphic locations for the 10 XRD and FTIR samples

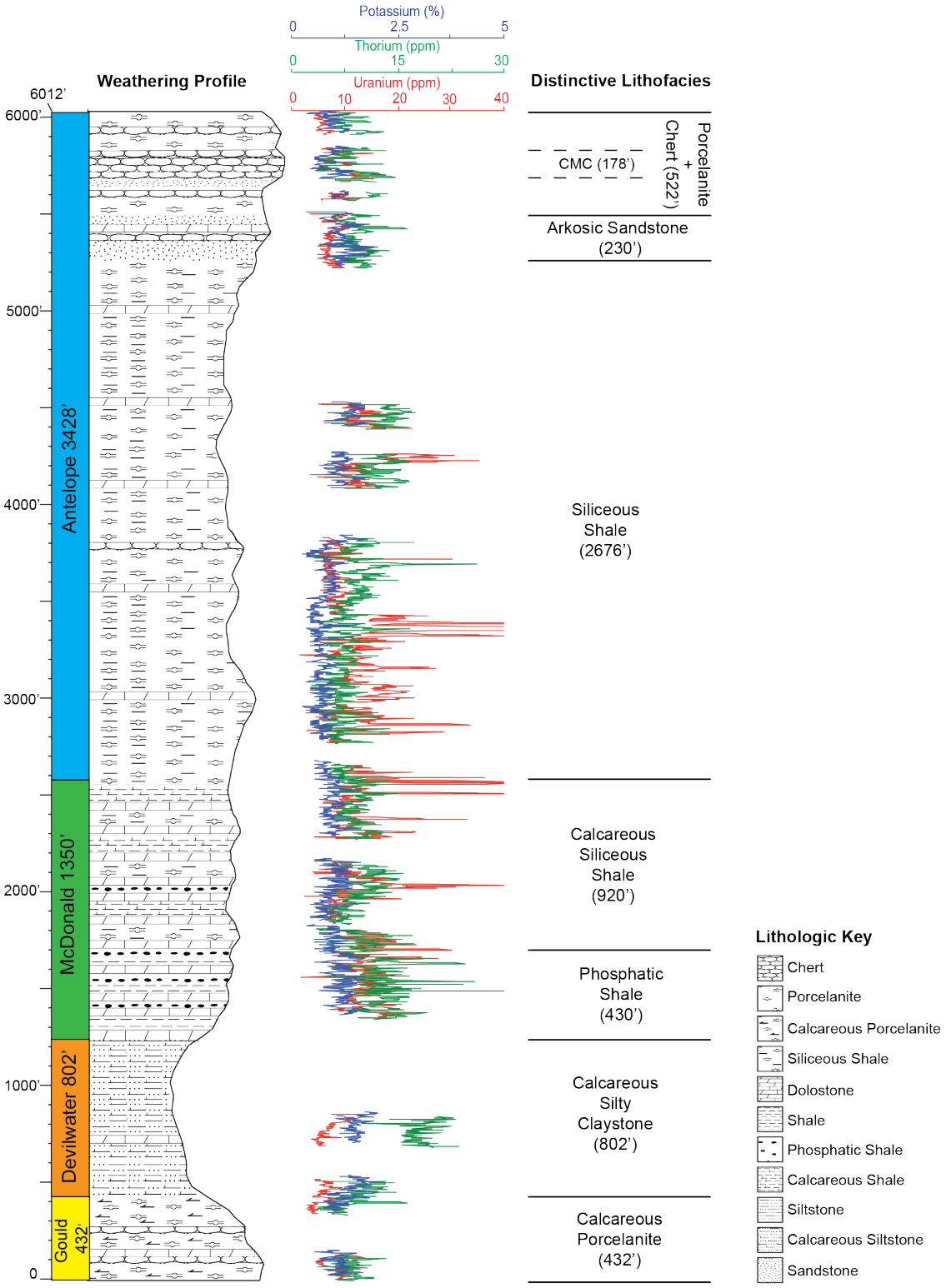

FIGURE 22. Generalized lithologic weathering profile with spectral gamma ray profile including uranium (ppm), thorium (ppm) and potassium (%) and the distinctive lithofacies at Chico Martinez Creek.

the other Monterey Formation members by the abundance of calcareous porcelanite (figs. 21 and 22). This member is highly calcareous overall with abundant microfossil molds. Although also siliceous, the section alternates between thin-bedded, clay-rich intervals and thin to medium-bedded, siliceous zones with local highly fractured chert beds (fig. 23). Siliceous, one to two-foot-thick dolostone beds are common throughout the section. Based on XRD and FTIR analysis, the porcelanite is quartz phase (Table 1). Average uranium, thorium, potassium and total gamma-ray values are 7.0 (ppm), 5.1 (ppm), 1.1 (%) and 81.9 API, respectively (Table 2), and the average calculated TOC (weight %) for this member is 1.3.

FIGURE 23. Typical Gould Shale lithofacies. Thicker blocky calcareous porcelanite beds interbedded with less competent siliceous shale.

Devilwater Shale

The Devilwater Shale member of the Monterey Formation is estimated to be 802 feet thick with approximately 560 feet covered (30 % exposure). Its contact with the underlying Gould Shale is transitional and is defined by a shift from dense dark yellowish-orange siliceous strata to light bluish-gray silty shale (figs. 21, 22 and 24, Plate 1). Overall there is an increase in clastic detritus in this interval, which is dominantly silty, becoming slightly sandy locally. A shift in rock competency due to the decrease in silica content is expressed in the geomorphology of the landscape, which abruptly changes from hilly to highly eroded flat topography (fig. 20). The base of the Devilwater Shale is composed of calcareous silty claystone with an increase in clay content up

FIGURE 24. Typical calcareous silty claystone lithofacies. Note blocky to conchoidal fracture pattern without distinct bedding.

TABLE 1. Composition of Spot Samples within Lithologic Intervals Based on XRD (X-ray diffraction) and FTIR (Fourier transform infrared spectroscopy) Analysis.

Lithofacies (sample depth)	Composition	Interpretation
Chert and Porcelanite (5732')	Major: tridymite and cristobalite	Opal-CT chert and porcelanite
Arkosic Arenite (5302')	Major: detrital quartz Minor: anorthite, microcline, illite, tridymite and cristobalite	Opal-CT porcelanite with sandstone lenses. Sandstone is a arkosic arenite with an illite clay matrix
Siliceous Shale (4202', 3412', 2852', 2552')	Major: tridymite and cristobalite Minor: quartz, minor illite content at 2852' and 2552'	Opal-CT siliceous shale with minor detrital quartz grains
Calcareous Siliceous Shale (2142')	Major: quartz Minor: tridymite, cristobalite and illite	Mostly quartz phase siliceous shale with illite clays. Minor opal-CT siliceous shale.
Phosphatic Shale (1352')	Major: quartz Minor: illite	Mostly quartz phase siliceous shale with illitic clays
Calcareous Silty Shale (722')	Major: illite Minor: muscovite and quartz	Illite-rich claystone with minor detrital quartz and muscovite
Calcareous Porcelanite (52')	Major: quartz	Quartz porcelanite

TABLE 2. Average Uranium, Thorium, Potassium and Total Gamma-ray Values in Distinct Lithologic Intervals

Lithofacies	Average Uranium (ppm)	Average Thorium (ppm)	Average Potassium (%)	Average Total Gamma (API)
Porcelanite and Chert	7.8	5.5	0.9	99.9
Arkosic Arenite	7.5	6.1	1.2	102.9
Siliceous Shale	12.9	5.9	0.8	140.2
Calcareous Siliceous Shale	12.5	6.2	0.9	139.7
Phosphatic Shale	14.3	8.9	1.2	169.0
Calcareous Silty Claystone	6.6	10.4	1.5	118.5
Calcareous Porcelanite	6.7	5.2	1.1	81.9

section. The claystone alternates between non-calcareous and highly calcareous intervals, but the overall lithology of is fairly homogenous. One to two-foot-thick dolostone beds are common at the base of the section, becoming less common towards the top. XRD and FTIR analysis indicate mostly illite, with minor detrital quartz and muscovite (Table 1). Average uranium, thorium, potassium and total gamma-ray values are 6.6 (ppm), 10.4 (ppm), 1.5 (%) and 118.5, respectively (Table 2), and the average calculated TOC (weight %) for this member is 1.3.

McDonald Shale

The McDonald Shale member of the Monterey Formation is estimated to be 1350 feet thick with approximately 228 feet covered (83 % exposure), making it the most completely described section in CMC. Its contact with the underlying Devilwater Shale is transitional and is defined by a shift from silty claystone to phosphatic shale (figs. 21 and 22, Plate 1). The contact is easily identified in the field by an abrupt change in slope from an eroded ravine to highly resistant ridge (fig. 20). The shift from light green to dark green vegetation also defines this boundary. The McDonald Shale is subdivided into two intervals based on distinctive lithology: the lower phosphatic shale and the upper calcareous siliceous shale (figs. 21 and 22). The average calculated TOC (weight %) for this member is 6.1, the highest in the CMC section.

Phosphatic shale lithofacies. This 430-foot interval is organic-rich with abundant carbonate-fluorapatite nodules. Nodules range in size from small mm-scale white irregular blebs along bedding planes to large cm-scale pinkish-white features (fig. 25). This interval is characteristically darker in color and more dense than the overlying unit in the McDonald which is characteristically more siliceous. Evenly spaced, almost

cyclic, one to two-foot-thick dolostone beds occur throughout this section. XRD and FTIR analysis indicate quartz phase siliceous shale with an illitic clay (Table 1), a common intercalated lithology. Average uranium, thorium, potassium and total gamma-ray values are 14.3 (ppm), 8.9 (ppm), 1.2 (%) and 169.0 API, respectively (Table 2).

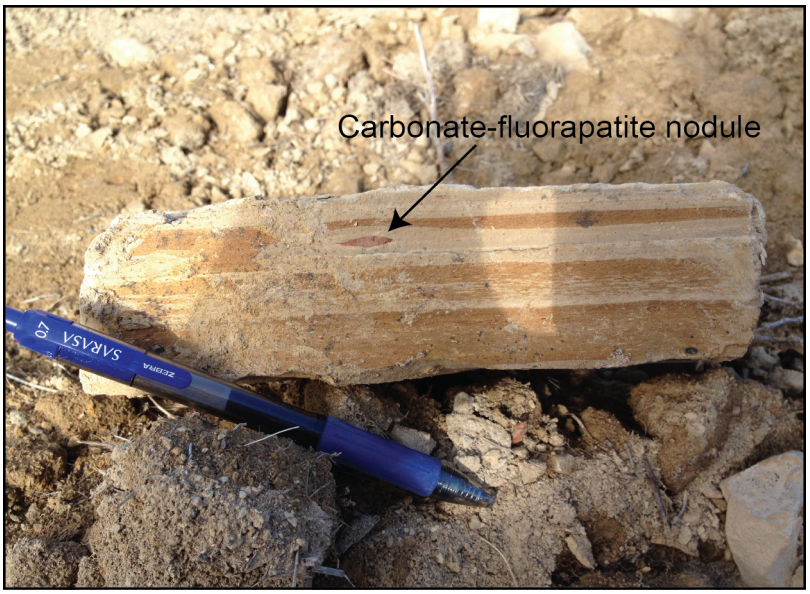

FIGURE 25. Typical phosphatic shale lithofacies.

Calcareous siliceous shale lithofacies. The upper 920 feet of the McDonald Shale member is defined by a transition from dark yellowish-brown phosphatic shale to light yellowish brown calcareous-siliceous shale with a distinct increase in silica content. This section alternates between calcareous-siliceous shale and non-calcareous siliceous shale at a scale of 1 inch to several feet, with discrete laminations being distinctly more calcareous in some intervals. Microfossil molds are easily visible with a hand lens in calcareous intervals. In comparison to the lower phosphatic lithofacies, dolostone beds are less frequent. This interval becomes increasingly siliceous towards the top with

common 1-inch porcelanite beds becoming more abundant, ultimately grading at its top into the Antelope Shale. Average uranium, thorium, potassium and total gamma ray values are 12.5 (ppm), 6.2 (ppm), 0.9 (%) and 139.7 API, respectively (Table 2).

Antelope Shale

The Antelope Shale member of the Monterey Formation is estimated to be 3428 feet thick with approximately 1310 feet covered (62 % exposure). Its contact with the underlying McDonald Shale is very gradational and is defined by a gradual shift to increasingly siliceous facies over approximately 900 feet. The contact was placed 2586 feet from the base of the section in conjunction with an abrupt increase in uranium values (figs. 21 and 22) that also marks the top of the organic-rich McDonald Shale in the subsurface gamma-ray profile from 51X-33 ST and Bacon #1 wells. Gaps in data could not be filled from the nearby well USL 57-11 (figs. 14 and 16) for the majority of the Antelope Shale because the well did not penetrate this upper interval. The Antelope Shale is subdivided into three stratigraphic intervals based on distinctive lithofacies: lower siliceous shale, middle arkosic sandstone and upper porcelanite and chert (figs. 21 and 22). The average calculated TOC (weight %) for this member is 5.0.

Siliceous shale lithofacies. This lower 2676-foot interval of the Antelope Shale is predominantly composed of siliceous shale and is fairly homogenous throughout the section with limited and very localized porcelanite beds and rare cherty intervals (fig. 26). It is the thickest distinctive lithofacies in the entire CMC succession (figs. 21 and 22). The siliceous shale facies is overall lighter in color than the lower McDonald Shale, varying from dark yellowish brown to pale yellowish brown. Across this 900-foot transition zone, there is also an apparent decrease in bulk density likely associated with

FIGURE 26. Typical siliceous shale lithofacies.

increased porosity or a change in bulk silica phase. This interval is generally non-calcareous, becoming only slightly calcareous in limited strata. The section alternates from light-colored, highly siliceous shale (almost porcelanite) to darker, detrital-rich siliceous shale. Dolostone beds are less common in this section than in the underlying McDonald Shale, averaging approximately 1 bed every 50 to 100 feet. XRD and FTIR indicate opal-CT phase siliceous shale with minor detrital quartz grains and greater illite clay content lower in the section (Table12). Average uranium, thorium, potassium and total gamma ray values are 12.9 (ppm), 5.9 (ppm), 0.9 (%) and 140.2 API, respectively (Table 2).

Arkosic sandstone. This upper 230-foot interval is characterized by an abundance of thin arkosic sandstone beds and laminations, and is the coarsest clastic-rich interval in

CMC. Although the most characteristic feature, the sandstone comprises only about 20% of the interval, and it is intercalated with the predominant lithologies – siliceous shale and porcelanite. The section alternates between 6 to 8-inch siliceous shale beds, 1 to 3-inch porcelanite beds and very localized 1 to 2-inch chert beds. Sandstone is present as both 1 to 2-inch thick continuous thin beds and ½-inch thick (cm-scale) continuous laminations and is mostly composed of quartz and feldspar with minor muscovite and undifferentiated lithic grains (fig. 27). Individual sand grains are predominantly fine to very fine-grained, and are subangular to subrounded. The sandstones are typically moderately sorted and are grain-supported. Sandstones typically have point and long grain contacts and are only lightly compacted and easily friable. Based on XRD and FTIR analysis, the fine-grained

FIGURE 27. Typical arkosic arenite sandstone lithofacies. Photo on the left illustrates a discontinuous sandstone lens; the photo on the right illustrates a thin planar bed of sandstone between siliceous shale.

components of this lithofacies are composed of opal- CT phase porcelanite and mudrocks, and sandstone is mostly composed of quartz and feldspar with a minor illite clay matrix (Table 1). Average uranium, thorium, potassium and total gamma-ray values are 7.5(ppm), 6.1 (ppm), 1.2 (%), and 102.9 API respectively (Table 2).

Porcelanite and chert. This upper 522-foot interval is characterized by a high silica content and is dominantly composed of chert and porcelanite. A interval 178 feet thick is especially chert-rich, and was referred to as the Chico Martinez Cherts (CMC) by Foss and Blaisdell (1968), Dibblee (1973), Graham and Williams (1985), and Heitman (1986) (figs. 21 and 22). Individual chert beds are 1 to 6 inches thick and are interbedded with less fractured porcelanite and shale (fig. 28). Sandstone and siltstone lenses are relatively rare, and dolostones are mostly present as discontinuous nodules and beds.

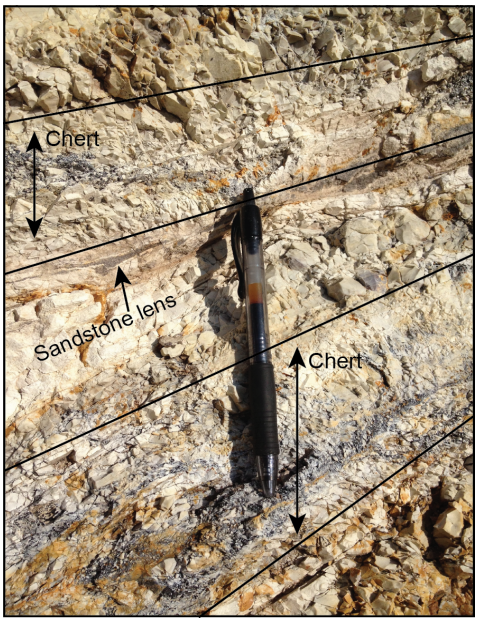

FIGURE 28. Typical porcelanite and chert lithofacies. Note the presence of highly fractured cherts interbedded with more massive porcelanite beds.

XRD and FTIR analysis indicates that the cherts and porcelanites are composed of opal-CT phase silica (Table 1). Average uranium, thorium, potassium and total gamma-ray values are 6.7 (ppm), 5.2 (ppm), 1.1 (%), and 81.9 API, respectively (Table 2).

Chronostratigraphy

Biostratigraphic Ages

Benthic foraminifera are prolific in the lower Gould, Devilwater and McDonald Shale members, and siliceous diatoms are sporadically preserved in the upper Antelope Shale member (Heitman, 1986) with most having been destroyed by burial diagenesis. In addition, calcareous nanofossils occur sporadically through the lower calcareous Gould and Devilwater Shales, but they yield inadequate biostratigraphic control (Heitman, 1986). On the basis of benthic foraminiferal and diatom biostratigraphy from the Unocal (Heitman, 1986) and Shell (Bell, 1937) studies, four distinct biostratigraphic horizons, A, B, C and D, were identified in the CMC section (fig. 29). Biostratigraphic intervals are based on the siliceous diatom zones of Barron (1981a, 1981b) and benthic foraminiferal stages of Kleinpell (1938), and numerical ages were assigned ages based on Barron and Isaacs (2001) chronostratigraphic framework (fig. 30).

Both the Unocal and Shell studies were unable to provide age control for the base of the Monterey; therefore, an age of 16 Ma is assigned based on the literature (Scheirer Magoon, 2007). This age was derived from Foss and Blaisdell's 1968 study in which Relizian foraminifers of the *Siphogenerina branneri* zone were reported in the Gould Shale. According to Bartow (1992), this zone is equivalent to the lower to middle part of the N8 planktonic foraminiferal zone (16.5 to 15.5 Ma). Thus the base of the Monterey is assigned an approximate age of 16 Ma.

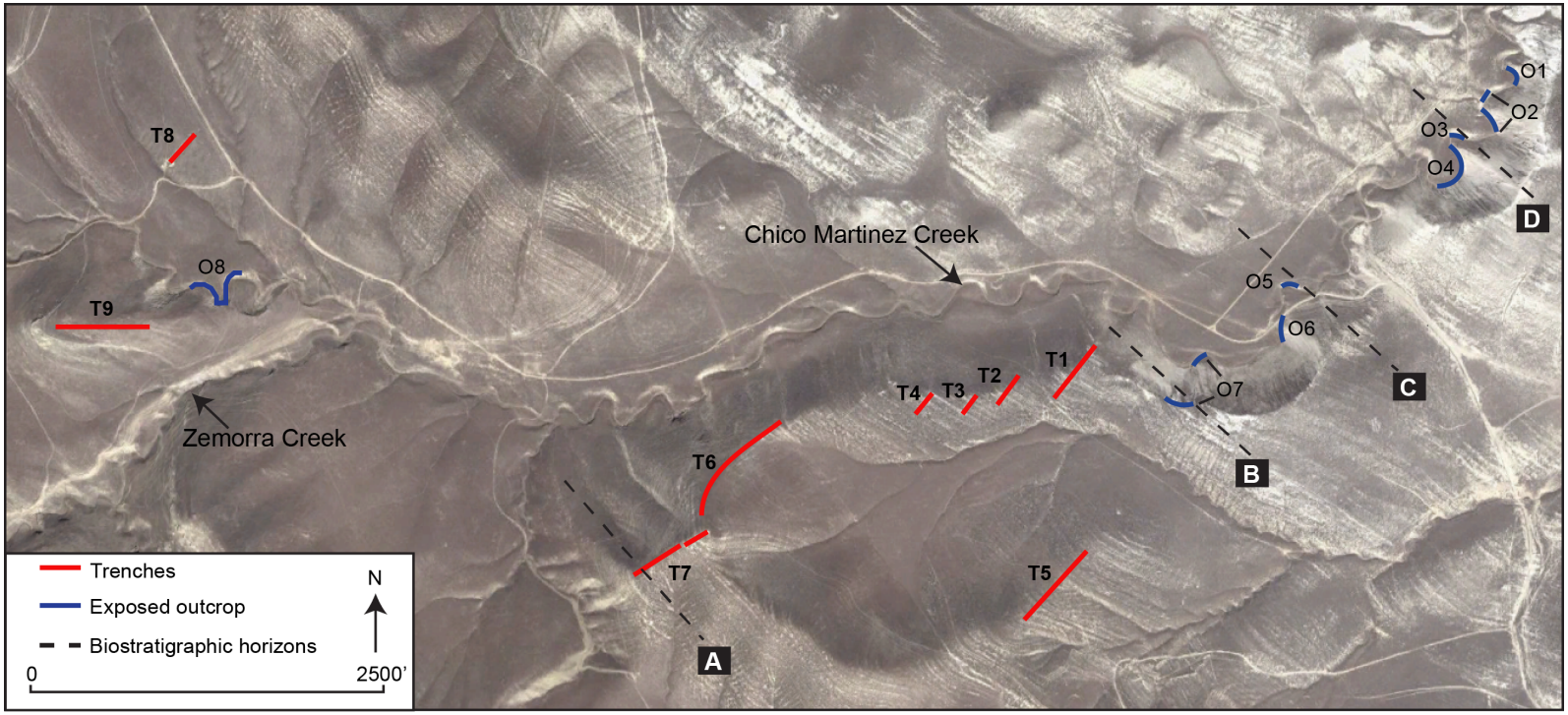

FIGURE 29. Location of biostratigraphic horizons tied into the section from previous studies conducted by Shell (1937) and Unocal (1986). A = Top Mohnian, B = Denticulopsis hustedtii-Denticulposis lauta (c), C = Denticulopsis hustedtii-Denticulposis lauta (d) and D = Denticulopsis hustedtii.

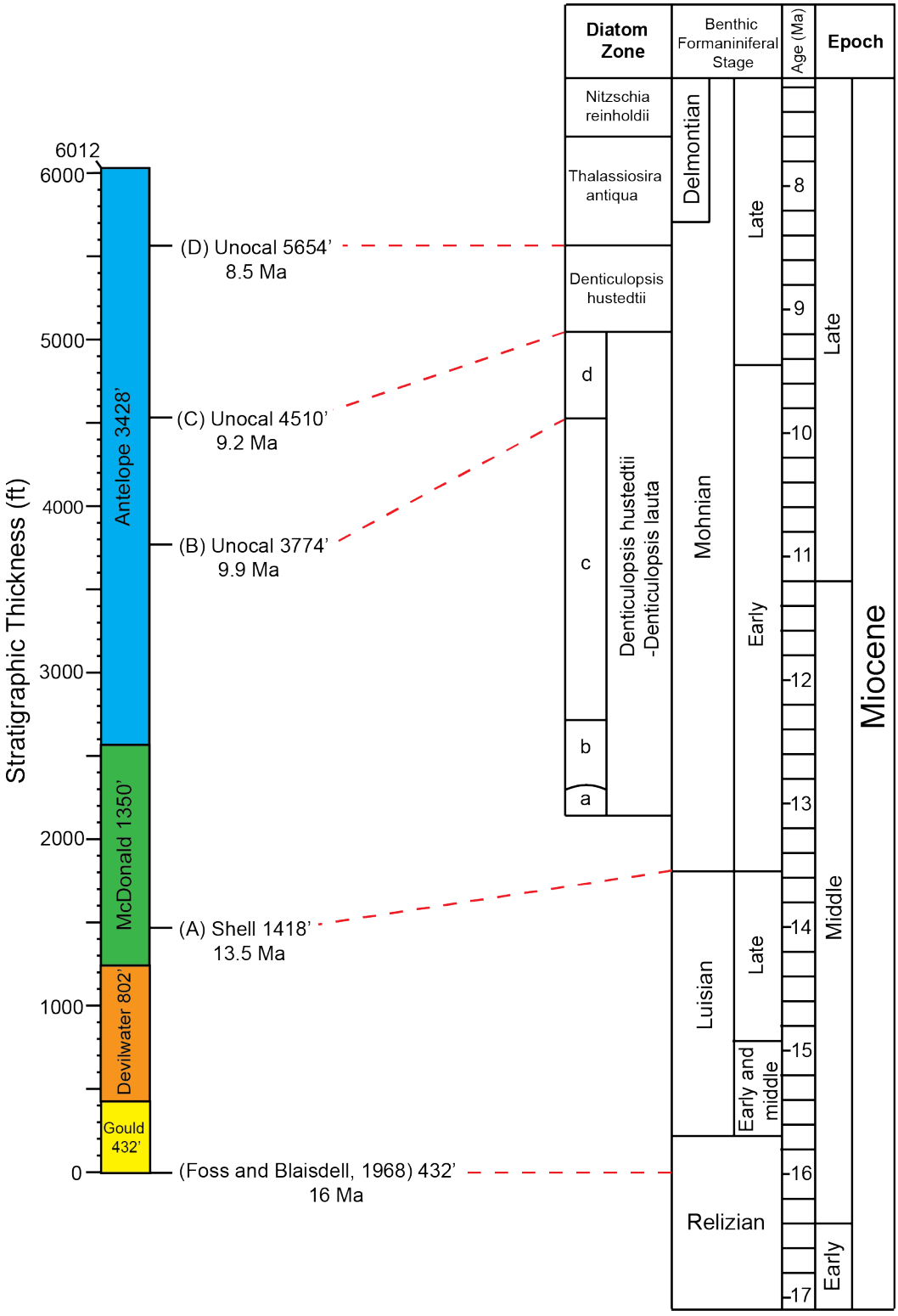

FIGURE 30. Correlation of biostratigraphic datums identified in the Chico Martinez Creek section with ages of zones from Barron and Isaacs (2001).

The following 4 horizons mark the top of formaniferal stages and diatom zones and thus provide the youngest ages of these zones. Horizon A marks the Mohnian-Luisian Stage boundary and is the most clearly defined benthic forminiferal horizon in the CMC section with a large abundance of diverse species in the Gould Shale member followed by an abrupt extinction of many species in the lower McDonald Shale (fig. 29). This horizon is clearly identified in the studies conducted by Unocal and Shell, but the Shell horizon was most easily integrated into this study because it was identified in the area of the re-excavated trenches. The Mohnian-Luisian boundary was placed 1418 feet from the base of the section, just above the base of the McDonald Shale and is assigned an age of 13.5 Ma (fig. 30).

Horizons B, C and D are boundaries of diatom zones identified by Unocal (Heitman, 1986) and were directly integrated into the section measured along the creek (Fig. 25). The top of diatom zones *Denticulopsis hustedtii-Denticulposis lauta* (c), *Denticulopsis hustedtii-Denticulposis lauta* (d) and *Denticulopsis hustedtii* were placed 3774, 4510 and 5254 feet from the base of the section and assigned ages of 9.9, 9.2 and 8.5 Ma, respectively (fig. 30). No age was determined for the top of the Monterey due to the lack of biostratigraphic control. This inability to assign an age to the top of the Antelope is a common problem in the San Joaquin basin where diagenetic alteration of diatoms makes microfossil identification nearly impossible (Graham and Williams, 1985). This is further complicated by the time-trangressive nature of the top of the Antelope, which varies significantly in age from one part of the basin to another (Graham and Williams, 1985). According to Scheirer and Magoon (2007), the top of the Antelope can be generally placed at 6.5 Ma in the San Joaquin basin; however, the 8.5 Ma datum

(Horizon A) positioned only 358 feet below the top of the section suggests the top of the Antelope is likely closer to 8 Ma at CMC.

Paleomagnetic Ages

Of the 33 dolostone beds drilled in the McDonald Shale, 18 were determined to retain normal polarity, 9 reversed polarity, and 6 were indeterminate (fig. 31). Biostratigraphic horizon A (defined by the Luisian-Mohnian benthic stage boundary) and horizon B (defined by the top of diatom zone *Denticulopsis hustedtii-Denticulopsis lauta* subzone c) were used to provide age control for these paleomagnetic reversals. To a major extent, paleomagnetic age assignment is highly interpretive because long gaps in time are not accounted for between dolostone samples and data resolution is limited to the presence and frequency of dolostone beds. Conservative age estimates that assumed relatively constant sedimentation rates were used to assign dolostones to normal and reversed polarity intervals within chrons. This is demonstrated in Figure 31 by the approximately equivalent slope of the lines that tie the dolostones to the geologic timescale.

Sediment Accumulation Rates

Linear sediment accumulation rates were calculated as the slope between biostratigraphic and magnetostratigraphic datums (fig. 32). The Gould and Devilwater Shales are constrained by only two datums, which yield a combined sedimentation rate of approximately 585 ft/Myr (178 m/Myr). On average, the sediment accumulation rate in the McDonald Shale is 335 ft/Myr (102 m/Myr), nearly half the rate of the underlying section. The sediment accumulation rate in the Antelope Shale is by far the greatest at approximately 1900 ft/Myr (579 m/Myr), on average.

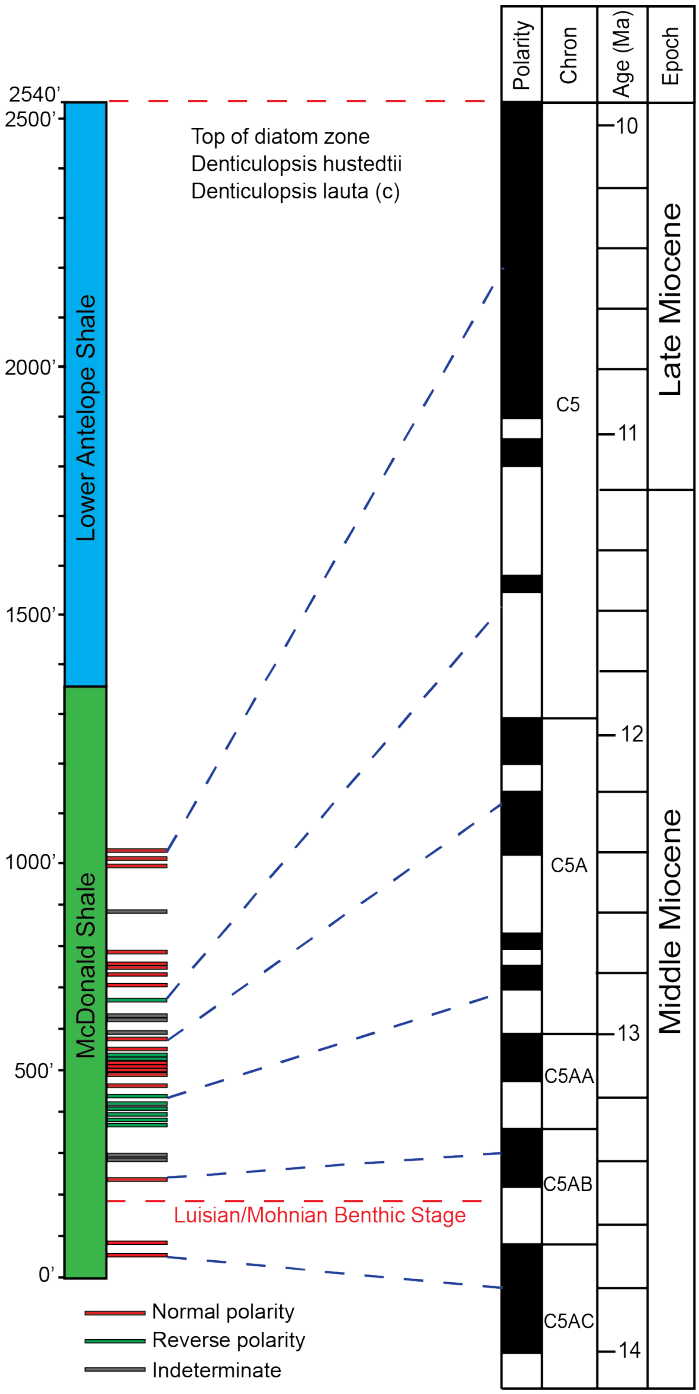

FIGURE 31. Correlation of paleomagnetic data derived from dolostones to the geologic timescale of Barron and Isaacs (2001).

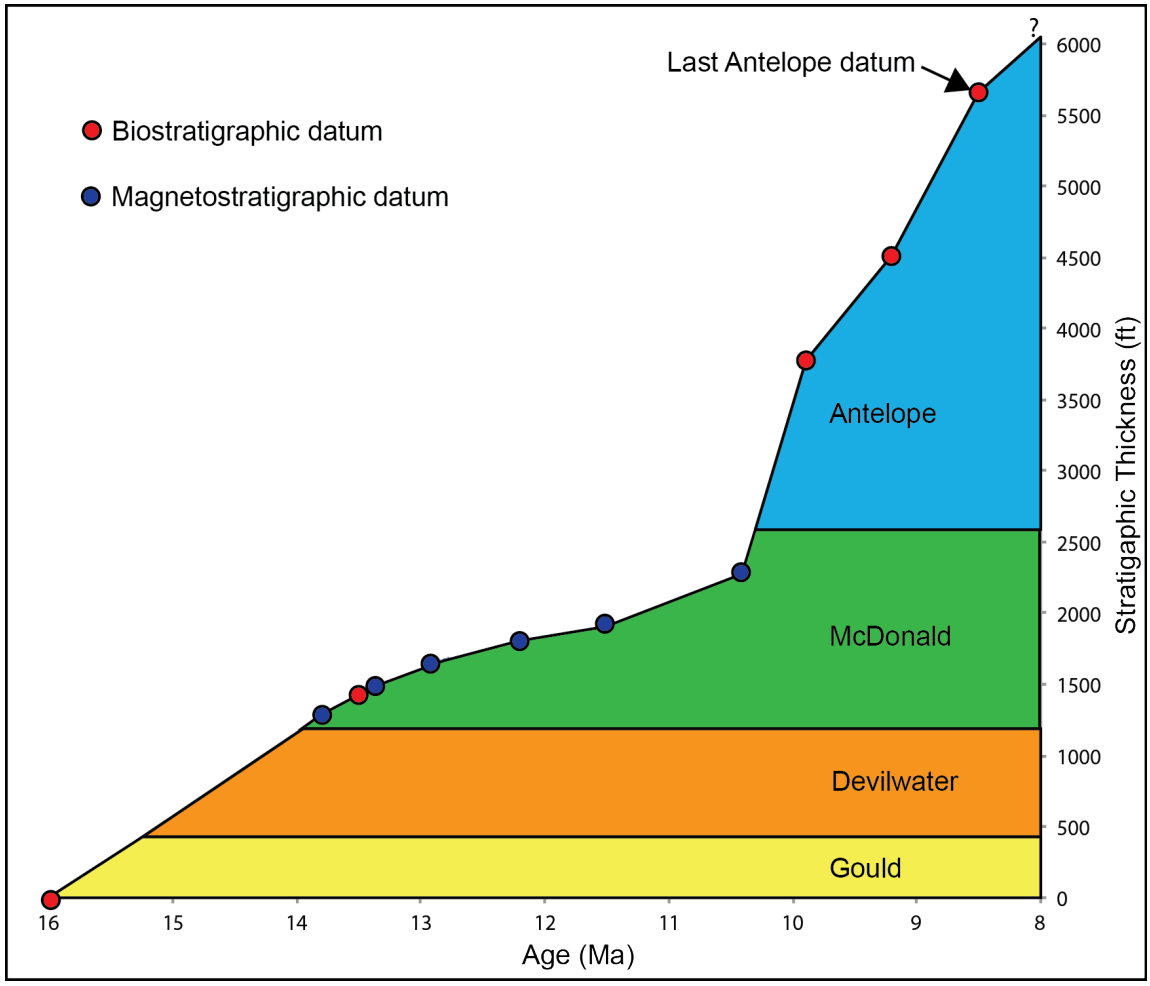

FIGURE 32 Sediment accumulation curve based on biostratigraphic (red circles) and magnetostratigraphic (blue circles) datums. Note the large increase in sedimentation rate between the McDonald and overlying Antelope Shale.

Subsurface Correlation

Gamma-ray logs from both 51X-33 ST and Bacon #1 wells were hung on a datum at the top of the McDonald, which is defined by a sharp total gamma-ray increase (figs. 21 and 22). This gamma ray signature proved to be one of the most useful tools for correlation between the CMC section and the subsurface well data. Additionally, the

identification of the Luisian-Mohnian boundary in 51X-33 ST enhanced correlation to the northeast.

From CMC to 51X-33 ST, located 4.5 miles to the northeast, member thicknesses decrease with the exception of the Devilwater Shale (fig. 33). The Gould Shale thins from 432 feet in CMC to 374 feet to the northeast. The Devilwater Shale thickens slightly from 802 feet to 929 feet to the northeast. The McDonald and Antelope Shales decrease in thickness from the southwest to northeast from 1350 and 3428 feet, to 1100 and 2747 feet, respectively. Overall, there is a decrease in Monterey thickness of 862 feet from CMC to 51X-33 ST to the northwest.

From CMC to Bacon #1, located 3.5 miles to the north, the Monterey increases in thickness overall by 107 feet (fig. 34). Both the Gould and McDonald Shale members decrease in thickness to the north, while the Devilwater and Antelope Shales increase in thickness. The Gould Shale thins from 432 to 345 feet and the McDonald decreases in thickness from 1350 to 1089 feet. The Devilwater and Antelope Shales increase in thickness from the south to north from 802 and 3428 feet, to 1008 and 3677 feet, respectively.

In summary, the Monterey thins slightly to the northeast and thickens to the north. At 432 and 1350 feet, respectively, the Gould and McDonald Shale members reach their maximum thickness at CMC, while the Devilwater and Antelope Shales reach their maximum thickness to the north at Bacon #1. Despite minor thickness variations within members, the overall Monterey Formation maintains its thickness 3.5 miles north and 4.5 miles northeast. This is expected because the wells have very little deviation in dip angle from the CMC section and there were no obvious folds or faults in either subsurface.

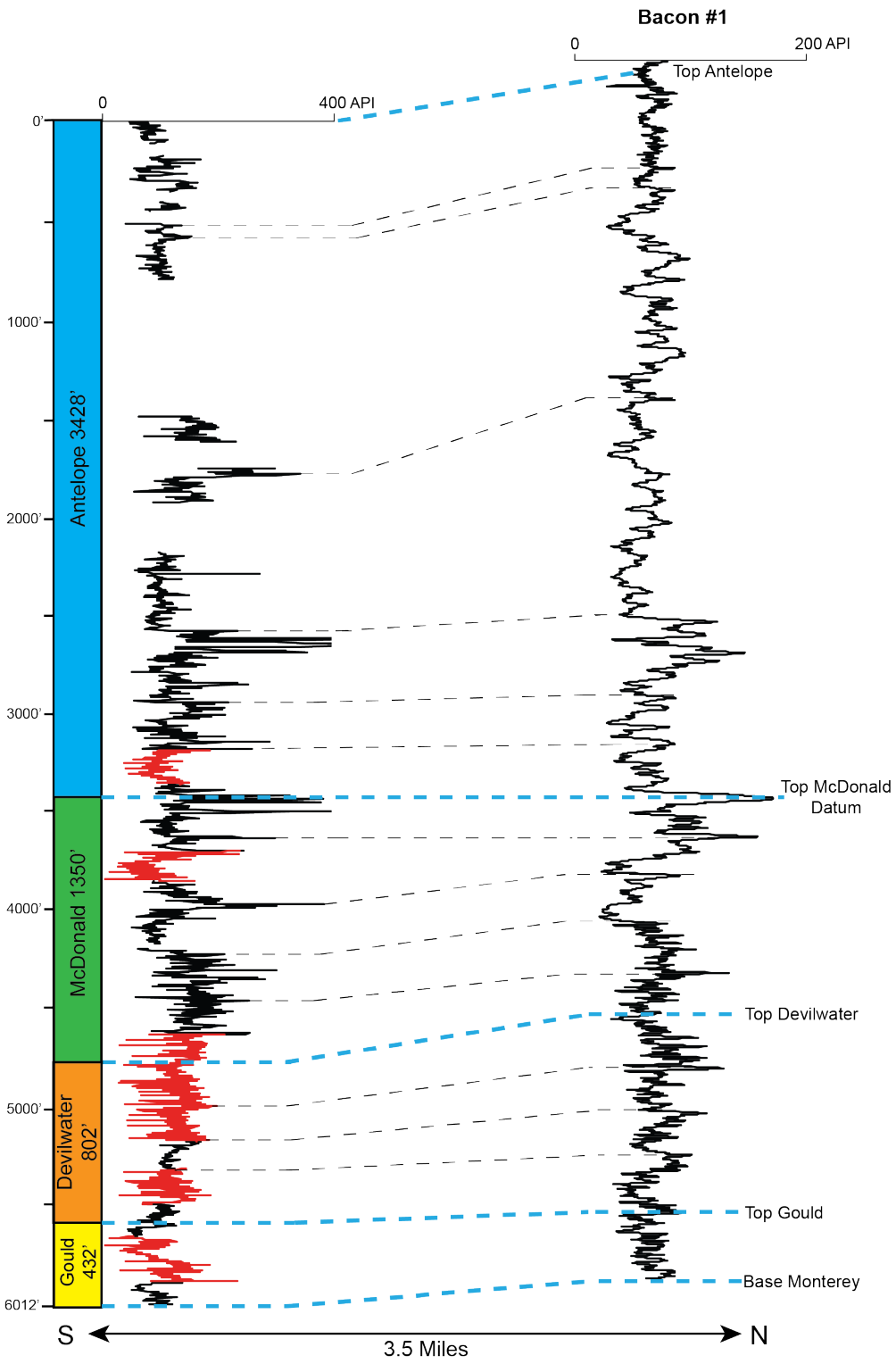

FIGURE 33. Correlation of the Chico Martinez Creek section to well Bacon #1. Thick blue dashed lines illustrate correlation of Monterey members and thin black dashed lines illustrate inter-member correlations.

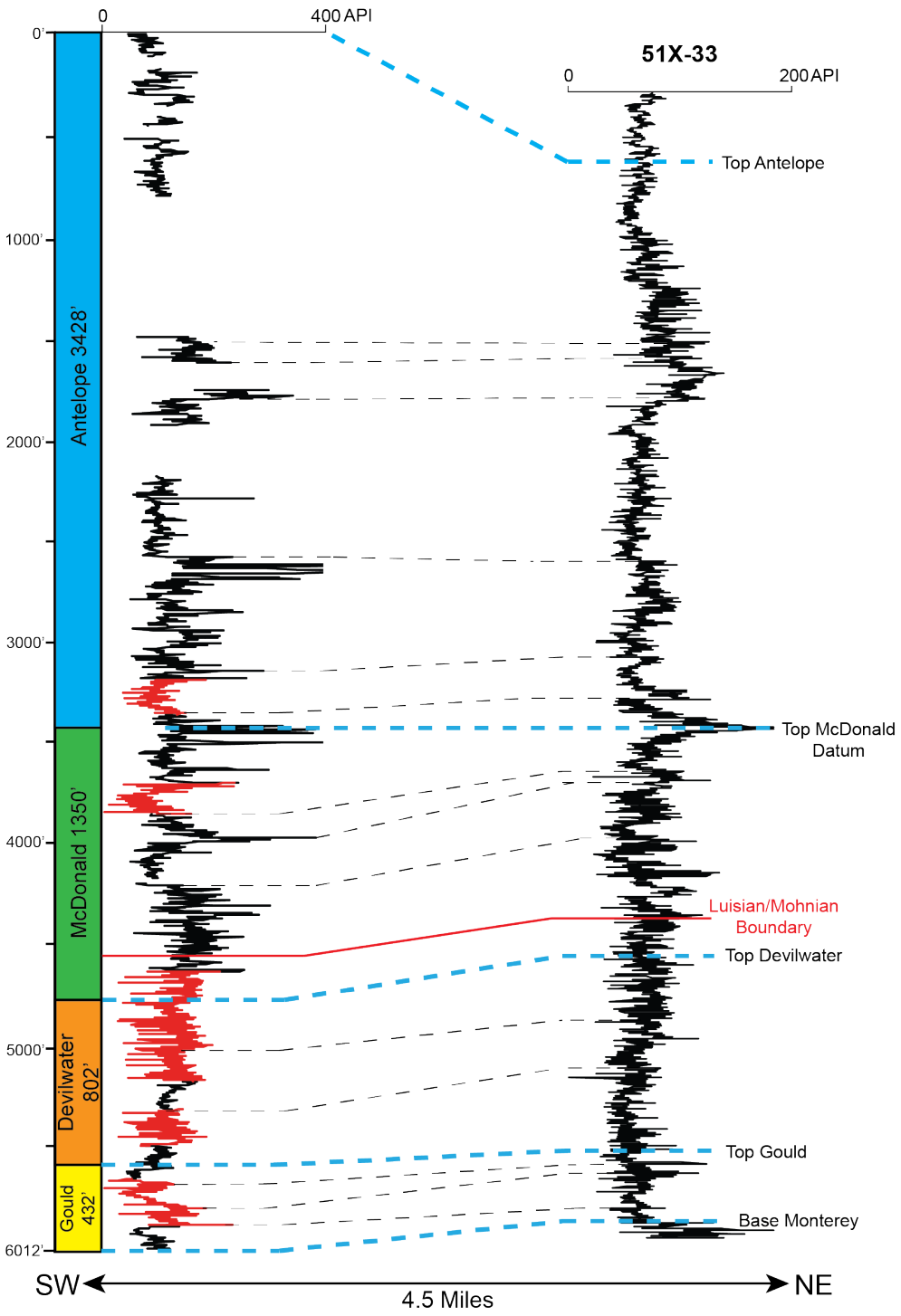

FIGURE 34. Correlation of the Chico Martinez Creek section to well 51X-33 ST. Thick blue dashed lines illustrate correlation of Monterey members, thin black dashed lines illustrate inter-member correlations and the solid red line demarks the Luisian/Mohnian boundary.

section. Furthermore, there was no biostratigraphic evidence, or other indications in the gamma-ray logs to suggest missing or repeated section in either well.

CHAPTER 4

DISCUSSION

This chapter examines the most important findings and implications of the investigation of the Chico Martinez Creek section. Ages of Monterey Formation members are compared to those reported in the literature for elsewhere in the San Joaquin basin. Members are also interpreted in a sequence stratigraphic context based on comparison of the refined ages of the sedimentary sequence with the global coastal onlap curve of Haq et al. (1987a,b, and 1988), later modified by Johnson et al. (2005). Changes in sedimentation rate are analyzed in relation to sea-level fluctuations and global climatic events that impacted rates in other basins along the California continental margin. The paleoceanographic and tectonic significance of subsurface gamma-ray correlations is explored, along with potential applications of CMC data for petroleum geologists.

Ages of Monterey Formation Members at CMC

Approximate age estimates for the members of the Monterey Formation at CMC are assigned based on new ages for previously identified biostratigraphic datums and new magnetostratigraphic correlations (fig. 32). In all cases, member contacts lie between biostratigraphic and magnetostratigraphic horizons and are thus estimated based on stratigraphic position between datums. The following ages were determined for the Monterey members at CMC: the Gould Shale is 16 to 15.5 Ma, Devilwater Shale is 15.5 to 14.0 Ma, McDonald Shale is 14.0 to 10.3 Ma and the Antelope Shale is 10.3 to

reported in the literature from basin-wide compilations, such as Scheirer and Magoon (2007) who concluded that the Gould Shale was deposited between 16.5 and 15.5 Ma, the Devilwater Shale between 15.5 and 13.5 Ma, the McDonald Shale between 13.5 and 10.0 Ma, and the Antelope Shale between 10.0 and 6 Ma. The large differences in ages reported for the top of the Antelope Shale in the literature and here for the CMC can be attributed to the time-transgressive nature of the top of the Antelope, which is diachronous throughout the San Joaquin basin (Graham and Williams, 1985) and to the lack of biostratigraphic data at CMC in the poorly exposed upper part of the section.

Sequence Stratigraphic Interpretation

Members of the Monterey Formation at CMC can be interpreted in a sequence stratigraphic context when compared to the global coastal onlap curve, newly calibrated to magnetostratigraphic and biostratigraphic datums (fig. 35). The conformable contact between the Buttonbed Sandstone and the overlying Gould Shale member marks a marine transgression and major shift from a macrofossil-rich, clastic-dominated shelf and slope to a distal deepwater environment (fig. 8, Johnson and Graham, 2004). The transition from the calcareous porcelanite lithofacies of the Gould Shale to the calcareous silty claystone of the Devilwater Shale is synchronous with a short-lived drop in sea level at approximately 15.3 Ma (Haq et al., 1987a,b). This minor sea level regression was accompanied by an increase in clastic input that was either sourced from the Salinian Block to the west or the eastern Sierra Nevada (Graham and Williams, 1985). Sea level continued to fall in stages during deposition of the McDonald Shale and marked a shift from the clastic-rich claystone of the Devilwater Shale to phosphatic, organic-rich shale.

A major sea-level fall occurred during deposition of the McDonald at approximately 11.5 Ma (Haq et al., 1987) and was followed by accumulation of the siliceous, upper McDonald and Antelope Shales (fig. 35). Callaway (1990) considered the most siliceous interval, near the top of the Antelope – the Chico Martinez cherts (figs. 21 and 22) – to be a condensed interval associated with a maximum flooding surface, however the coastal onlap curve indicates that the upper Antelope was actually deposited during the longest, and one of the lowest, sea-level lowstands of the Monterey succession.

This prominent change in lithology associated with sea-level fall is not the simple, gradual increase in detritus that would be expected during regression near the basin margin. Instead, it indicates a relative increase in hemipelagic and authigenic components requiring either increased biogenic sediment accumulation or decreased dilution by detritus. Condensed, biogenic- and authigenic-rich successions are most commonly associated with the upper surfaces of transgressive systems tracts, not regressional sequences (Loutit et al., 1988). Several scenarios may explain this, however, data to critically evaluate them are not available. These may reflect marginal changes in sedimentation related to eustatic or relative sea level, tectonics, or to changes in the intensity or location of upwelling centers.

On one hand, the change in composition may relate to local isolation of this part of the basin from terrigenous input. This could be due to changes in sediment migration pathways, such as slope bypass via incised submarine canyons or relative sediment starvation Terrigenous-poor Monterey sediments are postulated to have accumulated in lowstand systems tracts in the Santa Maria and Santa Barbara basin where sediment

supply was hindered as a consequence of sea-level fall (Bohacs, 1993). Although the western San Joaquin depocenter is more proximal than these outer basins, the same sediment trapping and sequestration may have occurred to decrease siliciclastic sediments at CMC.

Alternately, decreased terrigenous sedimentation may reflect more regional changes in the continental supply of siliciclastic detritus to the margin due to contemporaneous climatic cooling and aridification along the western North American margin (Retallack, 2004). Yet another hypothesis may be that long-distance drainage patterns from the continental interior were diverted from the central California margin by mid-Miocene extensional faulting in the Basin and Range province (Wernicke, 2011) or by rejuvenated uplift of the paleo-Sierra Nevada that likely began ~10 Ma (Henry, 2009).

Sedimentation Rates

The lithology of the Monterey Formation varies at scales from laminations to members as a result of changes in relative accumulation rates and relative abundances of organic and terrigenous sediment. Fluctuations in the influx of these constituents also control trends in bulk sedimentation rates (Isaacs, 1983). Terrigenous input may be influenced by a number of factors. Tectonic uplift controls both relief and the size of drainage areas and exposures to erosion and also can block or modify sediment transport routes. Changes in eustatic or relative sea level can either promote or choke off the transport of eroded sediment to the basin. Sediment supply is also influenced by changes in climate and precipitation through the amount of continental runoff. Accumulation rates of siliceous sediment–diatoms, radiolarians or silicoflagellates–is primarily controlled by nutrient supply and primary productivity and enhanced preservation by rapid burial.

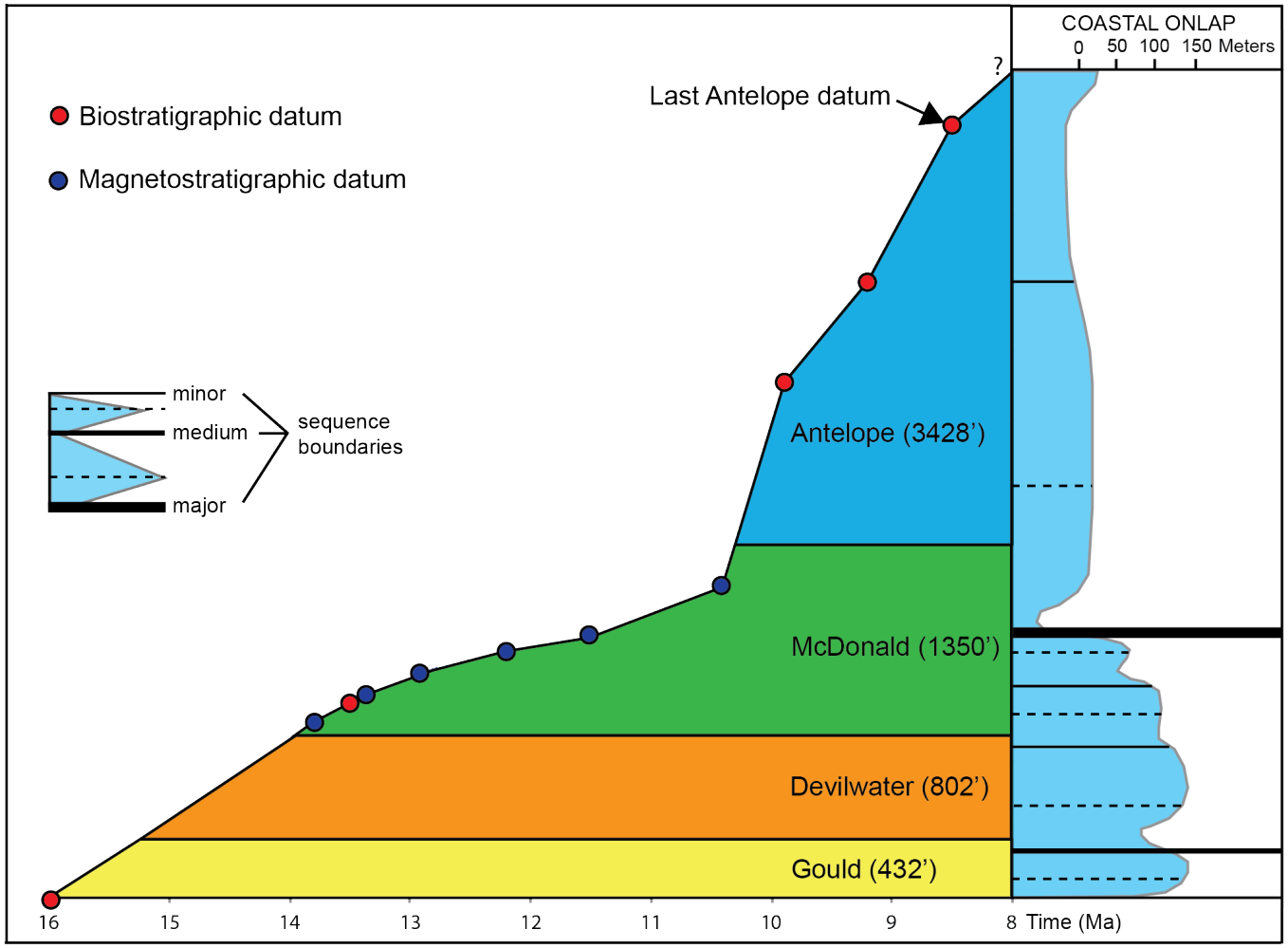

FIGURE 35. Sedimentation rate vs. coastal onlap curve from McDougall (2007) scaled to biostratigraphic and magnetostratigraphic datums. Dashed lines indicate maximum coastal onlap.

Finally, accumulation and preservation of organic matter is controlled by biologic productivity and basin anoxia, but its concentration can be further enhanced by reduction of terrigenous input, the deposition of which can dilute or disperse the biogenic component. Based on biostratigraphic and magnetostratigraphic age datums, linear sediment accumulation rates are moderate from 16 to 13.8 Ma (585 ft/Myr or 178 m/Myr), slow from 13.8 to 10.4 Ma (335 ft/Myr or 102 m/Myr) , and significantly increase from 10.4 to 8 Ma (1900 ft/Myr or 579 m/Myr). The largest change in sedimentation rate occurs within the upper McDonald Shale where there is a nearly 6-

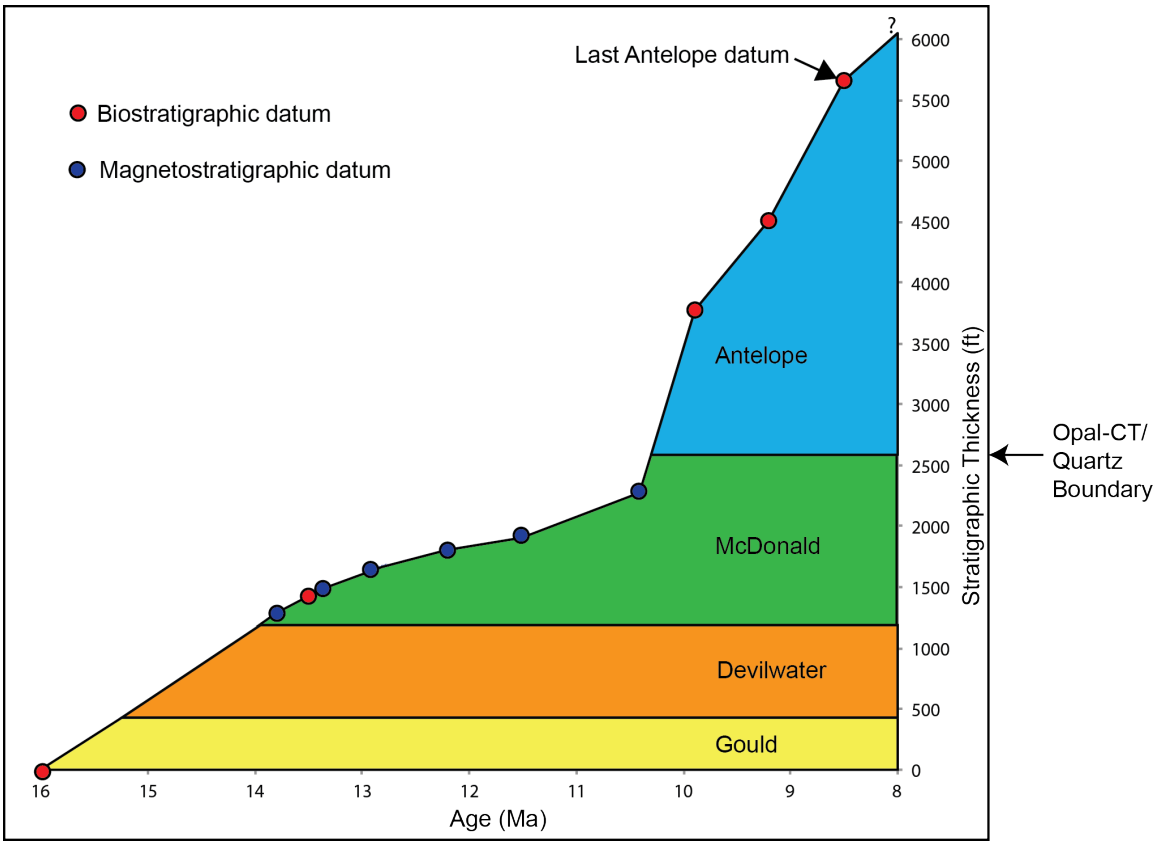

FIGURE 36. Stratigraphic position of the opal-CT to quartz transition. Note the large increase in the rate of sediment accumulation at this boundary.

fold increase from 335 ft/Myr to 1900 ft/Myr. Understanding this shift is the focus of this discussion as it occurs synchronously with a major sea level regression at ~11.5 Ma (fig. 35), a lithologic shift to increasingly siliceous lithofacies (fig. 21 and 22) and the opal-CT to quartz diagenetic transition boundary (fig 36, Table 2). These changes provide multiple, nonexclusive potential explanations for the dramatic change in the rate of sediment accumulation.

Biosiliceous sediments are unique in their dramatic stepwise loss of porosity with burial transition from opal-A to opal-CT to quartz phase silica. The substantial water loss and compaction associated with the phase transition from opal-CT to quartz results in a marked increase in bulk density due to the combined effects of decreased porosity and increased grain density. In order to assess if the large increase in linear sediment accumulation rate between 10.4 and 9.9 Ma is an artifact of diagenetic state, sediment thicknesses must be compared under similar silica phase conditions.

Although a large portion of the increase in accumulation rate at 10.4 Ma can be attributed to diagenesis, calculations show the sedimentation rate above this transition boundary would still exceed the rate below by 2 times if they were compared under the same quartz phase conditions of grain density and porosity using values based on empirical data from Monterey Formation sediments in the San Joaquin basin (Chaika and Dvorkin, 2000). The combined effects associated with the diagenetic transition from opal-CT (44 % porosity, 2.15 g/cm^3 grain density) to quartz phase (26 % porosity, 2.65 g/cm^3 grain density) would result in overall rock volume decrease of 60 %, reducing the sediment accumulation rate from 1900 to 760 ft/Myr. Although accounting for a

significant amount of the increased sediment accumulation rate, the normalized rate above the transition is still twice that of below.

The increase in sediment accumulation rate also occurs after a major fall in sea level at approximately 11.5 Ma (fig. 35). This regression is associated with the formation or expansion of the Antarctic ice sheet. In addition to expected changes in sedimentation related to regression, this major global cooling event is thought to be associated with an increase in diatom productivity (Ingle, 1981; Barron, 1986). This surge in biologic production and accumulation was likely a major factor contributing to the increase in continued sediment accumulation and silica content in the upper McDonald and lower Antelope. A similar peak in biogenic opaline silica accumulation between approximately 9.5 and 8 Ma can also be seen in deep-sea cores along the length of the California margin (Lyle et al., 2000), far outside of the restricted bathymetry of the Miocene borderland, indicating that the increased accumulation of siliceous sediment was a regional phenomenon rather than a local environmental event. It is also possible that the combined effects of increased diatom and organic matter sedimentation overwhelmed subsidence in the CMC depocenter, resulting in reduction in area as the basin filled and shallowed.

Paleobasin Conditions Interpreted from Th/U, Th/K Ratios And CGR

Thorium-uranium (Th/U) and thorium-potassium (Th/K) ratios from spectral gamma-ray data have been applied in numerous studies to provide insight into paleobasin anoxia and the relative proportion of illite with respect to other clay minerals (i.e., smectite, kaolinite and k-feldspar) (Adams and Weaver, 1958; Hesselbo, 1996; Dypvik and Harris, 2001; Doveton and Merriam, 2004). Th/U values are sensitive to oxidizing or

reducing depositional conditions where low values indicate basin anoxia (Adams and Weaver, 1958). Low Th/K are associated with the presence of illite, mica or other high-K minerals, whereas high Th/K values are associated with other detrital clay minerals (Hesselbo, 1996; Doveton and Merriam, 2004). The computed gamma-ray (CGR) log incorporates only potassium and thorium values, eliminating the influence of organic content associated with high uranium (Doveton and Merriam, 2004). Thus the analysis of the CGR log is a purely lithologic approach that allows for assessment of relative detrital clay content.

Based on the Th/U ratios, the succession switched from suboxic and oxic conditions to anoxia and then back to weaker anoxic conditions through the succession. Strongest anoxic conditions prevailed from 14 to 10 Ma (fig. 37). The prominent shift from oxidizing basin conditions in the Gould and Devilwater shales to reducing conditions in the McDonald and lower Antelope shales partially explains the transition from organic-poor (1.3 weight % TOC) calcareous silty claystone to organic-rich (5.0 to 6.1 weight % TOC) phosphatic and siliceous shales.

A gradual regression from the Devilwater Shale into the McDonald Shale (~14 to 11 Ma) may have both isolated the depocenter from clastic source pathways as previously described and possibly allowed the oxygen minimum zone to intercept the western basin margin resulting in basin anoxia and the onset of McDonald Shale deposition (fig. 38). It may also have helped isolate the entire San Joaquin basin by restricting connection to the Pacific. It also corresponds to the slowest sediment accumulation rate of the entire succession. Condensed sedimentation during a gradual regression may be related to rates of thermal and isostatic subsidence similar to those demonstrated in other Neogene pull-

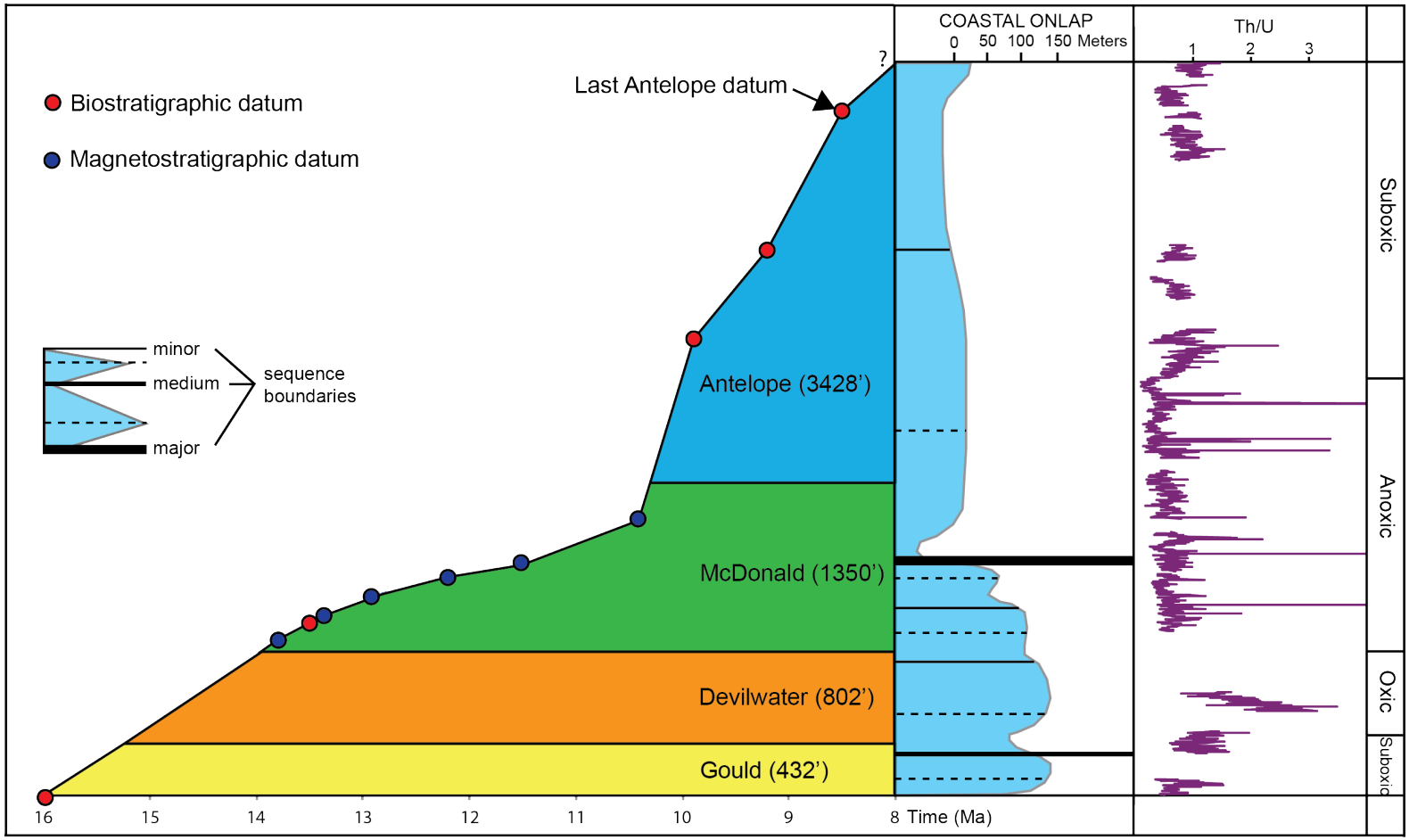

FIGURE 37. Sedimentation rate vs. coastal onlap curve from McDougall (2007) compared to Thorium/Uranium ratios at Chico Martinez Creek. Low Th/U is indicative of anoxic basin conditions; high Th/U is indicative of oxic basin conditions.

apart basins in California (Compton, 1991) outstripping sea-level fall for a resulting relative sea-level rise. This environment of isolated, deep basin conditions would allow for the slow sediment accumulation and preservation of organic-rich, phosphatic shales characteristic of the lower McDonald. Basin anoxia could have been intensified due to a large marine regression that occurred during deposition of the upper McDonald - this may have further isolated the basin from the Pacific Ocean (fig. 38). Accumulation of abundant organic matter continued along with biosiliceous sedimentation through deposition of the upper McDonald to lower Antelope.

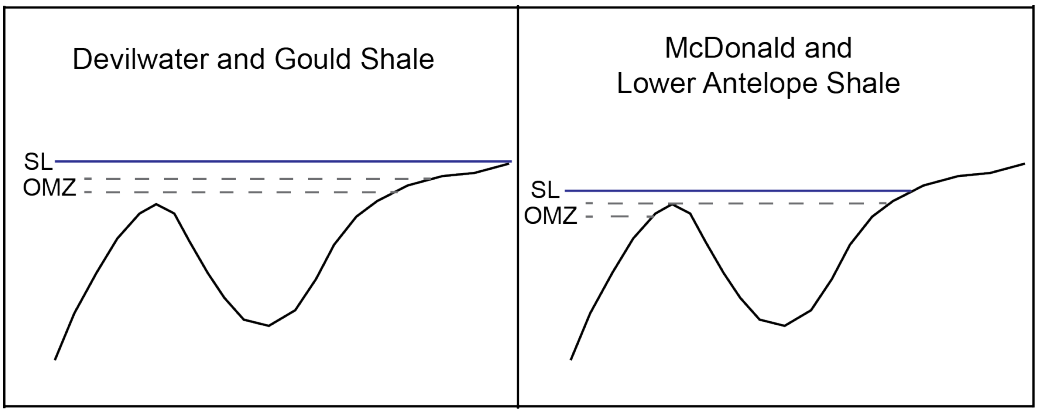

FIGURE 38. Schematic model of paleobasin conditions during McDonald and Antelope Shale deposition. SL = Sea-level and OMZ = Oxygen mimimum zone.

The CGR log indicates low clay content in the Gould Shale, upper McDonald and lower Antelope shales, and moderate clay in the upper Antelope. The highest clay content interval is present from the Devilwater Shale to the lower McDonald Shale (fig. 39). The low clay content interval in the upper McDonald and lower Antelope is significant because it is approximately synchronous with anoxic basin conditions. This further supports the theory that the CMC depocenter became isolated from detrital input

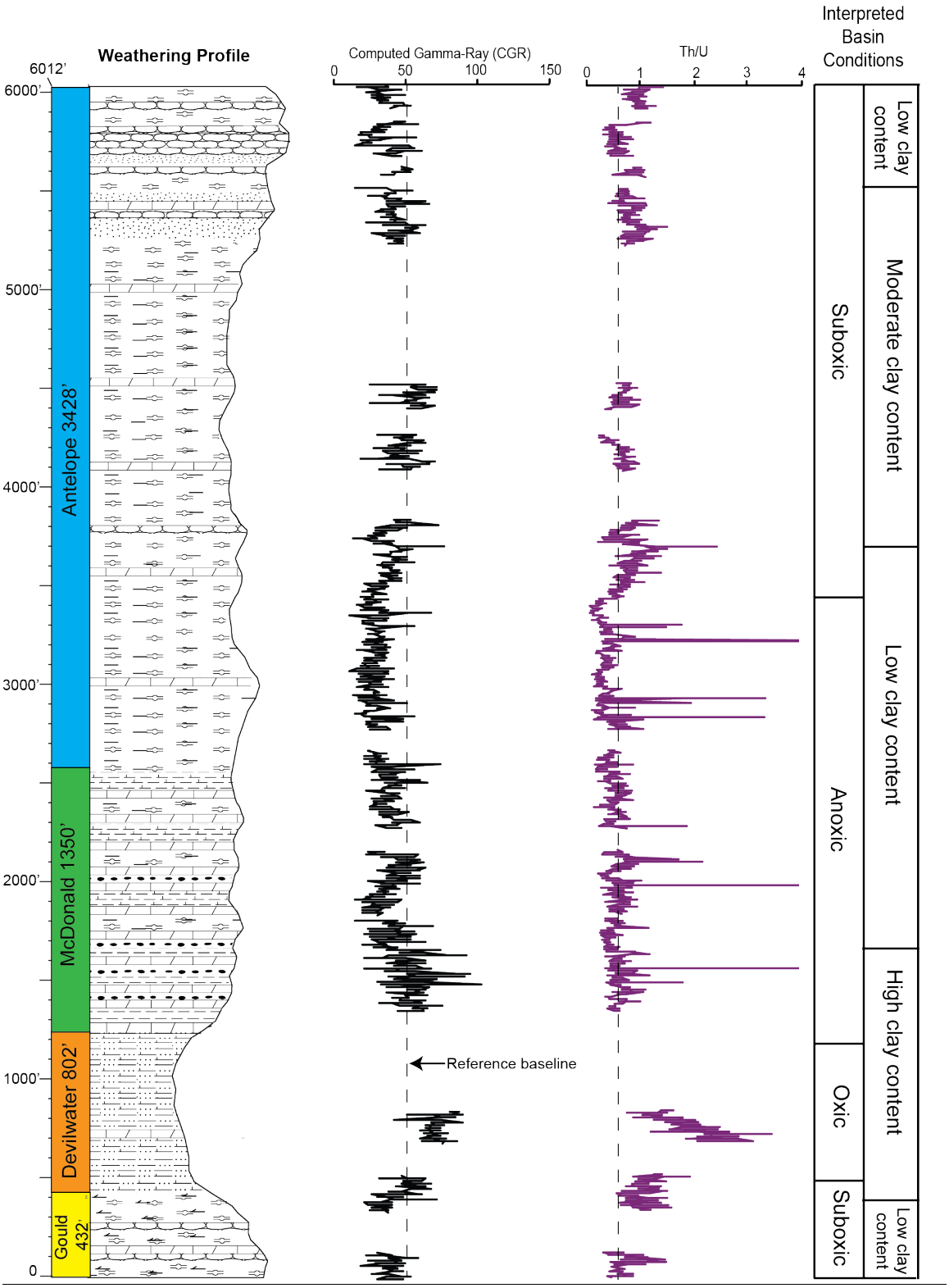

FIGURE 39. Paleobasin conditions interpreted from CGR and Th/U ratios.

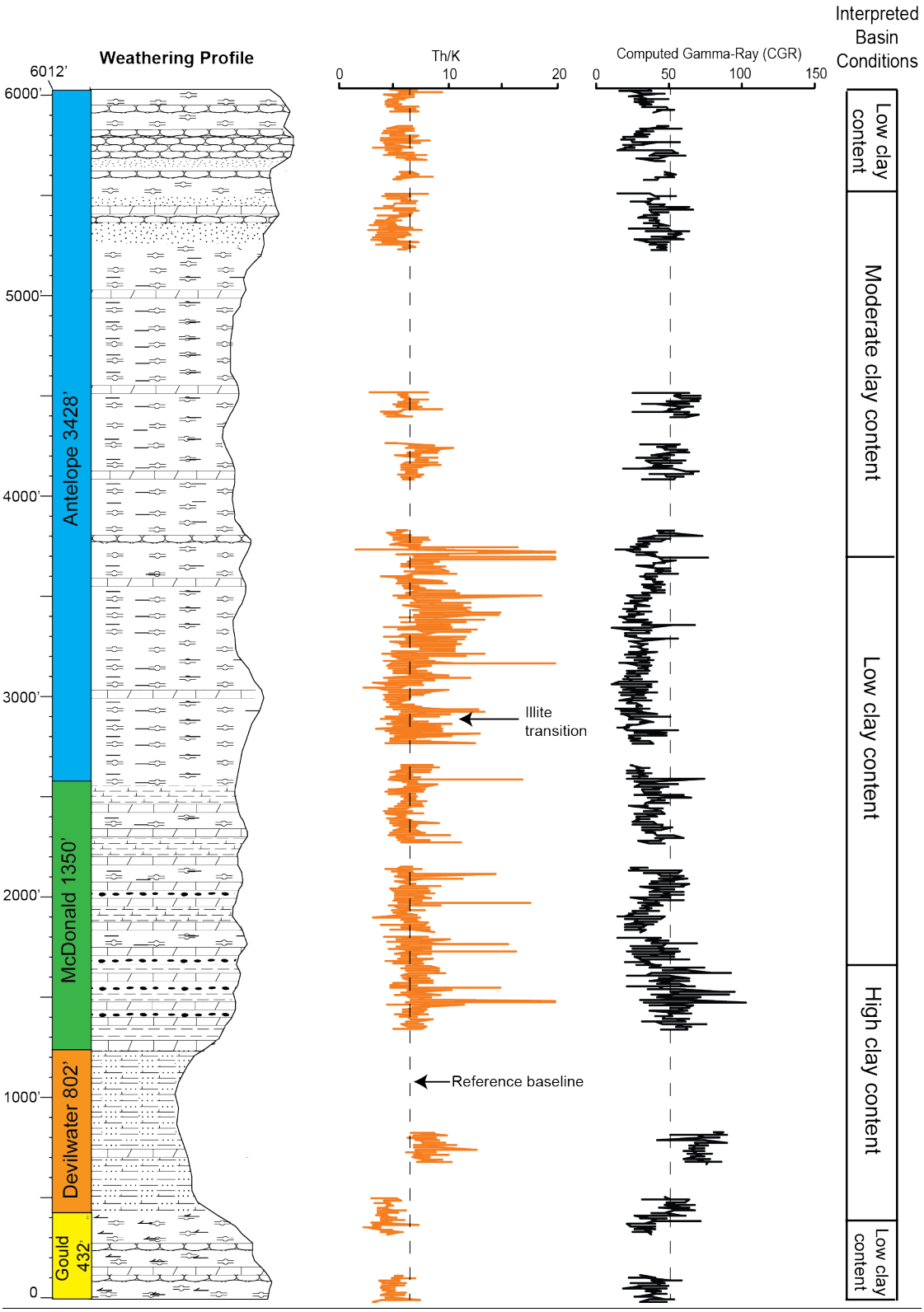

FIGURE 40. Relative clay content and illite content interpreted from CGR and Th/U ratios.

subsequent to sea-level regression.

High Th/K values in the Devilwater Shale can be attributed to high thorium throughout this member, which is almost twice that of most other distinctive lithofacies in the CMC section (fig. 40). The reason for high Th values in this detrital-rich interval are unknown, but are likely related to provenance. There is also a prominent transition from high to low Th/K values in the lower Antelope that occurs synchronous with the smectite-to-illite transition based on XRD and FTIR data (Table 1). Below this point, values continue to remain low (with the exception of the Devilwater Shale) providing further support that this is a mineralogic transition to illite clays.

Comparison of Sedimentation Rates in Proximal Neogene Basins

Sediment accumulation rates at CMC (San Joaquin basin) were compared to rates determined from previous studies (fig. 41) in Pismo basin (Omarzai, 1992), Santa Maria basin (McCrory et al., 1996) and Santa Barbara basin (DePaolo and Finger, 1991). Similarities in sedimentation patterns provide strong support that the processes that controlled sedimentation at CMC were widespread, not just restricted to the San Joaquin basin. Discrepancies would suggest basin-specific localized mechanisms controlled the precise timing of changes in rate and type of deposition.

Similar to CMC, the sedimentation records from Pismo, Santa Maria and Santa Barbara basins reflect a major lull in sedimentation from approximately 14 to 10 Ma (fig. 42). The magnitude of this decrease in rate of accumulation varies from very slow rates in the San Joaquin and Pismo basins to almost complete depositional hiatuses in the Santa Maria and Santa Barbara basins. In all basins, diminished accumulation rates could have been associated with basin isolation on a complex margin similar to the modern

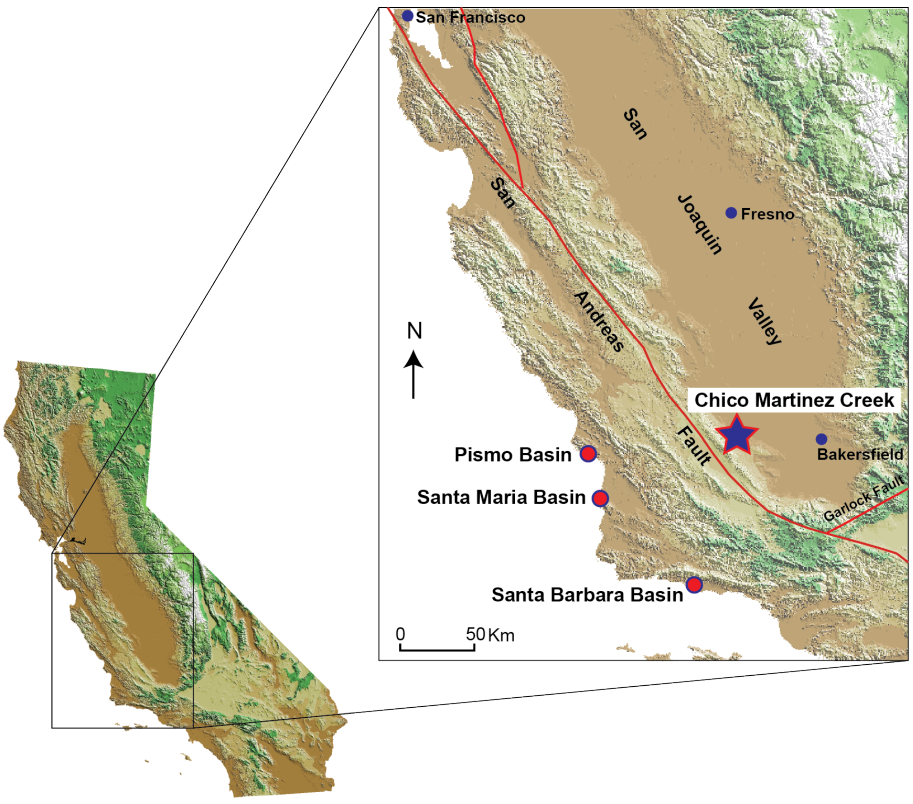

FIGURE 41. Location of studied sections shown in Figure 41 from other Neogene basins in relation to Chico Martinez Creek.

California Continental Borderland due to sea level fall, or, if subsidence was fast enough, to sediment starvation from reduced supply from the continent. The formation of the East Antarctic Ice Sheet and subsequent sea level fall was a global event that would have had a similar and relatively isochronous impact on many Neogene basins along the California margin. Simultaneously, aridification due to global cooling may have decreased precipitation, run-off and terrigenous sediment transport to the continental margin (Retallack, 2004).

The onset and termination of the sedimentation rate decrease is diachronous across all four basins. In CMC sedimentation rate decreases substantially from

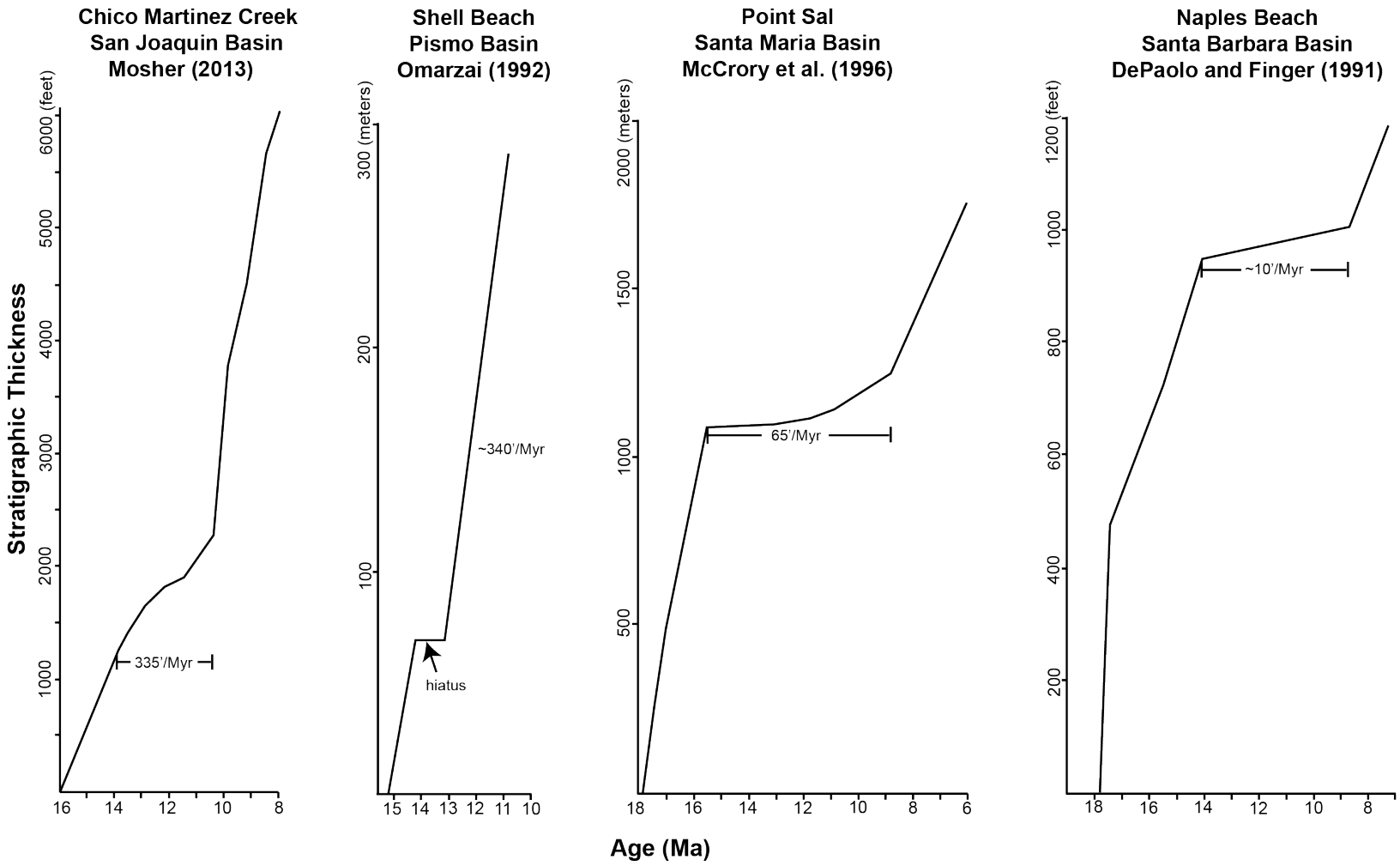

FIGURE 42. Comparison of sediment accumulation rates determined at Chico Martinez Creek to Pismo basin (Omarzai, 1992), Santa Maria basin (McCrory, 1996) and Santa Barbara basin (DePaolo and Finger, 1991).

approximately 13.8 to 10.4 Ma, whereas in the Santa Maria basin, rates begin to drop at approximately 16 Ma and increase at 9 Ma. Variation in the onset of condensed sedimentation may be attributed to San Andreas-related tectonics, which opened and isolated basins at different times independent of global sea level change (Blake et al., 1978). The abrupt increase in rates following slow sedimentation in CMC, Santa Maria, and Santa Barbara basins occurred between 10 and 9 Ma. This change sedimentation rate is unknown in Pismo basin because of the lack of published data. The increased sedimentation rate has been attributed to increased diatom productivity that dominated the California margin in the Late Miocene due to increased upwelling (Ingle, 1981). However, variation in the magnitude of the increase in sedimentation rate may have been influenced by the geographic location of these basins with the San Joaquin basin having filled more rapidly than Santa Maria and Santa Barbara basins. This is likely attributed to the more inboard geographic position of the San Joaquin basin relative to the two outboard basins, which were more isolated from terrigenous sources. It was not until the late Miocene to early Pliocene (approximately 6.8 Ma) that these outboard basins experience a major increase in sedimentation rate marked by the deposition of the Sisquoc Formation (Isaacs, 2001).

Subsurface Correlation

Subsurface gamma-ray correlations to 51X-33 ST and Bacon #1, located 3.5 miles north and 4.5 miles northeast, respectively, indicate relatively minor variation in total thickness of the Monterey Formation over this distance. The Monterey Formation decreases in thickness by 862 feet from CMC to 51X-33 ST and increases in thickness by

107 feet from CMC to Bacon #1. This lack of lateral variation in thickness has tectonic and paleobathymetric implications.

It is apparent that these three areas did not experience substantial syndepositional tectonic deformation observed in other Monterey sediments in the San Joaquin basin (Harding, 1976). If this were the case, there would be more lateral variation in thickness reflecting the differential accommodation space in structurally formed bathymetric highs and lows. It can be interpreted that, overall, this small area of the basin remained tectonically quiescent during deposition of the Monterey, then underwent post-depositional deformation resulting in uplift and exposure of the sediments at CMC (and northwest-southeast along the foothills of the Temblor Range), but burying them to the north and northeast. The relatively constant thickness of the Monterey also indicates relatively flat paleobathymetry and the lack of local sills and bank tops in this limited area of the San Joaquin depocenter.

CHAPTER 5

CONCLUSIONS

This study provides the most detailed lithostratigraphic and chronostratigraphic characterization of the Monterey Formation at the Chico Martinez Creek section, a classic exposure visited by thousands of geologists over the years and a key reference section for the San Joaquin basin. In spite of its acknowledged significance, no continuous detailed description existed previously in the public domain. The Monterey Formation, previously divided into 4 lithostratigraphic members–the Gould, Devilwater, McDonald and Antelope shales–has been further subdivided into 7 distinctive lithofacies with unique spectral gamma-ray character and composition. A chronostratigraphic framework has now been established based on 5 previously unpublished biostratigraphic datums and 6 new paleomagnetic ages. These new data allowed for determination of linear sediment accumulation rates at CMC that could then be compared with other Neogene basins in California. The following are the most significant findings based on the data collected from the CMC:

1. The Monterey Formation is 6012 ft thick at CMC and has been subdivided into 7 distinct lithofacies in age-ascending order: calcareous porcelanite (432 ft), calcareous silty claystone (802 ft), phosphatic shale (430 ft), calcareous siliceous shale (920 ft), siliceous shale (2676 ft), arkosic sandstone (230 ft), and porcelanite and chert (522 ft). Certain distinctive lithofacies have the following unique defining spectral gamma-ray

characteristics:

a. The calcareous silty claystone lithofacies has the highest average thorium (10.4 ppm) and potassium values (1.5 %).

b. The phosphatic shale lithofacies has the highest uranium value (14.3 ppm).

2. The ages and durations of Monterey members at Chico Martinez Creek are relatively consistent (generally within 0.5 Ma) with values in the published literature. The only exception being the large discrepancy in age reported for the top of the Antelope Shale, which is time-transgressive.

3. Major changes in distinctive lithofacies observed at Chico Martinez Creek have sequence stratigraphic significance and can be directly correlated to eustatic sea-level fluctuations.

4. The shift from the clastic-rich claystone of the Devilwater Shale to the phosphatic, organic-rich shales of the lower McDonald Shale and siliceous shales of the upper McDonald and Antelope shales is correlated to a fall in sea-level; this marine regression is related to the advancement of the East Antarctic Ice Sheet and a prolonged period of global cooling.

5. The prominent increase in siliceous composition starting in the upper McDonald Shale indicates either an increase in diatom productivity associated with global cooling, or a decrease in dilution by detritus. Several different scenarios, or a combination of them, may explain this increase in the silica:detrital ratio:

a. This area of the basin was isolated from terrigenous input due to changes in sediment migration pathways, i.e. slope bypass via submarine canyons.

b. Aridification along the western North American margin associated with global cooling decreased sediment transport to the ocean.

c. Drainage pathways from the continental interior were diverted by mid-Miocene extensional faulting in the Basin and Range provenance or rejuvenation of uplift of the Sierra Nevada approximately 10 Ma.

6. Sediment accumulation rates surged during deposition of the upper McDonald through Antelope siliceous facies. Since these sediments are detrital-poor, increased diatom productivity was likely a major factor contributing to this large influx in accumulation rates.

7. Th/U ratios from spectral gamma-ray data reveal that anoxic basin conditions prevailed during the deposition of the upper McDonald and lower Antelope. Basin isolation from the Pacific Ocean due to the synchronous marine regression may explain these conditions. The computed total gamma-ray (CGR) log confirms that this interval had low detrital clay content providing further support that the increase in linear sediment accumulation rates is attributed to increased diatom productivity.

8. Similarities in sedimentation rate patterns with Pismo, Santa Maria and Santa Barbara basins provide strong support that the processes that controlled sedimentation at CMC were widespread. This comparison shows that the advancement of the East Antarctic Ice Sheet and consequent sea-level fall impacted many Neogene basins along the California margin similarly.

9. Correlation of surface total gamma-ray data to proximal wells in the western San Joaquin basin indicate relatively minor variation in the total thickness of the

Monterey Formation. This lack of lateral variation implies tectonic quiescence and relatively flat paleobathymetry during Monterey Formation deposition.

CHAPTER 6

FUTURE WORK

This thesis is a foundational study on which future projects can expand. Future work recommendations range in scope from increasing the resolution of data collected at the CMC section to applying the interpretations made and technical analysis conducted at CMC to other areas of the San Joaquin basin and other Neogene basins throughout California. The following are recommendations for future work.

Data Refinement

1. Compositional XRD and FTIR analysis was limited to only 10 samples. Extending the compositional analysis to a much higher stratigraphic resolution would better characterize compositional variation. The addition of x-ray fluorescence (XRF) analysis would provide a suite of elemental data that would aid in paleoceanographic correlation and interpretation. These data would permit calculation of detailed mass accumulation rates of geochemically important components, such as organic carbon, phosphorous, and biogenic silica that could be used to test fundamental questions about the role of the Monterey in Miocene global change.

2. Thorium-Uranium ratios from the spectral gamma-ray data were used as a proxy for identifying paleobasin conditions. The environmental significance of these ratios needs to be confirmed by direct geochemical data; the CMC sections would be a good place to conduct this test.

3. The generated magnetostratigraphic record was limited to the lower to middle McDonald Shale. Extending the magnetostratigraphic record above and below this interval would help refine the chronostratigraphy at CMC, which would provide a more detailed record of changes in sediment and mass accumulation rates. Identification of more subtle changes in sediment accumulation may provide more insight into the paleoceanographic and paleoclimatic mechanisms that controlled these fluctuations.

Subsurface Correlation

1. This study highlights the importance of collecting spectral gamma-ray data in subsurface wells and outcrop studies, which compliment a total gamma-ray dataset by providing a means to interpret paleobasin environmental conditions, in addition to correlating similarities in lithology and log character. Due to the limited availability of subsurface spectral gamma-ray data from older wells, such correlations could not be conducted in this thesis, but should be attempted when more data become publicly available.

2. Consistent with previous studies, this thesis demonstrates that Th/U ratios derived from spectral gamma-ray data can be used a means to interpret paleobasin conditions. These ratios would offer a powerful subsurface correlation tool that could be used to correlate sediments that were deposited under similar basin conditions. This would provide a low-resolution method of correlation in addition to correlating total gamma-ray character. This application would be of particular use in the McDonald and lower Antelope members of the Monterey Formation, which were deposited in anoxic basin conditions; these conditions were not just specific to the CMC location, but were widespread and somewhat diachronous throughout California. The high TOC values

associated with this interval in CMC (5.0 to 6.1 weight %) make it a viable source rock in the San Joaquin basin. By integrating data from numerous wells with spectral gamma-ray measurements and calculated Th/U values, it could be possible to build an isopach map that predicts the lateral and vertical extent of anoxia and deposition of the related source rock strata in the San Joaquin basin.

3. The potential for subsurface correlation of distinctive lithofacies by their unique spectral log character is also a valuable application of this study. This could be particularly useful in the Devilwater Shale member where the lithology and spectral gamma-ray signature is strikingly dissimilar to the rest of the Monterey Formation. Unlike the other Monterey members at CMC, the thorium is much higher than the uranium in this silty claystone interval, resulting in crossover and curve separation. This distinct log signature could be applied to mark the base of the organic-rich McDonald Shale and to construct subsurface isopach maps of the Devilwater Shale should it ever prove to be an economic reservoir in the San Joaquin basin.

Basin Comparison

1. This thesis compared sediment accumulation rates to those in 3 other Neogene basins in California. This comparison could be expanded not only to additional paleobasins in California, but also to other Miocene depocenters along the Pacific Rim that experienced correlative eustatic sea-level changes and global cooling events. This would provide confirmation or refutation that the processes that controlled sedimentation in California were broadly regional, if not global in nature.

APPENDIX A

PLATE 1

Surface lithology, spectral gamma-ray and total gamma-ray log of the Monterey Formation at Chico Martinez Creek, CA

Annie Mosher, 2013

(Plate 1)

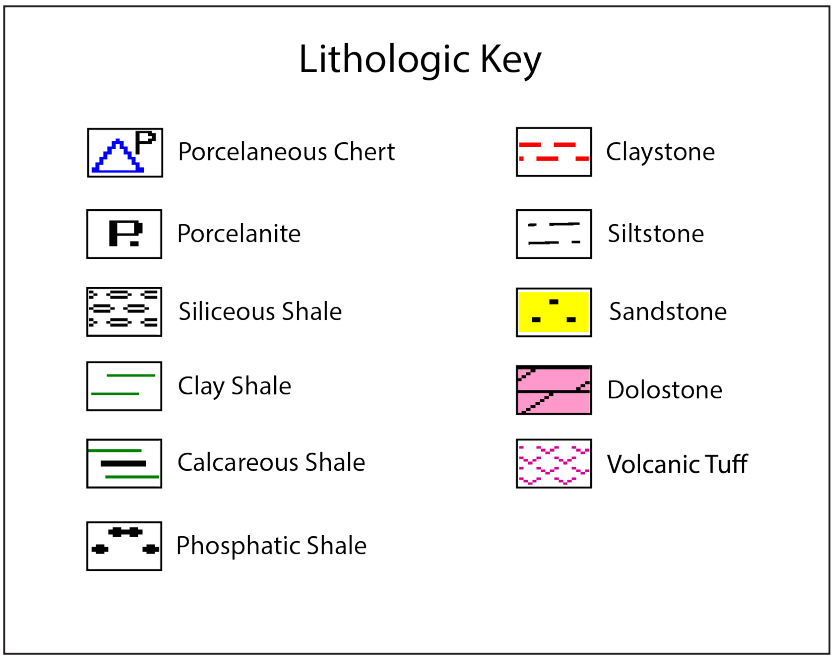

Software provided courtesy of Epoch Well Services Inc.

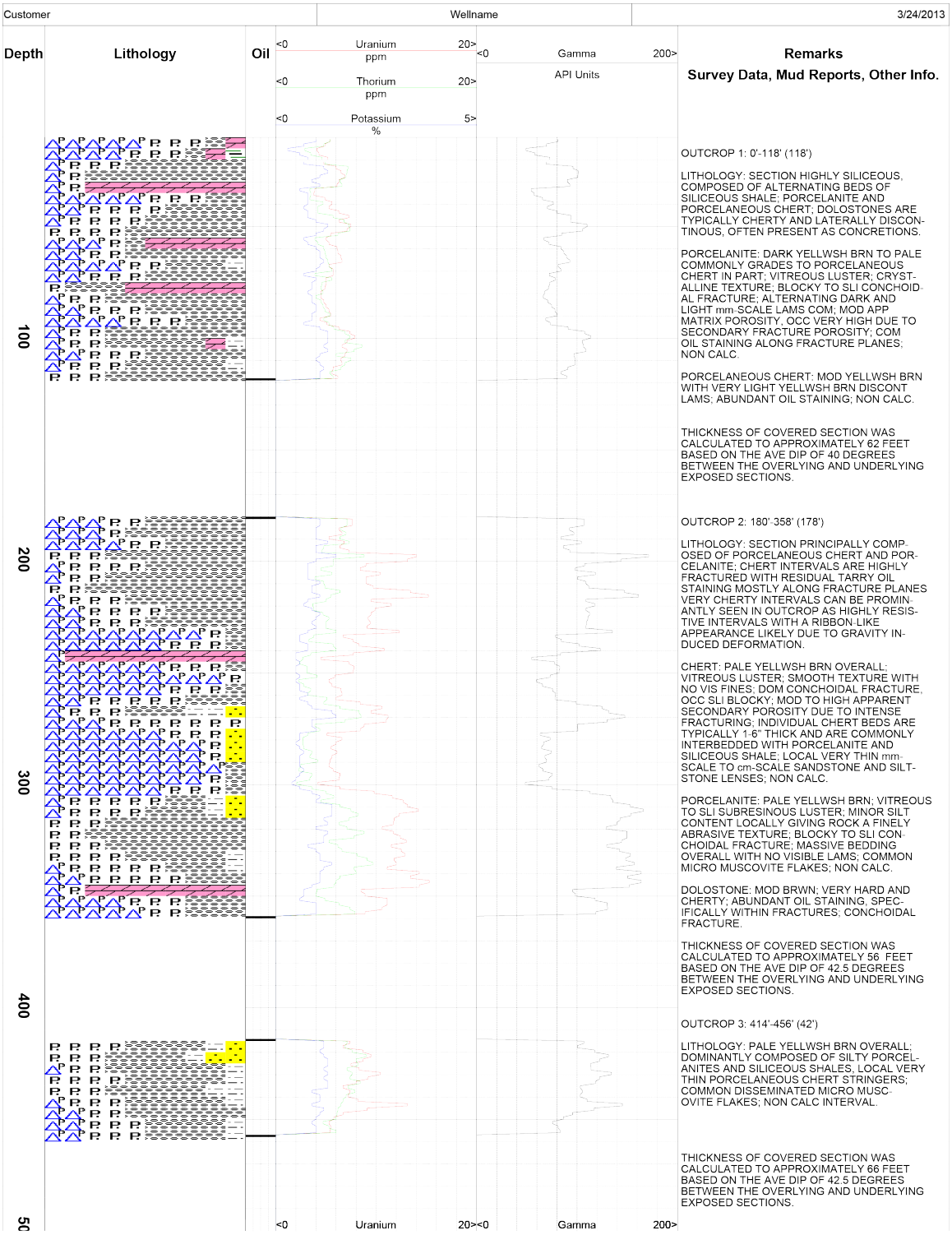

OUTCROP 1: 0'-118' (118')

LITHOLOGY: SECTION HIGHLY SILICEOUS, COMPOSED OF ALTERNATING BEDS OF SILICEOUS SHALE; PORCELANITE AND PORCELANEOUS CHERT; DOLOSTONES ARE TYPICALLY CHERTY AND LATERALLY DISCONTINOUS, OFTEN PRESENT AS CONCRETIONS.

PORCELANITE: DARK YELLWSH BRN TO PALE COMMONLY GRADES TO PORCELANEOUS CHERT IN PART; VITREOUS LUSTER; CRYSTALLINE TEXTURE; BLOCKY TO SLI CONCHOIDAL FRACTURE; ALTERNATING DARK AND LIGHT mm-SCALE LAMS COM; MOD APP MATRIX POROSITY, OCC VERY HIGH DUE TO SECONDARY FRACTURE POROSITY; COM OIL STAINING ALONG FRACTURE PLANES; NON CALC.

PORCELANEOUS CHERT: MOD YELLWSH BRN WITH VERY LIGHT YELLWSH BRN DISCONT LAMS; ABUNDANT OIL STAINING; NON CALC.

THICKNESS OF COVERED SECTION WAS CALCULATED TO APPROXIMATELY 62 FEET BASED ON THE AVE DIP OF 40 DEGREES BETWEEN THE OVERLYING AND UNDERLYING EXPOSED SECTIONS.

OUTCROP 2: 180'-358' (178')

LITHOLOGY: SECTION PRINCIPALLY COMPOSED OF PORCELANEOUS CHERT AND PORCELANITE; CHERT INTERVALS ARE HIGHLY FRACTURED WITH RESIDUAL TARRY OIL STAINING MOSTLY ALONG FRACTURE PLANES VERY CHERTY INTERVALS CAN BE PROMINANTLY SEEN IN OUTCROP AS HIGHLY RESISTIVE INTERVALS WITH A RIBBON-LIKE APPEARANCE LIKELY DUE TO GRAVITY INDUCED DEFORMATION.

CHERT: PALE YELLWSH BRN OVERALL; VITREOUS LUSTER; SMOOTH TEXTURE WITH NO VIS FINES; DOM CONCHOIDAL FRACTURE, OCC SLI BLOCKY; MOD TO HIGH APPARENT SECONDARY POROSITY DUE TO INTENSE FRACTURING; INDIVIDUAL CHERT BEDS ARE TYPICALLY 1-6" THICK AND ARE COMMONLY INTERBEDDED WITH PORCELANITE AND SILICEOUS SHALE; LOCAL VERY THIN mm-SCALE TO cm-SCALE SANDSTONE AND SILTSTONE LENSES; NON CALC.

PORCELANITE: PALE YELLWSH BRN; VITREOUS TO SLI SUBRESINOUS LUSTER; MINOR SILT CONTENT LOCALLY GIVING ROCK A FINELY ABRASIVE TEXTURE; BLOCKY TO SLI CONCHOIDAL FRACTURE; MASSIVE BEDDING OVERALL WITH NO VISIBLE LAMS; COMMON MICRO MUSCOVITE FLAKES; NON CALC.

DOLOSTONE: MOD BRWN; VERY HARD AND CHERTY; ABUNDANT OIL STAINING, SPECIFICALLY WITHIN FRACTURES; CONCHOIDAL FRACTURE.

THICKNESS OF COVERED SECTION WAS CALCULATED TO APPROXIMATELY 56 FEET BASED ON THE AVE DIP OF 42.5 DEGREES BETWEEN THE OVERLYING AND UNDERLYING EXPOSED SECTIONS.

OUTCROP 3: 414'-456' (42')

LITHOLOGY: PALE YELLWSH BRN OVERALL; DOMINANTLY COMPOSED OF SILTY PORCELANITES AND SILICEOUS SHALES, LOCAL VERY THIN PORCELANEOUS CHERT STRINGERS; COMMON DISSEMINATED MICRO MUSCOVITE FLAKES; NON CALC INTERVAL.

THICKNESS OF COVERED SECTION WAS CALCULATED TO APPROXIMATELY 66 FEET BASED ON THE AVE DIP OF 42.5 DEGREES BETWEEN THE OVERLYING AND UNDERLYING EXPOSED SECTIONS.

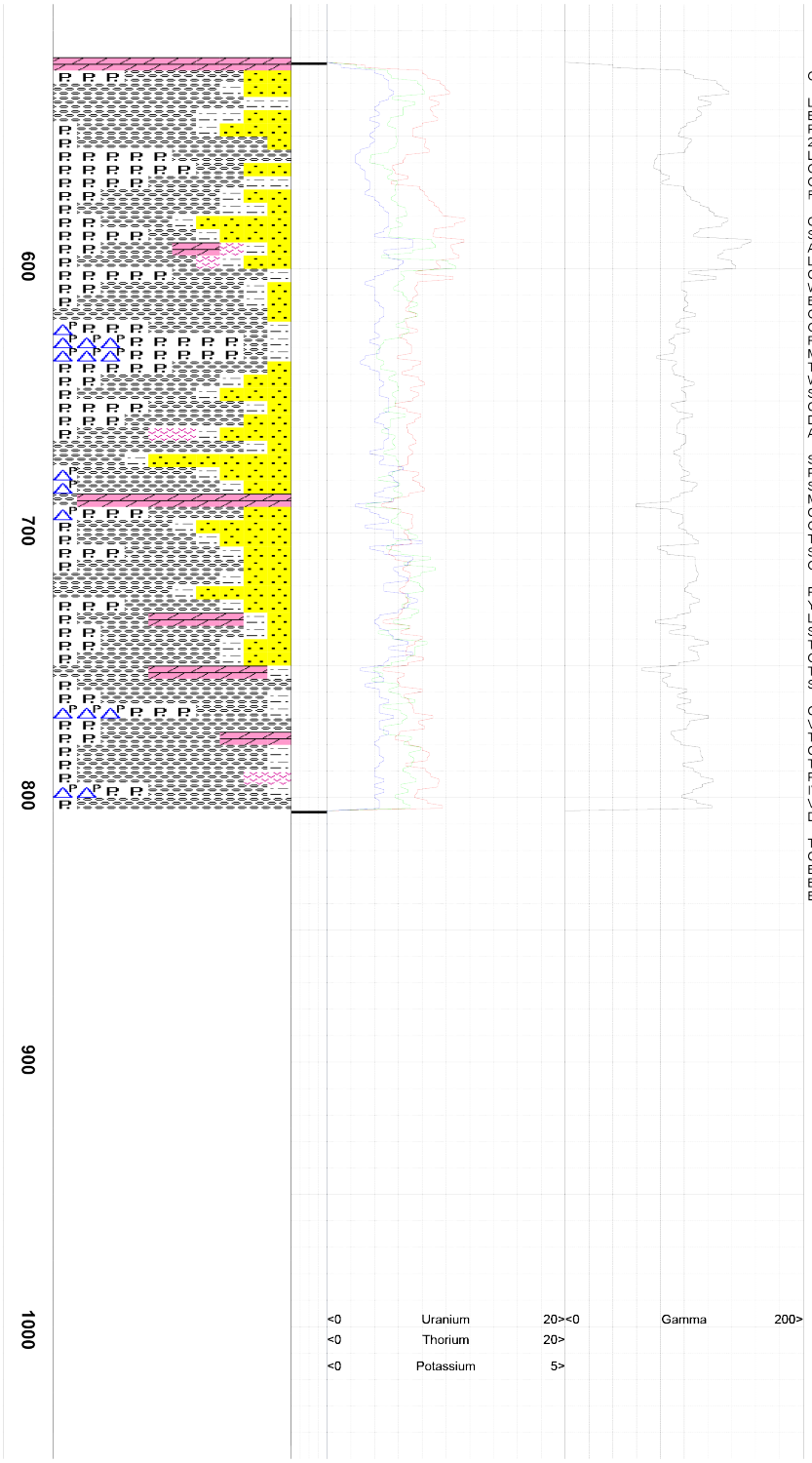

OUTCROP 4: 522'-804' (282')

LITHOLOGY: OVERALL SECTION ALTERNATES BETWEEN 6-8" SILICEOUS SHALE BEDS; 1-3" PORCELANITE BEDS AND VERY LOCALLIZED 1-2" CHERT BEDS; ABUNDANT SANDSTONES LENSES AND BEDS THROUGHOUT SECTION. OVERALL MOST CLASTIC-RICH SECTION OBSERVED IN THE CHICO MARTINEZ CREEK FIELD AREA.

QUARTZ ARENITE SANDSTONE: PRESENT IN SECTION LOCALLY AS 1-2" CONTINOUS BEDS AND LENSES AND VERY THIN cm-SCALE LENSES AND LAMINATIONS; SAND IS MOSTLY COMPOSED OF K-FELDPAR AND QUARTZ WITH MINOR MUSCOVITE AND UNDIFFER-ENTIATED LITHIC FRAGS; FINE TO VERY FIN GRAINED, OCC UPPER FINE TO LOWER MED GRAINED; SUBANGULAR TO OCC SLI SUB-ROUNDED GRAINS; MOD SORTED; VARB MATRIX AND GRAIN SUPPORTED; MATRIX TYPICALLY COMPOSED OF SILICEOUS CLAY WITH FLOATING GRAINS; GRAIN SUPPORTED SANDSTONE GRAINS TYPICALLY HAVE POINT CONTACT OR LONG CONTACT; SANDSTONE IS DOMINANTLY FIRM FRIABLE; MOD TO HIGH APPARENT POROSITY; NON CALC.

SILICEOUS SHALE: DARK YELLWSH BRWN TO PALE YELLWSH BRN; DULL EARTHY LUSTER; SMOOTH TO SLI SILTY TEXTURE DUE TO MINOR SILT CONTENT, OCC VERY SILTY; COMMON QUARTZ AND K-FELDSPAR SAND GRAIN INCLUSIONS; IRREGULAR FRACTURE; TYPICAL cm-SCALE AND mm-SCALE SAND-STONE LENSES; VERY HIGH APPARENT POR-OSITY AND LOW DENSITY; NON CALC.

PORCELANITE: DARK YELLWSH BRN TO PALE YELLWSH BRWN; SUBRESINOUS TO VITREOUS LUSTER; FINELY ABRASIVE TEXTURE DUE TO SILT CONTENT; BLOCKY FRACTURE; BRITTLE TENACITY; MASSIVE WITH NO VISIBLE LAMS OR BANDING; NON CALC; PRESENT AS THIN 1-3" BEDS WITHIN A PRINCIPALLY SAN SILICEOUS SHALE SECTION.

CHERT: PALE YELLWSH BRN; PORCELANEOUS VITREOUS LUSTER; SMOOTH TO CRYSTALLINE TEXTURE, SLI ABRASIVE DUE TO MINOR SILT CONTENT; PORCELANITE TYPICALLY GRADES TO PORCELANITE ALONG THE SAME BEDDING PLANE, LATERALLY DISCONTINUOUS; MASS-IVELY BEDDED WITH NO VIS LAMS; NON CALC VERY LOW APPARENT POROSITY; MOD DENSITY.

THICKNESS OF COVERED SECTION WAS CALCULATED TO APPROXIMATELY 698 FEET BASED ON THE AVE DIP OF 35 DEGREES BETWEEN THE OVERLYING AND UNDERLYING EXPOSED SECTIONS.

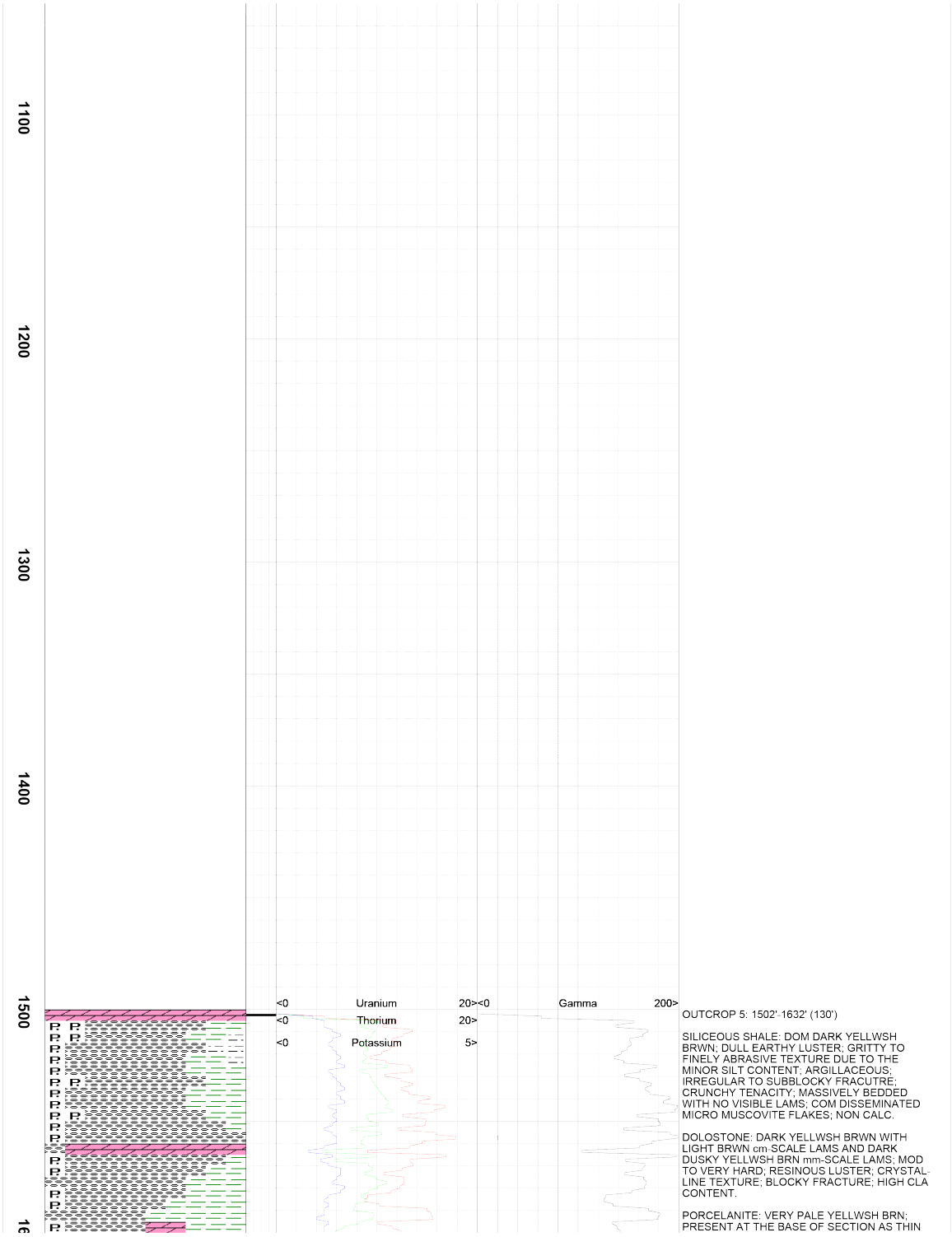
1100
1200
1300
1400
1500
<0
Uranium
20><0
Gamma
200>
<0
Thorium
20>
<0
Potassium
5>
OUTCROP 5: 1502'-1632' (130')
SILICEOUS SHALE: DOM DARK YELLWSH BRWN; DULL EARTHY LUSTER; GRITTY TO FINELY ABRASIVE TEXTURE DUE TO THE MINOR SILT CONTENT; ARGILLACEOUS; IRREGULAR TO SUBBLOCKY FRACUTRE; CRUNCHY TENACITY; MASSIVELY BEDDED WITH NO VISIBLE LAMS; COM DISSEMINATED MICRO MUSCOVITE FLAKES; NON CALC.
DOLOSTONE: DARK YELLWSH BRWN WITH LIGHT BRWN cm-SCALE LAMS AND DARK DUSKY YELLWSH BRN mm-SCALE LAMS; MOD TO VERY HARD; RESINOUS LUSTER; CRYSTALLINE TEXTURE; BLOCKY FRACTURE; HIGH CLA CONTENT.
PORCELANITE: VERY PALE YELLWSH BRN; PRESENT AT THE BASE OF SECTION AS THIN

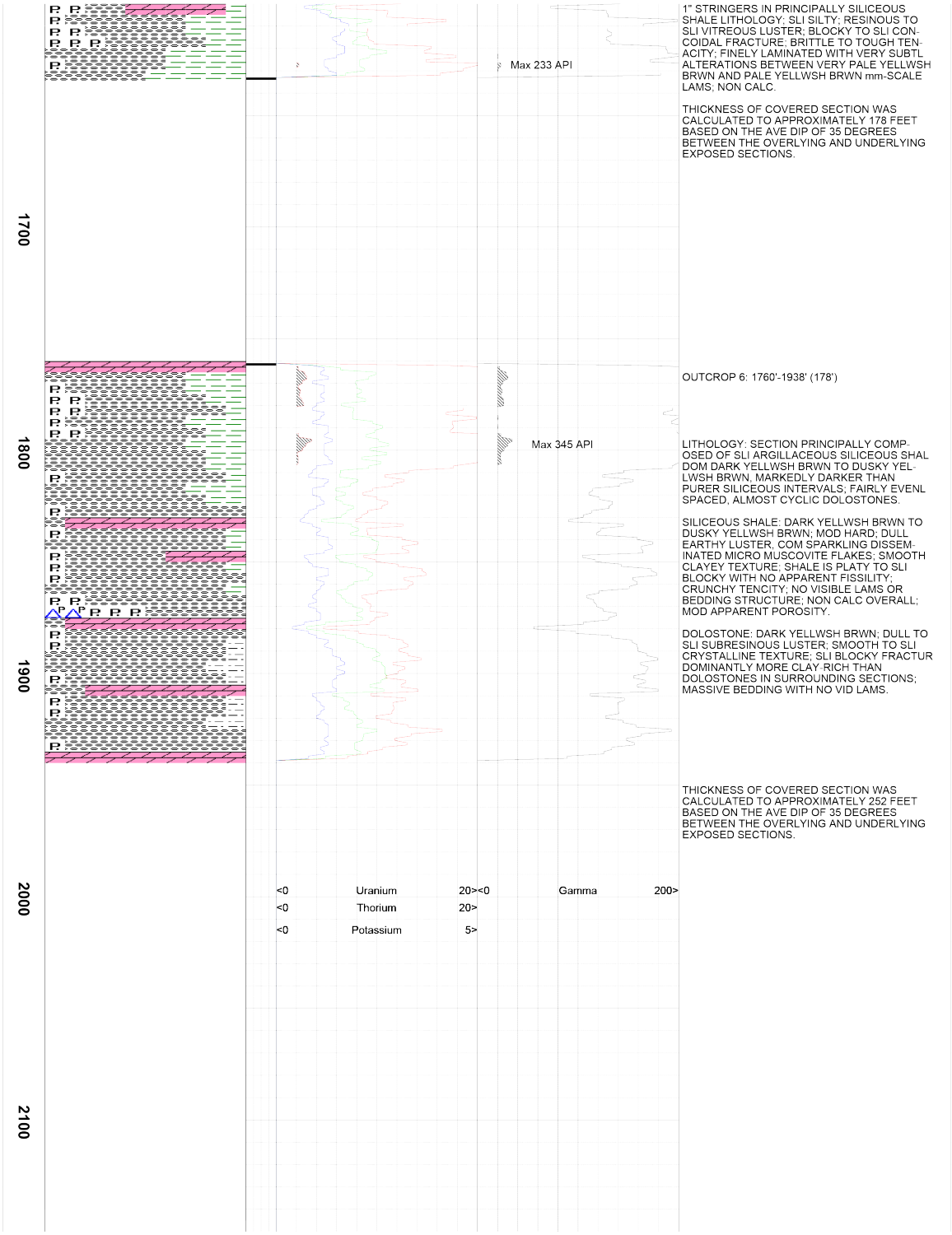

1" STRINGERS IN PRINCIPALLY SILICEOUS SHALE LITHOLOGY; SLI SILTY; RESINOUS TO SLI VITREOUS LUSTER; BLOCKY TO SLI CONCOIDAL FRACTURE; BRITTLE TO TOUGH TENACITY; FINELY LAMINATED WITH VERY SUBTL ALTERATIONS BETWEEN VERY PALE YELLWSH BRWN AND PALE YELLWSH BRWN mm-SCALE LAMS; NON CALC.

THICKNESS OF COVERED SECTION WAS CALCULATED TO APPROXIMATELY 178 FEET BASED ON THE AVE DIP OF 35 DEGREES BETWEEN THE OVERLYING AND UNDERLYING EXPOSED SECTIONS.

OUTCROP 6: 1760'-1938' (178')

LITHOLOGY: SECTION PRINCIPALLY COMPOSED OF SLI ARGILLACEOUS SILICEOUS SHAL DOM DARK YELLWSH BRWN TO DUSKY YELLWSH BRWN, MARKEDLY DARKER THAN PURER SILICEOUS INTERVALS; FAIRLY EVENL SPACED, ALMOST CYCLIC DOLOSTONES.

SILICEOUS SHALE: DARK YELLWSH BRWN TO DUSKY YELLWSH BRWN; MOD HARD; DULL EARTHY LUSTER, COM SPARKLING DISSEMINATED MICRO MUSCOVITE FLAKES; SMOOTH CLAYEY TEXTURE; SHALE IS PLATY TO SLI BLOCKY WITH NO APPARENT FISSILITY; CRUNCHY TENCITY; NO VISIBLE LAMS OR BEDDING STRUCTURE; NON CALC OVERALL; MOD APPARENT POROSITY.

DOLOSTONE: DARK YELLWSH BRWN; DULL TO SLI SUBRESINOUS LUSTER; SMOOTH TO SLI CRYSTALLINE TEXTURE; SLI BLOCKY FRACTUR DOMINANTLY MORE CLAY-RICH THAN DOLOSTONES IN SURROUNDING SECTIONS; MASSIVE BEDDING WITH NO VID LAMS.

THICKNESS OF COVERED SECTION WAS CALCULATED TO APPROXIMATELY 252 FEET BASED ON THE AVE DIP OF 35 DEGREES BETWEEN THE OVERLYING AND UNDERLYING EXPOSED SECTIONS.

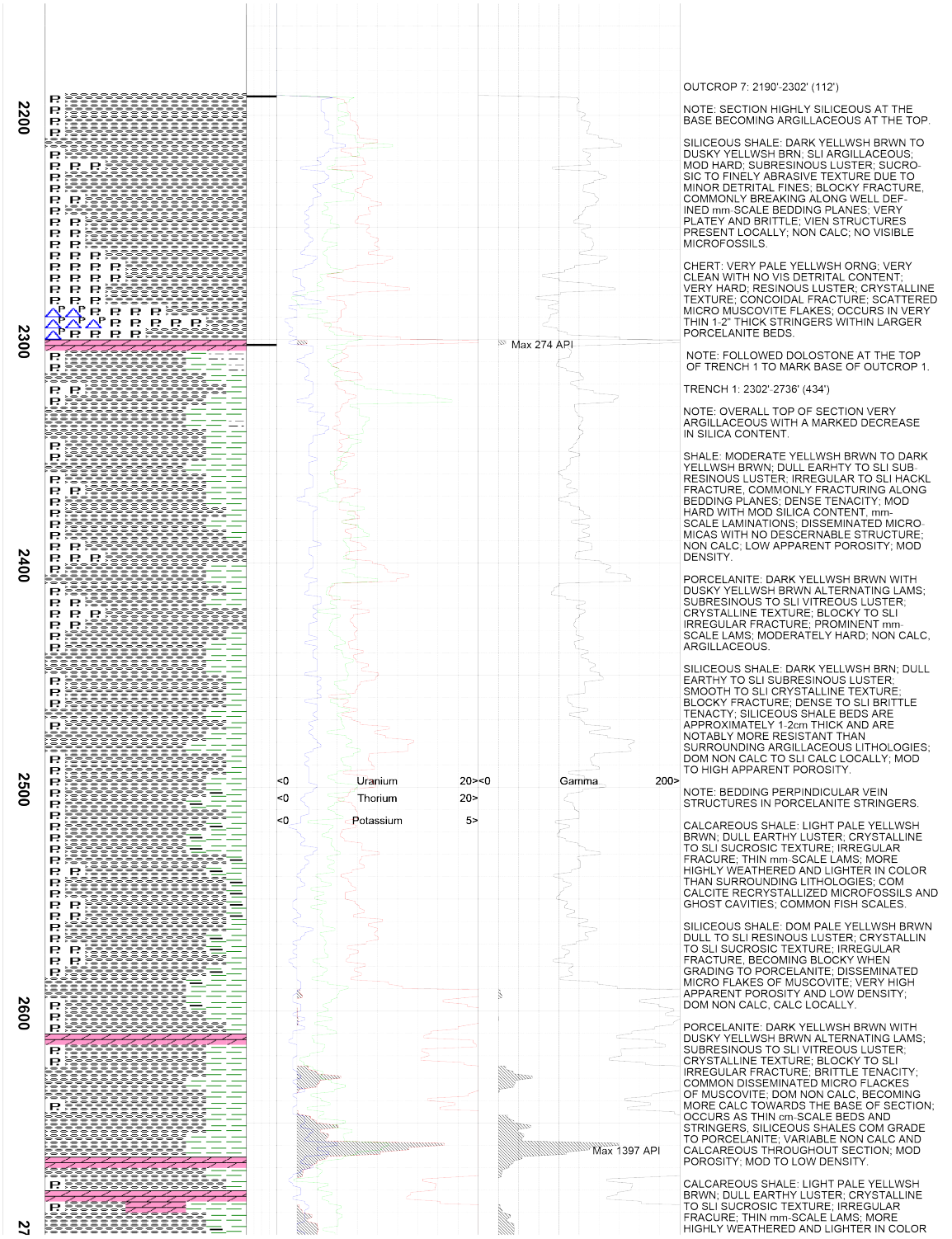

OUTCROP 7: 2190'-2302' (112')

NOTE: SECTION HIGHLY SILICEOUS AT THE BASE BECOMING ARGILLACEOUS AT THE TOP.

SILICEOUS SHALE: DARK YELLWSH BRWN TO DUSKY YELLWSH BRN; SLI ARGILLACEOUS; MOD HARD; SUBRESINOUS LUSTER; SUCROSIC TO FINELY ABRASIVE TEXTURE DUE TO MINOR DETRITAL FINES; BLOCKY FRACTURE, COMMONLY BREAKING ALONG WELL DEFINED mm-SCALE BEDDING PLANES, VERY PLATEY AND BRITTLE; VIEN STRUCTURES PRESENT LOCALLY; NON CALC; NO VISIBLE MICROFOSSILS.

CHERT: VERY PALE YELLWSH ORNG; VERY CLEAN WITH NO VIS DETRITAL CONTENT; VERY HARD; RESINOUS LUSTER; CRYSTALLINE TEXTURE; CONCOIDAL FRACTURE; SCATTERED MICRO MUSCOVITE FLAKES; OCCURS IN VERY THIN 1-2" THICK STRINGERS WITHIN LARGER PORCELANITE BEDS.

NOTE: FOLLOWED DOLOSTONE AT THE TOP OF TRENCH 1 TO MARK BASE OF OUTCROP 1.

TRENCH 1: 2302'-2736' (434')

NOTE: OVERALL TOP OF SECTION VERY ARGILLACEOUS WITH A MARKED DECREASE IN SILICA CONTENT.

SHALE: MODERATE YELLWSH BRWN TO DARK YELLWSH BRWN; DULL EARHTY TO SLI SUBRESINOUS LUSTER; IRREGULAR TO SLI HACKL FRACTURE, COMMONLY FRACTURING ALONG BEDDING PLANES; DENSE TENACITY; MOD HARD WITH MOD SILICA CONTENT, mm-SCALE LAMINATIONS; DISSEMINATED MICRO-MICAS WITH NO DESCERNABLE STRUCTURE; NON CALC; LOW APPARENT POROSITY; MOD DENSITY.

PORCELANITE: DARK YELLWSH BRWN WITH DUSKY YELLWSH BRWN ALTERNATING LAMS; SUBRESINOUS TO SLI VITREOUS LUSTER; CRYSTALLINE TEXTURE; BLOCKY TO SLI IRREGULAR FRACTURE; PROMINENT mm-SCALE LAMS; MODERATELY HARD; NON CALC, ARGILLACEOUS.

SILICEOUS SHALE: DARK YELLWSH BRN; DULL EARTHY TO SLI SUBRESINOUS LUSTER; SMOOTH TO SLI CRYSTALLINE TEXTURE; BLOCKY FRACTURE; DENSE TO SLI BRITTLE TENACTY; SILICEOUS SHALE BEDS ARE APPROXIMATELY 1-2cm THICK AND ARE NOTABLY MORE RESISTANT THAN SURROUNDING ARGILLACEOUS LITHOLOGIES; DOM NON CALC TO SLI CALC LOCALLY; MOD TO HIGH APPARENT POROSITY.

NOTE: BEDDING PERPINDICULAR VEIN STRUCTURES IN PORCELANITE STRINGERS.

CALCAREOUS SHALE: LIGHT PALE YELLWSH BRWN; DULL EARTHY LUSTER; CRYSTALLINE TO SLI SUCROSIC TEXTURE; IRREGULAR FRACURE; THIN mm-SCALE LAMS; MORE HIGHLY WEATHERED AND LIGHTER IN COLOR THAN SURROUNDING LITHOLOGIES; COM CALCITE RECRYSTALLIZED MICROFOSSILS AND GHOST CAVITIES; COMMON FISH SCALES.

SILICEOUS SHALE: DOM PALE YELLWSH BRWN DULL TO SLI RESINOUS LUSTER; CRYSTALLIN TO SLI SUCROSIC TEXTURE; IRREGULAR FRACTURE, BECOMING BLOCKY WHEN GRADING TO PORCELANITE; DISSEMINATED MICRO FLAKES OF MUSCOVITE; VERY HIGH APPARENT POROSITY AND LOW DENSITY; DOM NON CALC, CALC LOCALLY.

PORCELANITE: DARK YELLWSH BRWN WITH DUSKY YELLWSH BRWN ALTERNATING LAMS; SUBRESINOUS TO SLI VITREOUS LUSTER; CRYSTALLINE TEXTURE; BLOCKY TO SLI IRREGULAR FRACTURE; BRITTLE TENACITY; COMMON DISSEMINATED MICRO FLACKES OF MUSCOVITE; DOM NON CALC, BECOMING MORE CALC TOWARDS THE BASE OF SECTION; OCCURS AS THIN cm-SCALE BEDS AND STRINGERS, SILICEOUS SHALES COM GRADE TO PORCELANITE; VARIABLE NON CALC AND CALCAREOUS THROUGHOUT SECTION; MOD POROSITY; MOD TO LOW DENSITY.

CALCAREOUS SHALE: LIGHT PALE YELLWSH BRWN; DULL EARTHY LUSTER; CRYSTALLINE TO SLI SUCROSIC TEXTURE; IRREGULAR FRACURE; THIN mm-SCALE LAMS; MORE HIGHLY WEATHERED AND LIGHTER IN COLOR

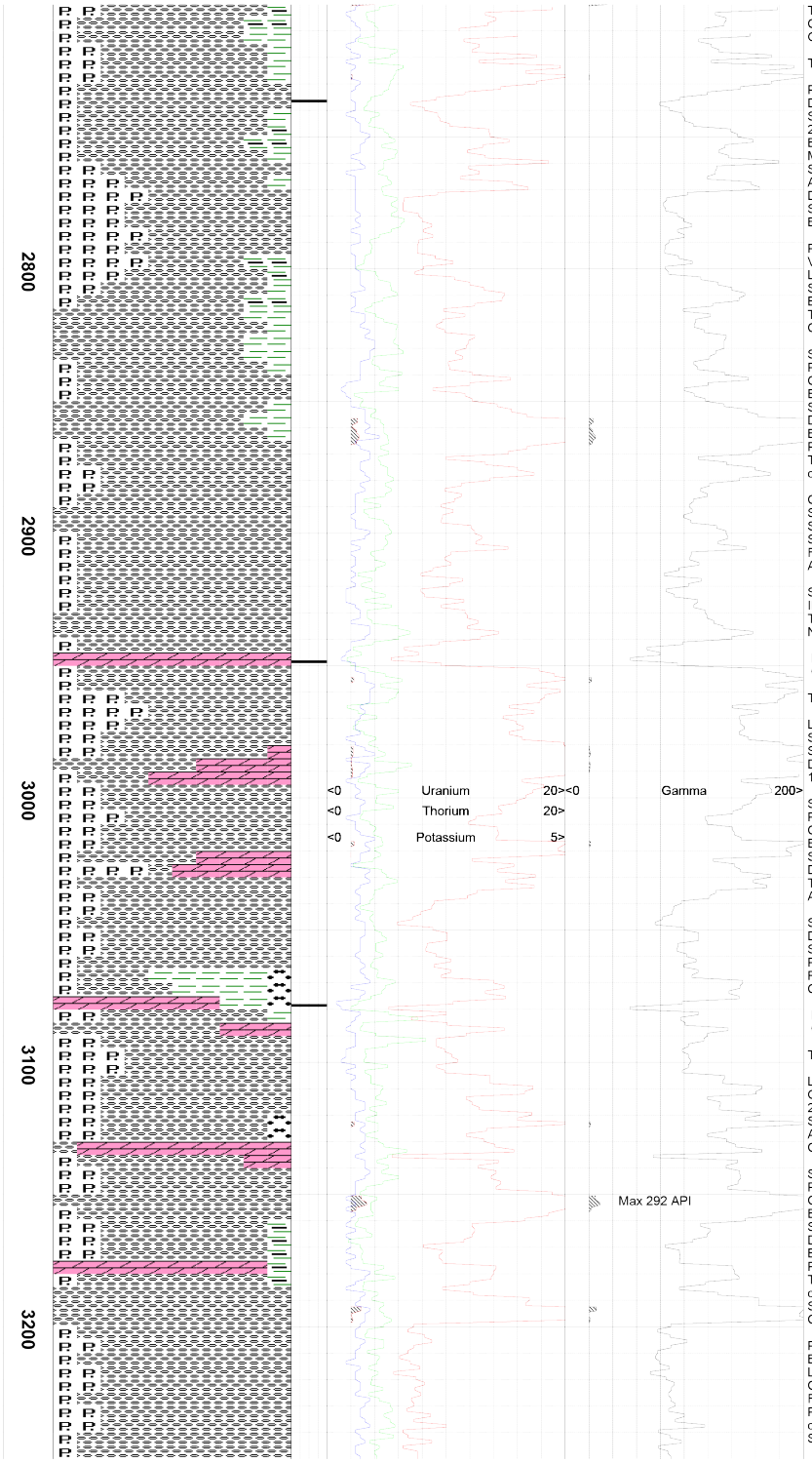

THAN SURROUNDING LITHOLOGIES; COM CALCITE RECRYSTALLIZED MICROFOSSILS AND GHOST CAVITIES.

TRENCH 2 2736'-2940' (212')

PORCELANITE: DARK YELLWSH BRN WITH DUSKY YELLWSH BRN FILLED VIEN STRUCTURES; VIEN STRUCTURES APPEAR AT 2880' AND OCCUR IN DISCRETE PORCELANITE BEDS THAT APPROXIMATELY 4-6" THICK, MOTTLED MOSAIC-LIKE APPEARANCE, STRUCTURES DOM OCCUR BOTH PARALLEL AND PERPENDICULAR TO BEDDING WITH A DOMIANT PARALLEL BEDDING PREFERENCE; SUBVITREOUS LUSTER; CRYSTALLINE TEXTURE BLOCKY FRACTURE; VERY DENSE; NON CALC.

PORCELANITE: DARK YELLWSH BRN WITH NO VIS ALTERNATING COLOR LAMS; DULL LUSTER; SMOOTH TEXTURE; BLOCKY TO SLI SPLINTERY FRACTURE WHEN VERY BRITTLE; BRITTLE TO CRUNCHY TENACITY, OCC VERY TOUGH; NO VISIBLE LAMINATIONS; NON CALC.

SILICEOUS SHALE: PALE YELLWSH BRWN TO PALE YELLWSH ORNG; OVERALL LIGHTER IN COLOR THAN UNDERLYING SECTION; DULL EARTHY TO SLI SUBRESINOUS LUSTER; SMOOTH MATTE TEXTURE WITH NO VIS DETRITAL CONTENT; IRREGULAR FRACTURE, BECOMING SLI BLOCKY WHEN GRADING TO PORCELANITE; BRITTLE TO SLI CRUNCHY TENACITY; THIN mm-SCALE LAMS TO OCC cm-SCALE LAMS; NON CALC.

CHERT: MOD YELLWSH BRN; OCCUR IN SECTION AS RARE VERY THIN 1" STRINGERS; SUBRESINOUS LUSTER; SMOOTH TO SLI CRYSTALINE TEXTURE; BLOCKY TO SLI CONCOIDA FRACTURE; VERY TOUGH TENACITY; COMPACTED FISH SCALES VISIBLE; NON CALC.

SILICEOUS SHALE: DARK YELLWSH BRWN; INTERVAL BECOMING MORE SHALEY TOWARDS THE BASE OF TRENCH; SECTION NON CALC.

NOTE: FOLLOWED DOLOSTONE AT THE TOP OF TRENCH 3 TO MARK BASE OF TRENCH 2.

TRENCH 3: 2948'-3078' (130')

LITHOLOGY: DOMINANTLY COMPOSED OF SILICEOUS SHALE WITH PORCELANITE STRINGERS AND LARGER BEDS; COMMON DOLOSTONE STRINGERS AND LARGER SCALE 1-2' BEDS.

SILICEOUS SHALE: PALE YELLWSH BRWN TO PALE YELLWSH ORNG; OVERALL LIGHTER IN COLOR THAN UNDERLYING SECTION; DULL EARTHY TO SLI SUBRESINOUS LUSTER; SMOOTH MATTE TEXTURE WITH NO VIS DETRITAL CONTENT; BRITTLE TO SLI CRUNCH TENACITY; NON CALC; COMMON FISH SCALES ALONG BEDDING PLANES.

SHALE: DOMINANTLY DARK YELLWSH BRWN; DECREASE IN SILICA CONTENT, BUT STILL S SILICEOUS; NOTABLE DECREASE IN APP POROSITY AND INCREASE IN DENSITY WITH RESPECT TO SURROUNDING LITHOLOGIES; COMMON FISH SCALES.

NOTE: FOLLOWED DOLOSTONE AT THE TOP OF TRENCH 4 TO MARK BASE OF TRENCH 3.

TRENCH 4: 3078'-3250' (172')

LITHOLOGY: INTERVAL DOMINANTLY COMPOSED OF SILICEOUS SHALE WITH 2 MAJOR 1-2' DOLOSTONE BEDS AND LOCAL DOLOSTONE STINGERS; MARKED INCREASE IN PORCELANITE THAN UNDERLYING SECTION; NON-CALCAREOUS OVERALL.

SILICEOUS SHALE: PALE YELLWSH BRWN TO PALE YELLWSH ORNG; OVERALL LIGHTER IN COLOR THAN UNDERLYING SECTION; DULL EARTHY TO SLI SUBRESINOUS LUSTER; SMOOTH MATTE TEXTURE WITH NO VIS DETRITAL CONTENT; IRREGULAR FRACTURE, BECOMING SLI BLOCKY WHEN GRADING TO PORCELANITE; BRITTLE TO SLI CRUNCHY TENACITY; THIN mm-SCALE LAMS TO OCC cm-SCALE LAMS; NON CALC; COMMON FISH SCALES ALONG BEDDING PLANES; COMMON CARBONATE-FLUORAPATITE.

PORCELANITE: ALTERNATING PALE YELLWSH BRWN WITH VERY PALE YELLWSH BRWN LAMS; VITREOUS TO SLI FROSTED LUSTER; CRYSTALLINE TEXTURE; VERY BLOCKY FRACTURE; BRITTLE DENSE TENACITY; PRESENT IN SECTION AS DOMINANTLY THIN cm-SCALE STRINGERS WITHIN LARGLY SILICEOUS SHALE SECTION.

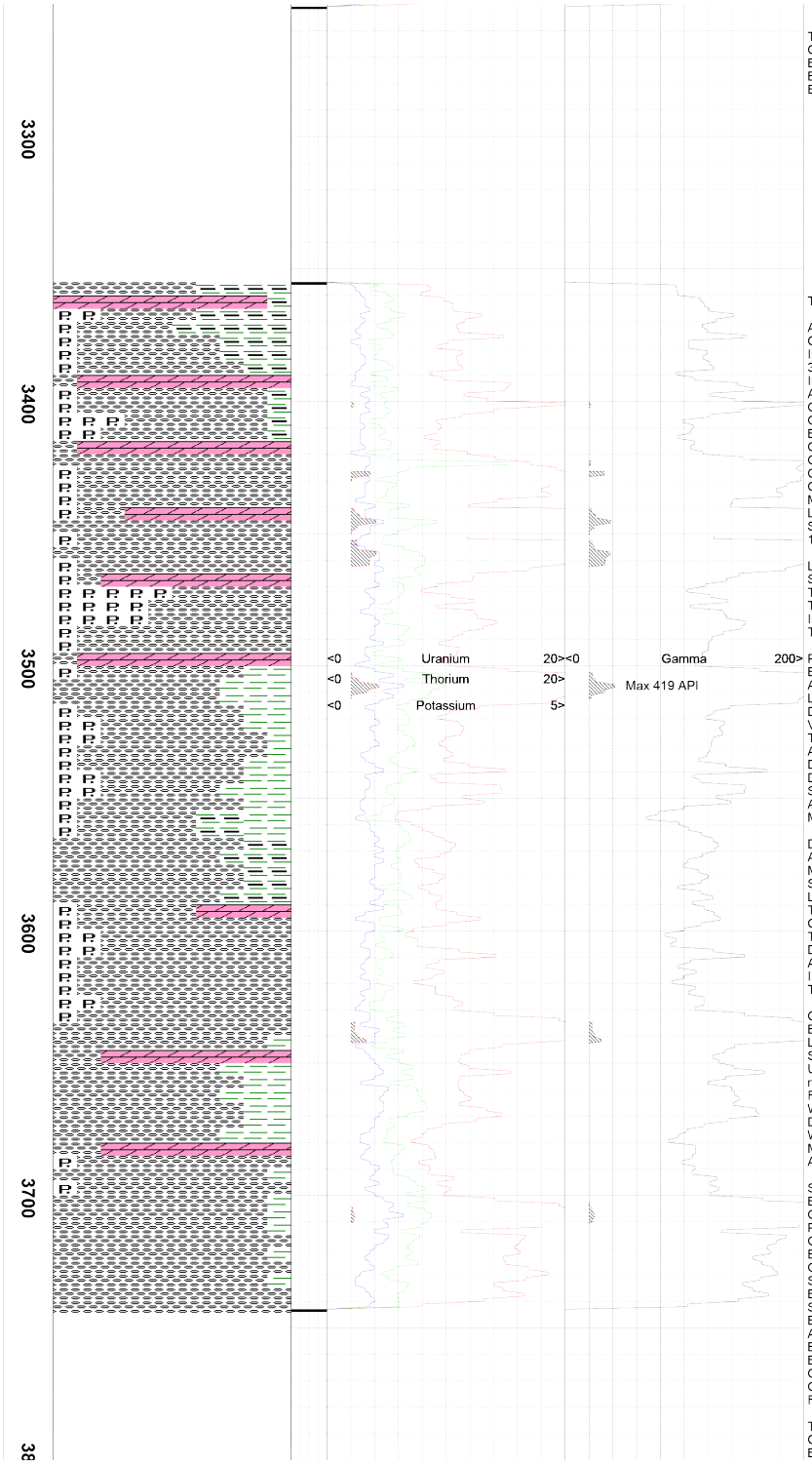

THICKNESS OF COVERED SECTION WAS CALCULATED TO APPROXIMATELY 104 FEET BASED ON THE AVE DIP OF 50 DEGREES BETWEEN THE OVERLYING AND UNDERLYING EXPOSED SECTIONS.

TRENCH 5: 3354'-3742' (388')

ANTELOPE-MCDONALD CONTACT: THIS CONTACT IS NOT ABRUPT, BUT GRADATIONAL IN NATURE; THE CONTACT WAS PLACED AT 3470' WHERE THERE APPEARS TO BE A LARGE INCREASE IN PORCELANITE, HOWEVER, SILIC APPEARS TO INCREASE GRADUALLY THROUG-OUT THE UPPER 900' OF THE MCDONALD; OVERALL THE MCDONALD IS CHARACTERIZED BY AN ABUNDACE OF PHOSPHATIC AND CALCAREOUS SHALES, AND DOLOSTONES COMPARED TO THE DOMINANTLY SILICEOUS COMPOSITION OF THE ANTELOPE; COLOR CHANGE FROM DARK YELLWSH BRN IN THE MCDONALD TO MORE PALE YELLWSH BRWN LITHOLOGIES IN THE ANTELOPE; TOTAL STRATIGRAPHIC THICKNESS OF MCDONALD = 1308'.

LITHOLOGY: SECTION DOM COMPOSED OF SILICEOUS SHALE AND SILICEOUS CALC SHAL THIN PORCELANITE BEDS AND STRINGERS THOUGHOUT THE SECTION BUT INCREASING IN FREQUENCY TOWARDS THE TOP OF TRENCH AT THE ANTELOPE CONTACT.

PORCELANITE: ALTERNATING PALE YELLWSH BRWN TO DARK YELLWSH BRWN LAMS WITH ALMOST BANDED APPEARANCE; VITREOUS LUSTER; GRITTY TO FINELY ABRASIVE TEXTU DUE TO THE PRESENCE OF DETRITAL FINES; VERY BLOCKY FRACTURE; TOUGH BRITTLE TENACITY; mm-SCALE LAMS; VARIABLE CALC AND NON-CALC, OCC ONLY CALC ALONG DISCRETE LAMS; MOD POROSITY; MOD DENSITY; MARKEDLY LOWER POROSITY THAN SILICEOUS SHALES; FIRST MAJOR PORCEL-ANITE INTERVALS AT THE TOP OF TRENCH 5, MARKS THE BASE OF THE ANTELOPE SHALE.

DOLOSTONE: ALT MOD YELLWSH BROWN AND PALE YELLWSH BRWN mm-SCALE LAMS MOD HARD TO OCC VRY HARD WHEN MORE SILICEOUS; DOM RESINOUS TO SLI FROSTED LUSTER; CRYSTALLINE TO SLI SUCROSIC TEXTURE; BLOCKY FRACTURE, BECOMING CONCOIDAL WHEN VERY SILICEOUS; PRESENT THROUGHOUT SECTION DOM AS THICK DISCRETE 1-2' BEDS, SCATTERED THIN BEDS AND STRINGERS; DOLOSTONE BEDS INCREASE IN ABUNDANCY TOWARDS THE TOP OF TRENCH 5.

CALCAREOUS SILICEOUS SHALE: DRK YELWSH BRWN TO MOD YELLWSH BRN; SUBRESINOUS LUSTER, OCC SLI EARTHY; SMOOTH TO OCC SLI SUCROSIC TEXTURE; BLOCKY TO SLI IRR ULAR FRACTURE; VARB THINLY LAMINTED ON mm-SCALE TO cm-SCALE LAMS; SHALE RANGE FROM DENSE AND BLOCKY TO HIGHLY WEATHERED AND PLATY EXHIBITING SOME DEGREE OF FISSILITY, THOUGH LIKELY A WEATHERING FEATURE; ABUNDANT GHOST MICROFOSSIL CAVITIES VIS LOCALLY; HIGH APP POROSITY; LOW DENSITY.

SILICEOUS SHALE: LIGHT MOD YELLWSH BROWN, NOTABLY LIGHTER IN COLOR THAN OTHER LITHOLOGIES WITH HIGHER APP POROSITY AND LOWER DENSITY; SUBRESIN-OUS LUSTER UNDER MICROSCOPE, DULL EARTHY LUSTER IN OUTCROP; SMOOTH TO OCC SLI FINELY ABRASIVE TEXTURE WHEN SILTY; IRREGULAR FRACTURE, BECOMING BLOCKY WHEN PORCELANEOUS; BRITTLE TO SLI CRUMBLY TENACITY; DOM mm-SCALE BEDDING WITH AN ALMOST BANDED APP ALTERNATING BETWEEN LIGHT MOD YELLOW BROWN BEDS AND DARKER YELLWSH BRN BEDS; VARIABLE SLI CALC TO NON CALC, OC ONLY CALC ALONG DISCRETE LAMINATONS OR WHERE CALCITE RECRYSTALLIZED MICRO-FOSSIL CAVITIES ARE PRESENT.

THICKNESS OF COVERED SECTION WAS CALCULATED TO APPROXIMATELY 116 FEET BASED ON THE AVE DIP OF 40 DEGREES

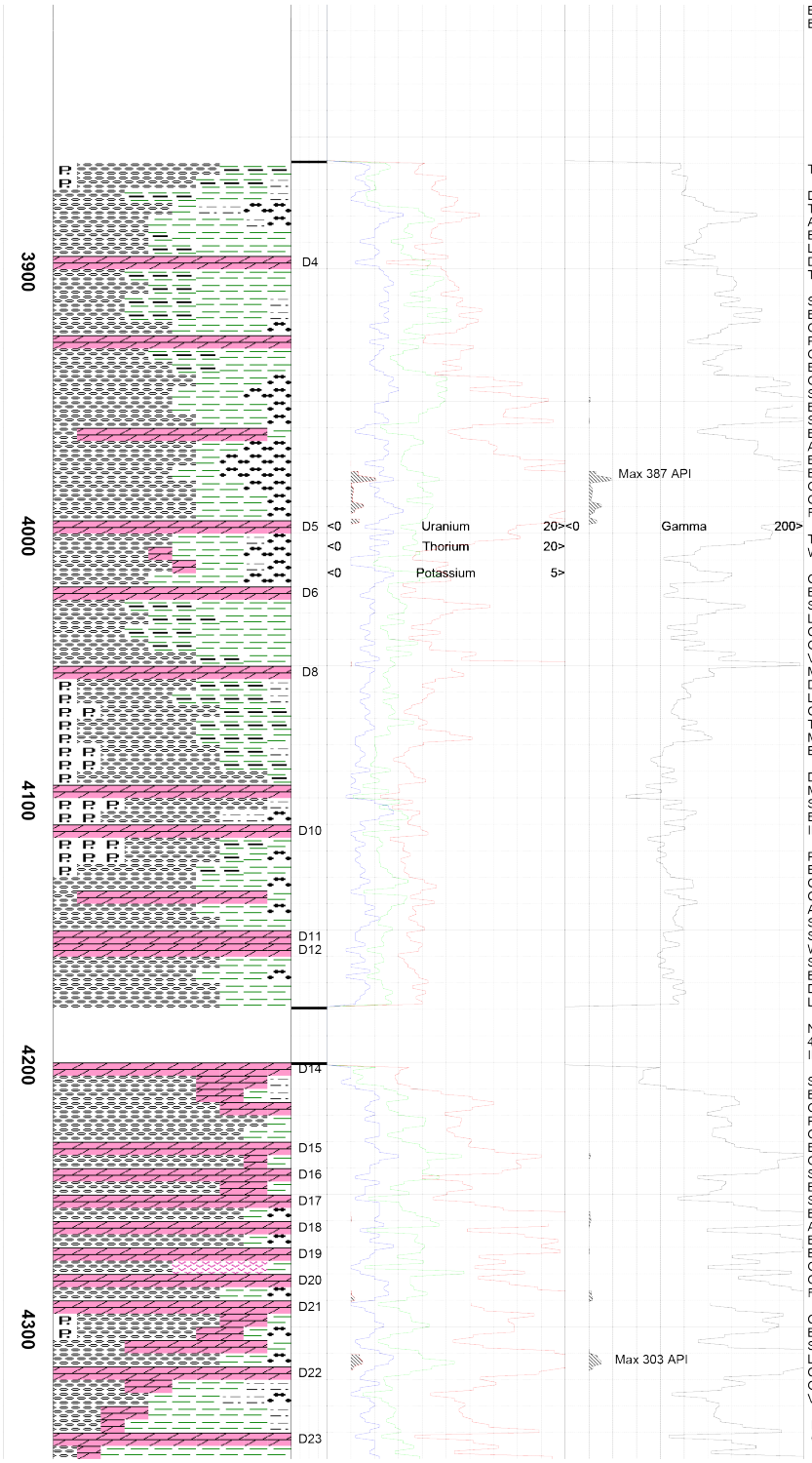

BETWEEN THE OVERLYING AND UNDERLYING EXPOSED SECTIONS.

TRENCH 6: 3858'-4346' (488')

DESCRIPTION: SLI INCREASE IN SILICA TOWARDS THE TOP OF TRENCH WITH HIGHER APP POROSITY AND LOWER DENSITY; BEGINNING TO TRANSITION INTO THE OVERLYING ANTELOPE SHALE MEMBER; MARKED DECREASE IN PHOSPHATIC SHALE COMPARED TO THE BASE OF THE MCDONALD.

SILICEOUS SHALE: LIGHT MOD YELLWSH BROWN, NOTABLY LIGHTER IN COLOR THAN OTHER LITHOLOGIES WITH HIGHER APP POROSITY AND LOWER DENSITY; SUBRESINOUS LUSTER UNDER MICROSCOPE, DULL EARTHY LUSTER IN OUTCROP; SMOOTH TO OCC SLI FINELY ABRASIVE TEXTURE WHEN SILTY; IRREGULAR FRACTURE, BECOMING BLOCKY WHEN PORCELANEOUS; BRITTLE TO SLI CRUMBLY TENACITY; DOM mm-SCALE BEDDING WITH AN ALMOST BANDED APP ALTERNATING BETWEEN LIGHT MOD YELLOW BROWN BEDS AND DARKER YELLWSH BRN BEDS: VARIABLE SLI CALC TO NON CALC, OC ONLY CALC ALONG DISCRETE LAMINATONS OR WHERE CALCITE RECRYSTALLIZED MICROFOSSIL CAVITIES ARE PRESENT.

TUFF: MODERATE ORNGSH-BRN WAXY TO SLI WAXY.

CALCAREOUS SHALE: DOM MOD YELLWSH BRN; SUBRESINOUS LUSTER UNDER MICROSCROPE, EXIBITING AN OVERALL DULL CHALK LUSTER IN OUTCROP; FINELY ABRASIVE CRYSTALLINE TEXTURE; PLANAR FRACTURE, OFTEN BREAKING ALONG BEDDING PLANES; VERY THIN mm-SCALE BEDDING, OCC SLI MORE MASSIVE IN SOME SECTIONS LIKELY DUE TO WEATHERING PATTERN; MOD TO LOW DENSITY; CRMBLY TENACTIY; COMMON CALCITE RECRYSTALLIZED MICROFOSSILS; TRACE TO SCATTERED MUSCOVITE FLAKES; SL MORE SILICEOUS THAN CALC SHALE AT THE BASE OF THE MCDONALD SECTION.

DOLOSTONE: DOM DARK YELLWSH BROWN; MOD TO HARD, BECOMING VERY HARD WHEN SILICEOUS; BECOMING INCREASING SILICEOUS AS SURROUNDING LITHOLOGY INCREASES IN SILICA CONTENT.

PHOSPHATIC SHALE: DOM DARK YELLWSH BROWN TO DSKY YELLWSH BROWN; SILICA CONTENT INCREASE IN THIS SECTION; COM CARBONATE-FLUOROAPATITE NODULES, NOT AS PROLIFIC AS BASE OF THE MCDONALD; SLI SUBRESINOUS TO EARTHY LUSTER, SMOOTH TO SLI FINELY ABRASIVE TEXTURE WHEN SILTY; DOM BLOCKY FRACTURE, OCC SLI IRREGULAR; DOM BLOCKY cm SCALE BEDDING, OCC THIN mm-SCALE BEDDING; DOM NON CALCAREOUS TO OCC SLI CALC LOCALLY.

NOTE: SECTION COVERED FROM 4180 TO 4200 DUE TO STEEP SLOPE AND CONSEQUENT INABILITY TO TRENCH.

SILICEOUS SHALE: LIGHT MOD YELLWSH BROWN, NOTABLY LIGHTER IN COLOR THAN OTHER LITHOLOGIES WITH HIGHER APP POROSITY AND LOWER DENSITY; SUBRESINOUS LUSTER UNDER MICROSCOPE, DULL EARTHY LUSTER IN OUTCROP; SMOOTH TO OCC SLI FINELY ABRASIVE TEXTURE WHEN SILTY; IRREGULAR FRACTURE, BECOMING BLOCKY WHEN PORCELANEOUS; BRITTLE TO SLI CRUMBLY TENACITY; DOM mm-SCALE BEDDING WITH AN ALMOST BANDED APP ALTERNATING BETWEEN LGHT MOD YELLWSH BROWN BEDS AND DARKER YELLWSH BRN BEDS: VARIABLE SLI CALC TO NON CALC, OC ONLY CALC ALONG DISCRETE LAMINATONS OR WHERE CALCITE RECRYSTALLIZED MICROFOSSIL CAVITIES ARE PRESENT.

CALCAREOUS SHALE: DOM MOD YELLWSH BRN; SUBRESINOUS LUSTER UNDER MICROSCROPE, EXIBITING AN OVERALL DULL CHALK LUSTER IN OUTCROP; FINELY ABRASIVE CRYSTALLINE TEXTURE; PLANAR FRACTURE, OFTEN BREAKING ALONG BEDDING PLANES; VERY THIN mm-SCALE BEDDING.

NOTE: FOLLOWED DOLOSTONE AT THE TOP OF TRENCH 7 TO MARK BASE OF TRENCH 6.

TRENCH 7: 4344'-4664' (318')

LITHOLOGY: OVERALL THIS SECTION IS COMOPOSED OF VERY DARK YELLWSH BRWN PHOSPHATIC SHALE IN THE LOWER 360' AND TRANSITIONS INTO A LIGHER MORE CALC-AREOUS SHALE TOWARDS THE TOP. SILICA CONTENT ALSO INCREASES TOWARDS THE TOP OF TRENCH; THE LOWER PHOSPHATIC ZONE CONTAINS ABUNDANT CARBONATE-FLUORAPATITE NODULES THAT RANGE IN SIZE FROM THIN mm-SCALE COMPACTED AND DEFORMED BLEBS ALONG BEDDING PLANES TO LARGER cm-SCALE NODULES; PHOS-PHATIC SHALES ARE CHARACTERISTICALLY MORE DENSE AND LOWER IN APPARENT POROSITY THAN OVERLYING SILICEOUS SHALES; SHALES TYPICALLY HAVE A FINELY ABRASIVE TEXTURE DUE TO MINOR SILT CONTENT.

CALCAREOUS SHALE: DOM MOD YELLWSH BRN; SUBRESINOUS LUSTER UNDER MICRO-SCROPE, EXIBITING AN OVERALL DULL CHALK LUSTER IN OUTCROP; FINELY ABRASIVE CRYSTALLINE TEXTURE; PLANAR FRACTURE, OFTEN BREAKING ALONG BEDDING PLANES; VERY THIN mm-SCALE BEDDING, OCC SLI MORE MASSIVE IN SOME SECTIONS LIKELY DUE TO WEATHERING PATTERN; MOD TO LOW DENSITY; CRMBLY TENACTIY; COMMON CALCITE RECRYSTALLIZED MICROFOSSILS; TRACE TO SCATTERED MUSCOVITE FLAKES; SL SILTY LOCALLY.

VOLCANIC TUFF: DOM DUSKY YELWSH BRN; SMOOTH WAXY TEXTURE; 2" THICK.

DOLOSTONE: DOM DARK YELLWSH BROWN; MOD TO HARD, BECOMING VERY HARD WHEN SILICEOUS; RESINOUS TO ALMOST CRYSTAL-LINE LUSTER; DOM SUCROSIC TEXTURE, BECOMING SMOOTHER WITH INCREASE IN CLAY CONTENT; COMMON THIN CALCITE FRACTURE HEALINGS; VARIABLE THINI mm to cm-SCALE BEDDING TO OCC MASSIVE BED-DING; VARIABLE SLI SILICEOUS TO SLI MOR CLAY-RICH, WITH VRY PROMINENT RESISTIVE CHERTY DOLOSTONE BEDS IN SOME SECTIONS VARIABLE 1-2' BEDS AND 1-2" STRINGERS.

PHOSPHATIC SHALE: DOM DARK YELLWSH BROWN TO DSKY YELLWSH BROWN WITH COMMON WHITE TO SLI PALE PINKISH WHITE CARBONATE-FLUOROAPATITE NODULES; NODULES RANGE IN SIZE FROM SMALL mm-SCALE DEFORMED BLEBS TO LARGE cm-SCALE NODULES; DOM DULL EARTHY LUSTER; SMOOTH TO OCC SLI GRITTY TEXTURE WHEN SILTY; DOM BLOCKY FRACTURE, OCC SLI IRR EGULAR; DOM BLOCKY cm-SCALE BEDDING, OCC THINLY BEDDED AND EXIBITIING A SLI FISSILITY; DOM NON CALCAREOUS TO SLI CALC LOCALLY.

THICKNESS OF COVERED SECTION WAS CALCULATED TO APPROXIMATELY 504 FEET BASED ON THE AVE DIP OF 40 DEGREES BETWEEN THE OVERLYING AND UNDERLYING EXPOSED SECTIONS.

NOTE: THE BASE OF THE MCDONALD IS POSITIONED AT 4778' BASED ON AN ABRUPT SLOPE BREAK 112' FROM THE BASE OF TRENCH 7. TOTAL STRATIGRAPHIC THICKNESS OF DEVILWATER SHALE = 802'.

TRENCH 8: 5168'-5324' (156')

LITHOLOGY: DOM LIGHT OLIVE TO SLI BLUIS GREY SILTY CALCAREOUS CLAYSTONE WITH ABUNDANT RECRYSTALLIZED MICROFOSSIL CAVITIES; LOCAL NON-CALCAREOUS INTER-VALS; OVERALL HIGHER DETRITAL CONTENT THAN THE UNDERLYING GOULD MEMBER. DOMINANTLY SILTY, BECOMING SLI SANDY LOCALLY; INTENSLY FRACTURED; ROCKS EXIBIT A SUBRESINOUS TO SLI SPARKLING LUSTER DUE TO DISSEMINATED MUSCOVITE; HIGHLY CALCAREOUS AT THE TOP OF TRENCH BECOMING DOM NON- CALCAREOUS BELOW 5290'; ASIDE FROM THE VARIATION BETWEEN CALC AND NON-CALC INTERVALS, THE LITHOLOGY IN THIS SECTION IS OVERALL FAIRLY HOMOGENOUS.

DOLOSTONE: DOM DARK YELLWSH ORNG; MOD DENSITY; DULL AND EARTHY TO SLI WAXY LUSTER; MATTE TEXTURE; SCATTERED SAND AND SILT GRAINS; NON SILICEOUS WIT HIGHER CLAY CONTENT THAN DOLOSTONE BEDS IN THE GOULD MEMBER.

NON CALCAREOUS SILTY CLAYSTONE: LIGHT OLIVE TO SLIGHTLY BLUISH GREY; CONCHOID AL FRACTURE; HIGHLY FRACTURED MAKING BEDDING ATTITUDE DIFFICULT TO DETERMINE DULL TO SLI SUBBRESINOUS LUSTER; ABUN-DANT FINE SAND AND SILTSTONE INCLUSIONS NO VISIBLE MICROFOSSIL CAVITIES.

THICKNESS OF COVERED SECTION WAS CALCULATED TO APPROXIMATELY 170 FEET BASED ON THE AVE DIP OF 35 DEGREES BETWEEN THE OVERLYING AND UNDERLYING EXPOSED SECTIONS.

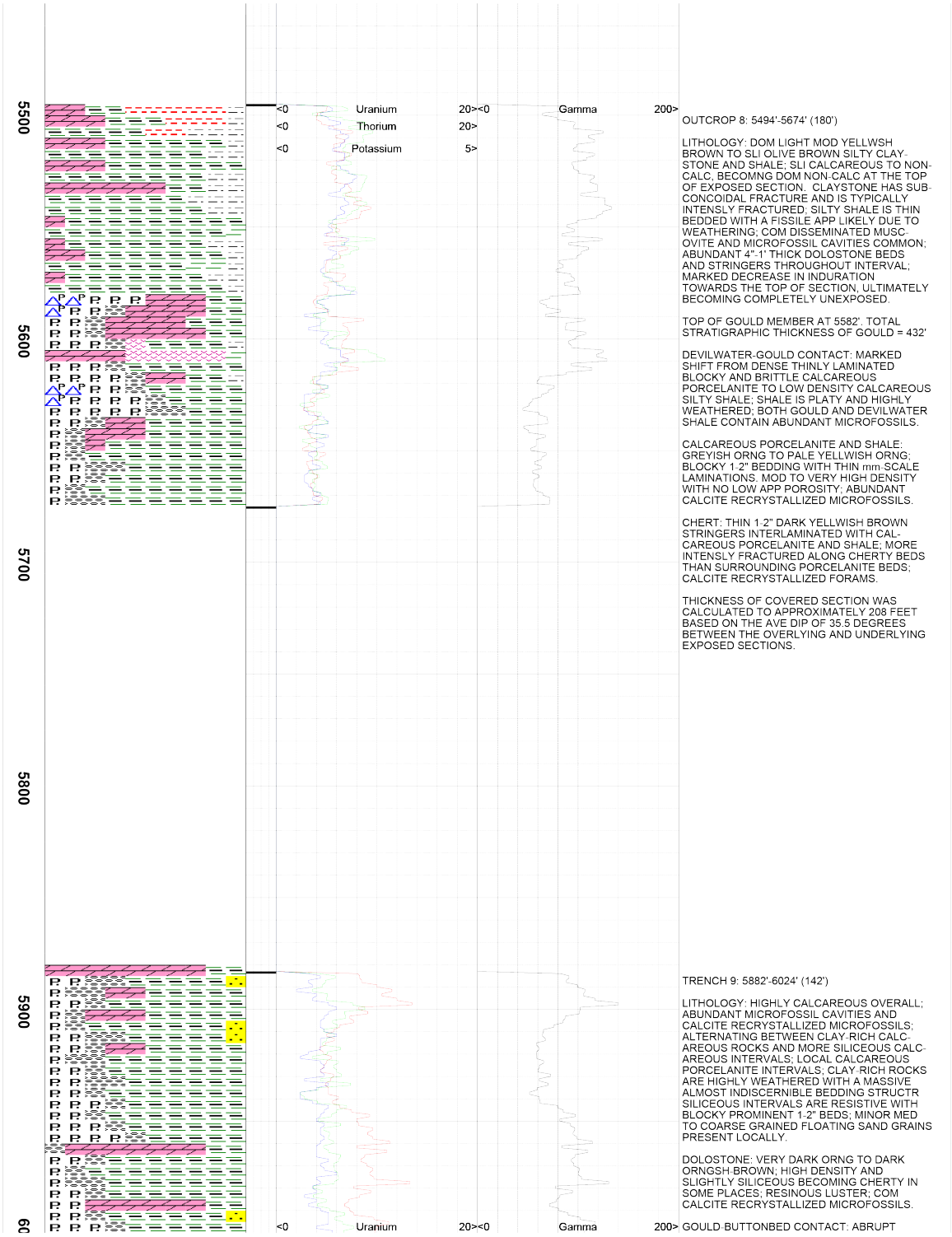
5500
5600
5700
5800
5900
<0
Uranium
20><0
Gamma
200>
<0
Thorium
20>
<0
Potassium
5>
OUTCROP 8: 5494'-5674' (180')
LITHOLOGY: DOM LIGHT MOD YELLWSH BROWN TO SLI OLIVE BROWN SILTY CLAYSTONE AND SHALE; SLI CALCAREOUS TO NON-CALC, BECOMNG DOM NON-CALC AT THE TOP OF EXPOSED SECTION. CLAYSTONE HAS SUB-CONCOIDAL FRACTURE AND IS TYPICALLY INTENSLY FRACTURED; SILTY SHALE IS THIN BEDDED WITH A FISSILE APP LIKELY DUE TO WEATHERING; COM DISSEMINATED MUSCOVITE AND MICROFOSSIL CAVITIES COMMON; ABUNDANT 4"-1' THICK DOLOSTONE BEDS AND STRINGERS THROUGHOUT INTERVAL; MARKED DECREASE IN INDURATION TOWARDS THE TOP OF SECTION, ULTIMATELY BECOMING COMPLETELY UNEXPOSED.
TOP OF GOULD MEMBER AT 5582'. TOTAL STRATIGRAPHIC THICKNESS OF GOULD = 432'
DEVILWATER-GOULD CONTACT: MARKED SHIFT FROM DENSE THINLY LAMINATED BLOCKY AND BRITTLE CALCAREOUS PORCELANITE TO LOW DENSITY CALCAREOUS SILTY SHALE; SHALE IS PLATY AND HIGHLY WEATHERED; BOTH GOULD AND DEVILWATER SHALE CONTAIN ABUNDANT MICROFOSSILS.
CALCAREOUS PORCELANITE AND SHALE: GREYISH ORNG TO PALE YELLWISH ORNG; BLOCKY 1-2" BEDDING WITH THIN mm-SCALE LAMINATIONS. MOD TO VERY HIGH DENSITY WITH NO LOW APP POROSITY; ABUNDANT CALCITE RECRYSTALLIZED MICROFOSSILS.
CHERT: THIN 1-2" DARK YELLWISH BROWN STRINGERS INTERLAMINATED WITH CALCAREOUS PORCELANITE AND SHALE; MORE INTENSLY FRACTURED ALONG CHERTY BEDS THAN SURROUNDING PORCELANITE BEDS; CALCITE RECRYSTALLIZED FORAMS.
THICKNESS OF COVERED SECTION WAS CALCULATED TO APPROXIMATELY 208 FEET BASED ON THE AVE DIP OF 35.5 DEGREES BETWEEN THE OVERLYING AND UNDERLYING EXPOSED SECTIONS.
TRENCH 9: 5882'-6024' (142')
LITHOLOGY: HIGHLY CALCAREOUS OVERALL; ABUNDANT MICROFOSSIL CAVITIES AND CALCITE RECRYSTALLIZED MICROFOSSILS; ALTERNATING BETWEEN CLAY-RICH CALCAREOUS ROCKS AND MORE SILICEOUS CALCAREOUS INTERVALS; LOCAL CALCAREOUS PORCELANITE INTERVALS; CLAY-RICH ROCKS ARE HIGHLY WEATHERED WITH A MASSIVE ALMOST INDISCERNIBLE BEDDING STRUCTR SILICEOUS INTERVALS ARE RESISTIVE WITH BLOCKY PROMINENT 1-2" BEDS; MINOR MED TO COARSE GRAINED FLOATING SAND GRAINS PRESENT LOCALLY.
DOLOSTONE: VERY DARK ORNG TO DARK ORNGSH-BROWN; HIGH DENSITY AND SLIGHTLY SILICEOUS BECOMING CHERTY IN SOME PLACES; RESINOUS LUSTER; COM CALCITE RECRYSTALLIZED MICROFOSSILS.
GOULD-BUTTONBED CONTACT: ABRUPT

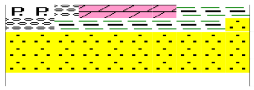

TRANSITION FROM DARK YELLWSH ORNG MOD TO POORLY SORTED, MED TO COARSE-GRAINED ARKOSIC ARENITE SANDSTONE TO CALCAREOUS SHALE AT 6012'.

The log data, interpretations and recommendation provided by Epoch are inferences and assumptions based on measurements of drilling fluids. Such inferences and assumptions are not infallible and reasonable professionals may differ. Epoch does not represent or warrant the accuracy, correctness or completeness of any log data, interpretations, recommendations or information provided by Epoch, its officers, agents or employees. Epoch does not and cannot guarantee the accuracy of any such interpretation of the log data, interpretations or recommendations and Company is fully responsible for all decisions and actions it takes based on such log data, interpretations and recommendations.

REFERENCES

Adams, J. A. S., and Weaver, C. E., 1958, Thorium-to-uranium ratios as indicators of sedimentary processes: example of concept of geochemical facies: AAPG Bulletin, v. 42, p. 387-440.

Atwater, T., 1970, Implications of plate tectonics for the Cenozoic tectonic evolution of western North America: Geologic Society of America Bulletin, v. 81, p. 3513-3535.

Atwater, T., and Molnar, P., 1973, Relative motion of the Pacific and North American plates deduced from sea-floor spreading in the Atlantic, Indian, and South Pacific Oceans, *in* Kovach, R. L., and Nur, A., eds., Proceedings of the conference on tectonic problems of the San Andreas fault system: Stanford University Publications in Geological Science, v. 13, p. 136-148.

Barron, J. A., 1981a, Late Cenozoic diatom biostratigraphy and paleoceanography of the middle latitude eastern north Pacific, Deep Sea Drilling Project Leg 63, *in* Initial reports of the Deep Sea Drilling Project: Washington, U. S., Government Printing Office, v. 63, p. 507-538.

Barron, J. A., 1981b, Middle Miocene diatom biostratigraphy of Deep Sea Drilling Project Site 77B in the eastern equatorial Pacific: Geoscience Journal, v. 2, no. 2, p. 137-144.

Barron, J. A., 1986, Paleoceanographic and tectonic controls on deposition of the Monterey Formation and related siliceous rocks in California: Palaeogeography, Palaeoclimatology, Palaeoecology v. 53, p. 27-15.

Barron, J. A., and Isaacs, C. M., 2001. Updated Chronostratigraphic framework for the California Miocene, *in* Isaacs, C. M., and Rullkotter, J., eds., The Monterey Formation: From Rocks to Molecules: Columbia University Press: New York, p. 393-395.

Bartow, J. A., 1991, The Cenozoic evolution of the San Joaquin Valley, CA: U.S. Geological Survey Professional Paper 1501, 40 p.

Bartow, J. A., 1992, Paleogene and Neogene time-scales for southern California: U.S. Geological Survey Open-File Report, p. 92-212.

Bell, F. W., 1937. Untitled Shell report, 507p.

Berrgren, W. A., 1972, A Cenozoic time-scale - some implications for regional geology and paleobiogeography: Lethaia, v. 5, no. 2, p. 195-215.

Berrgren, W. A., and Miller, K. G., 1989, Cenozoic bathyal and abyssal calcareous benthic foraminiferal zonation: Micropaleontology, v. 35, no. 4, p. 308-320.

Blake, M. C., Jr., Campbell, R. H., Dibblee, T. W., Jr., Howell, D. G., Nilsen, T. H., Normark, W. R., Vedder, J. C., and Silver, E. A., 1978, Neogene basin formation in relation to plate-tectonic evolution of San Andreas fault system, California: AAPG Bulletin, v. 62, p. 1173-1184.

Bohacs, K., 1993, Source quality variation tied to sequence development in the Monterey and associated formations, southwestern California, *in* Katz, B. J., and Pratt, L. M., AAPG Studies in Geology #37, Tulsa, Oklahoma, Ch. 12, p. 177-204.

Bramlette, M. N., 1946, The Monterey Formation of California and the origin of its siliceous rocks: U.S. Geological Survey Professional Paper 212, 57 p.

Bukry, D., 1973, Low-latitude coccolith biostratigraphic zonation, *in* Edgar, N. T., Kaneps, A. G., and Herring, J. R., eds., Initial reports of the Deep Sea Drilling Project, volume 15: Washington, D.C., U.S. Government Printing Office, p. 685-703.

Bukry, D., 1975, Coccolith and silicoflagellate stratigraphy, northwestern Pacific Ocean, Deep Sea Drilling Project Leg 32, *in* Gardner, J. V., ed., Initial reports of the Deep Sea Drilling Project, volume 32: Washington, D.C., U.S. Government Printing Office, p. 677-692.

Callaway, D. C., 1990, Organization of stratigraphic nomenclature for the San Joaquin basin, California, *in* Kuespert, J. G., and Reid, S. A., eds., Structure, stratigraphy, and hydrocarbon occurrences of the San Joaquin basin, California: Bakersfield, California, Pacific Section, Society of Economic Paleontologists and Mineralogists and Association of Petroleum Geologists, v. 64, p. 5-21.

Chaika, C.J., and Dvorkin, J., 2000, Porosity reduction during diagenesis of diatomaceous rocks: AAPG Bulletin, v. 84, p. 1173-1184.

Compton, J. S., 1991, Porosity reduction and burial history of siliceous rocks from the Monterey and Sisquoc Formations, Point Pedernales area, California: Geological Society of America Bulletin, v. 103, p. 625-636.

DePaolo, D. J., and Finger, K. L., 1991, High-resolution strontium-isotope stratigraphy and biostratigraphy of the Miocene Monterey Formation, central California: Geological Society of America Bulletin, v. 103, p. 112-124.

Dibblee, T. W., Jr., 2006, Geologic map of the Carneros Rocks and Belridge quadrangles, San Luis Obispo and Kern Counties, California: Dibblee Geological Foundation, Map DF-274 (Minch, J. A., ed.), scale 1:24,000.

Dibblee, T. W., Jr., 1973, Stratigraphy of the southern Coast Ranges near the San Andreas Fault from Cholame to Maricopa, Califronia: U.S. Geological Survey Professional Paper 764, 45 p.

Dickinson, W. R., and Seely, 1979, Structure and stratigraphy of forearc regions: AAPG Bulletin, v. 63, p. 2-31.

Dickinson, W. R., and Snyder, W. S., 1979, Geometry of triple junctions related to San Andreas transform: Journal of Geophysical Research, v. 84, p. 561-572.

Doveton, J. H., and Merriam, D. F., 2004, Borehole petrophysical chemostratigraphy of Pennsylvanian black shales in the Kansas subsurface: Chemical Geology, v. 206, p. 249-285.

Dypvik, H., and Harris, N. B., 2001, Geochemical facies analysis of fine-grained siliciclatics using Th/U, Zr/Rb and (Zr + Rb)/Sr ratios: Chemical Geology, v. 181, p. 131-146.

Ellis, Darwin V. 1987, Well Logging for Earth Scientists: Elsevier Science Publishing Co., Inc. page 190.

Foss, C. D., and Blaisdell, R., 1968, Stratigraphy of the west side southern San Joaquin Valley, *in* Karp, S. E., ed., Guidebook to geology and oil fields of the west side southern San Joaquin Valley: Pacific Section AAPG, SEG, SEPM Annual Field Trip Guidebook, p. 33-43.

Friedman, I., and Murata, K. J., 1979, Origin of dolomite in Miocene Monterey Shale and related formations in the Temblor Range, California: Geochimica et Cosmochimica Acta, 43(8), p. 1357-1366.

Gautier, D. L., Scheirer, A. H., Tennyson, M. E., Peters, K. E., Magoon L. B., Lillis, P. G., Charpentier, R. R., Cook, T. A., French, C. D., Klett, T. R., Pollastro, R. M., Schenk, C. J., 2003, Executive summary – assessment of undiscovered oil and gas resources of the San Joaquin Basin Province of California: U.S. Geological Survey Professional Paper 1713, ch. 1.

Gaylord, E. G., and Hanna, G. D., 1924, Correlation of organic shales in the southern end of the San Joaquin Valley: AAPG Bulletin, v. 9, p. 228-236.

Goudkoff, P. P., 1934, Subsurface stratigraphy of Kettleman Hills oil field, California: AAPG Bulletin, v. 18, p. 435-475.

Graham, S. A., and Williams L. A., 1985, Tectonic, depositional, and diagenetic history of the Monterey Formation (Miocene), central San Joaquin basin, California: AAPG Bulletin, v. 69, p. 385-341.

Hanna, G. D., 1928, The Monterey Shale of California at its type locality with a summary of its fauna and flora: AAPG Bulletin, v. 12, p. 969-983.

Harding, T. P., 1976, Tectonic significance and hydrocarbon trapping consequences of sequential folding synchronous with San Andreas faulting, San Joaquin Valley, California: AAPG Bulletin, v. 60, p. 356-378.

Haq , B. U., Hardenbol, J., and Vail, P. R., 1987a, Chronology of fluctuating sea levels since the Triassic: Science, v. 235, p. 1156-1167.

Haq, B. U., Hardenbol, J., and Vail, P. R., 1987b, The new chronostratigraphic basis of Cenozoic and Mesozoic sea level cycles, *in* Ross, C. A., and Harman, D., eds., Time and depositional history of eustatic sequences – Constraints on seismic stratigraphy: Cushman Foundation for Foraminiferal Research Special Publication 24, p. 7-13.

Haq, B. U., Hardenbol, J., and Vail, P, R., 1988, Mesozoic and Cenozoic chronostratigraphy and cycles of sea-level changes, *in* Wilgus, C. K., Hastings, B. S., Ross, C. A., Posamentier, H., Van Wagoner, J., and Kendell, C. G. S. C. eds., Sea-level changes – An integrated approach: Tulsa, Okla, Society of Economic Paleontologists and Mineralogists Special Publication 42, p. 71-108.

Heitman, H. L., 1986, The Chico Martinez/Zemorra Creek surface section; A west side San Joaquin Valley reference section (unpublished industry report), 107p.

Henry, C. D., 2009, Uplift of the Sierra Nevada, California: The Geological Society of America, v. 37, p. 575-576.

Hesselbo, S. P., 1996, Spectral gamma-ray logs in relationto clay mineralogy and sequence stratigraphy, Cenozoic of the Atlantic margin, offshore New Jersey, *in* Mountain, G. S., Miller, K. G., Blum, P., Poag, C. W., and Twichell, D. C., eds., Proceeding of the Ocean Drilling Program, Scientific Results, v. 150, p. 411-422.

Hudson, F. S., and White G. H., 1941, Thrust faulting and coarse clastics in Temblor Range, California: AAPG Bulletin, v. 25, p. 1327-1342.

Ingle, J. C., Jr., 1981, Origin of Neogene diatomites around the north Pacific rim, *in* Garrison, R. E., and Douglas, R. G., eds., The Monterey Formation and related

siliceous rocks of California: Los Angeles, Pacific Section, Society of Economic Paleontologists and Mineralogists, p. 159-179.

Isaacs, C. M., 1981, Field characterization of rocks in the Monterey Formation along the coast near Santa Barbara, California, *in* Isaacs, C. M., eds., Guide to the Monterey Formation in the California Coastal area, Ventura to San Luis Obispo: Pacific Section, AAPG, v. 52, p. 39-54.

Isaacs, C. M., 1983, Compositional variation and sequence in the Miocene Monterey Formation, Santa Barbara coastal area, California, *in* Larue, D. K., and Steel, R. J., eds., Cenozoic Marine Sedimentation, Pacific margin, USA. Pacific Section, Society of Economic Paleontologists and Minerologists Special Publication, p. 117-132.

Isaacs, C. M., 2001, Depositional framework of the Monterey Formation, California, *in* The Monterey Formation – from rocks to molecules: New York, Columbia University Press, p. 1-30.

John, C. M., Karner, G. D., Browning, E., Leckie, R. M., Mateo, Z., Carson, B., and Lowery, C., 2011, Timing and magnitude of Miocene eustasy derived from mixed siliciclastic-carbonate stratigraphic record of the northeastern Australian margin: Earth and Planetary Science Letters, v. 304, p. 455-467.

Johnson, C. L., Bloch, R. B., and Graham, S. A., 2005, Tertiary sequences of the central San Joaquin Basin, California – Age control and eustatic versus tectonic forcing factors: Pacific Section, American Association of Petroleum Geologists MP49, 1 sheet.

Johnson, C. L., and Graham, S. A., 2004, Middle Tertiary stratigraphic sequences of the San Joaquin basin, California *in* Petroleum systems and geologic assessment of oil and gas in the San Joaquin basin province, California: U.S. Geological Survey Professional Paper 1713, ch. 6.

Karp, S. E., Elliott, W. J., and Young, R. J., 1968, Guidebook geology and oilfields west side southern San Joaquin Valley, *in* 43rd Annual Pacific Section AAPG Meeting, 46 p.

Kleinpell, R. M., 1938, Miocene Stratigraphy of California: Tulsa Oklahoma, AAPG, 450 p.

Loutit, T. S., Hardenbol, J., Vail, P. R., Baum, G. R., 1988, Condensed sections: the key to age-dating and correlation of continental margin sequences, *in* Wilgus, C. K., Hastings, B. S., Kendall, C. G., St., C., Posamentier, H. W., Ross, C. A., Van Wagoner, J. C. Eds., Sea Level Changes – An Integrated Approach, v. 42, SEPM Special Publication, p. 183-213.

Lyle, M., Koizumi, I., Delaney, M. L., and Barron, J. A., 2000, Sedimentary record of the California current system, middle Miocene to Holocene: A synthesis of leg 167 results: Proceedings of the Ocean Drilling Program, Scientific Results, v. 167, p. 341-376.

Martini, E., 1970, Standard Paleogene calcareous nannoplankton zonation: Nature, v. 226, p. 560-561.

Martini, E., 1971, Standard Tertiary and Quaternary calcareous nannoplankton zonation, *in* Farinacci, A., ed., Proceedings of the second planktonic conference: Rome, Edizioni Teconscienza, p. 739-785.

Mawbey, E. M., and Lear, C. H., 2013, Carbon cycle feedbacks during the Oligocene-Miocene transient glaciation: Geology, v. 41 p. 963-966.

McCrory, P. A., Wilson, D. S., Ingle, J. C., and Stanley, R. G., 2005, Neogene geohistory analysis of Santa Maria Basin, California, and its relationship to transfer of Central California to the Pacific Plate: U.S. Geological Survey Bulletin, J1-J38.

McDougall, K., 2007, California Cenozoic Biostratigraphy - Paleogene *in* Petroleum systems and geologic assessment of oil and gas in the San Joaquin Basin province, California: U. S. Geological Survey Professional Paper, 18p, ch. 4.

McMichael, L. B., 1959, Formation, in Chico-Martinez Creek area, comprises (ascending) Gould shale, Devilwater silt, McDonald shale, Antelope shale, and Chico-Martinez chert (new) member: San Joaquin Geologic Society Guidebook Field Trip, p. 13.

Murata, K, J., and Nakata, J. K., 1974, Cristobalitic Stage in the Diagenesis of Diatomaceous Shale: Science, v 184, p. 567-568.

Murata, K. J., and Larsen, R. R., 1975, Diagenesis of Miocene siliceous shales, Temblor Range, California: U.S. Geological Survey Journal of Research, v. 3, n. 5, p. 553-556.

Murata, K. J., and Randall, R. G., 1975, Silica mineralogy and structure of the Monterey shale, Temblor Range, California: U.S. Geological Survey Journal of Research, v. 3, p. 567-572.

Murata, K. J., Friedman, I., and Gleason, J. D., 1977, Oxygen isotope relations between diagenetic silica minerals in Monterey shale, Temblor Range, California: American Journal of Science, v. 277, p. 259-272.

Okada, H., and Bukry, D., 1980, Supplementary modification and introduction of code numbers to the low-latitude coccolith biostratigraphy zonation (Bukry, 1973; 1975): Marine Micropaleontology, v. 5, n. 6, p. 321-325.

Omarzai, S. K., 1992, Monterey Formation of California at Shell Beach (Pismo Basin) – Its lithofacies, paleomagnetism, age, and origin, *in* Schwalbach, J. R., and Bohacs, K. M., eds., Sequence stratigraphy in fine-grained rocks – Examples from the Monterey Formation: Pacific Section, Society of Economic Paleontologists and Mineralogists, v. 70, p. 47-65.

Pisciotto, K. A., and Garrison, R. E., 1981, Lithofacies and depositional environments of the Monterey Formation, California, *in* Garrison, R. E., and Douglas, R. G., eds., The Monterey Formation and related siliceous rocks of California: Los Angeles, Pacific Section, Society of Economic Paleontologists and Minerologists, p. 97-122.

Retallack, G. J., 2004, Late Miocene climate and life on land in Oregon within a context of Neogene global change: Palaeogeography, Palaeoclimatology, Palaeoecology, v. 214, p. 97-123.

Scheirer, H. A., and Magoon, L. B., 2007, Age, distribution and stratigraphic relationship of rock units in the San Joaquin basin province, California, *in* Petroleum systems and geologic assessment of oil and gas in the San Joaquin basin province, California: U.S. Geological Survey Professional Paper 1713, ch. 5.

Scheirer, H. A., 2013, The three-dimensional geologic model used for 2003 National Oil and Gas Assessment of the San Joaquin Basin Province, California, *in* Hosford Scheirer, A., ed., Petroleum systems and geologic assessment of oil and gas in the San Joaquin basin province, California: U.S. Geological Survey Professional Paper 1713, ch. 7.

Schwalbach, J., and Bohacs, K., 1992, Field investigation techniques for analysis of the Monterey Formation, *in* Sequence stratigraphy in fine-grained rocks: examples from the Monterey Formation: Society of Economic Paleontology and Minerology, Pacific Section, ch. 3, p. 21.

Simpson, R. R., and Krueger, M. L., 1942, Crocker Flat landslide area, Temblor Range, California: AAPG Bulletin, v. 26, p. 1608-1631.

Taff, J. A., 1933, Geology of McKittrick oil field and vicinity, Kern County, California: AAPG Bulletin v. 17, p. 1-15.

Tearpock, D. J., and Bischke, R. E., 1991, Applied subsurface geologic mapping, first ed.: Upper Saddle River, NJ, Prentice-Hall, 648p.

Vail, P. R., and Hardenbol, J., 1979, Sea level changes during the Tertiary: Oceanus, v. 22, p. 71-79.

Vincent, E., and Berger, W. H., 1985, Carbon dioxide and global cooling in the Miocene: The Monterey hypothesis, *in* Sundquist, E. T., and Broecker, W. S., eds., The carbon cycle and atmospheric CO_2: Natural variations Archean to present: American Geophysical Union Geophysical Monographs 32, p. 455-468.

Ward, D. L., 1982, Surface radiometric surveys for uranium using gross and spectral gamma-ray measurements: Bendix Field Engineering Corporation, 36p.

Wernicke, B., 2011, The California River and its role in carving the Grand Canyon: Geological Society of America Bulletin, v. 123, p. 1288-1316.

Williams, L. A., 1982, Lithology of the Monterey Formation (Miocene) in the San Joaquin Valley, California, *in* Williams, L. A., and Graham, S. A., eds., Monterey Formation and associated coarse clastic rocks, central San Joaquin basin, California: Pacific Section, Society of Economic Paleontologists and Mineralogists Annual Field Trip Guidebook, p. 17-36.

Williams, L. A., 1990, Description of the Monterey Formation: Chico Martinez Creek area, western Kern County, California, *in* Field Trip Guide Book: Pacific Section, Society of Economic Paleontologists and Mineralogists, v 64, p. 347-346.

Williams, L. A., Cooley, S. A., Graham, S. A., and Philips, L., 1982, Road log: Monterey Formation and associated coarse clastics of the central San Joaquin Valley, *in* Williams, L. A., and Graham, S. A., eds., Monterey Formation associated coarse clastic rocks, central San Joaquin basin, California: Pacific Section SEPM Annual Field Trip Guidebook, p. 75-95.

Woodring, W. P., Stewart, R., and Richards, R. W., 1940, Geology of the Kettleman Hills oil field: U.S. Geological Survey Professional Paper, n. 195, 178 p.